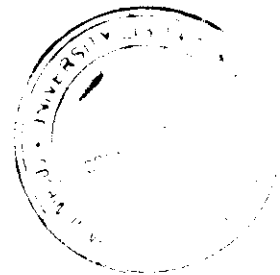


NONLINEAR DYNAMICS OF MULTIPLE  
QUANTUM WELL LASERS:  
Chaos and Multistability

A THESIS SUBMITTED TO  
COCHIN UNIVERSITY OF SCIENCE & TECHNOLOGY  
IN PARTIAL FULFILMENT OF THE REQUIREMENTS  
FOR AWARD OF THE DEGREE OF  
**Doctor of Philosophy**  
IN THE FACULTY OF SCIENCE



by

**Jijo P U**

International School of Photonics  
Cochin University of Science & Technology  
Cochin 682 022  
INDIA

August 2008

**Nonlinear Dynamics of Multiple Quantum Well Lasers:  
Chaos and Multistability**

*Ph.D Thesis in the field of Nonlinear Dynamics*

**Author:**

***Jijo P. U.***

T13

Research Fellow

International School of Photonics,  
Cochin University of Science and Technology,  
Cochin 682 022, India

E-mail: Paul.Jijo@gmail.com, jijo@rocketmail.com

**Research Advisor:**

***Dr. V. M. Nandakumaran***

Professor

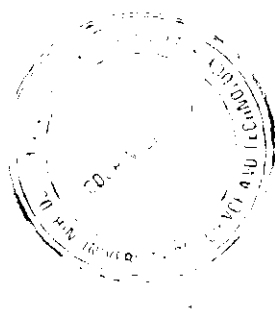
International School of Photonics,  
Cochin University of Science and Technology,  
Cochin 682 022, India

E-mail: nandak@cusat.ac.in

International School of Photonics,  
Cochin University of Science and Technology,  
Cochin, 682 022, India

URL: [www.photonics.cusat.edu](http://www.photonics.cusat.edu)

T  
621-375-826(043-2)  
J1J



**August 2008**

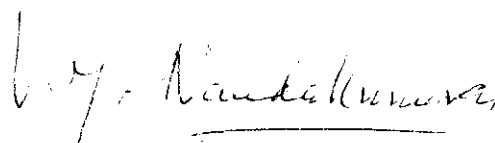
**Revised in April 2010**

TO

*My Loving Family*  
*and*  
*My Teachers*

***CERTIFICATE***

Certified that the work presented in the thesis entitled “*Nonlinear Dynamics of Multiple Quantum Well Lasers: Chaos and Multistability*” is based on the original work done by Mr. **Jijo P. U.**, under my guidance and supervision at the International School of Photonics, Cochin University of Science and Technology, Cochin 682 022, India and has not been included in any other thesis submitted previously for the award of any degree.



**Prof. V. M. Nandakumaran**

(Supervising Guide)

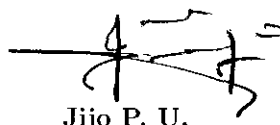
International School of Photonics, CUSAT

Kochi 22

August 29, 2008

## ***DECLARATION***

I do hereby declare that the work done in the thesis entitled “*Nonlinear Dynamics of Multiple Quantum Well Lasers: Chaos and Multistability*” is based on the original work done by me under the supervision of Dr. V. M. Nandakumaran, Professor, International School of Photonics, Cochin University of Science and Technology, Cochin 682 022, India and has not been included in any other thesis submitted previously for award of any degree.

A handwritten signature in black ink, consisting of several loops and a horizontal line, positioned above the name Jijo P. U.

**Jijo P. U.**

Kochi 22

August 29, 2008

## *Preface*

Semiconductor lasers have come a long way from their introduction as small and reliable source of coherent light energy to become the backbone of modern applications from communication to household electronic devices. The study of their dynamics has gathered momentum as their applications grew in number as the years go by. Along with the application front, the device fabrication technologies have also grown tremendously making the devices much smaller, faster and more reliable. In these contexts, the nonlinear dynamics of such lasers have become interesting to scientists and engineers owing to their typical application in areas like optical communication. Further, the understanding of device dynamics gave better feedback for improving the device performances.

Nonlinear dynamics of laser systems has become an interesting area of research in recent times. Lasers are good examples of nonlinear dissipative systems showing many kinds of nonlinear phenomena such as chaos, multistability and quasiperiodicity. The study of these phenomena in lasers has fundamental scientific importance since the investigations on these effects reveal many interesting features of nonlinear effects in practical systems. Further, the understanding of the instabilities in lasers is helpful in detecting and controlling such effects.

Chaos is one of the most interesting phenomena shown by nonlinear deterministic systems. It is found that, like many nonlinear dissipative systems, lasers also show chaos for certain ranges of parameters. Many investigations on laser chaos have been done in the last two decades. The earlier studies in this field were concentrated on the dynamical aspects of laser chaos. However, recent developments in this area mainly belong to the control and synchronization of chaos. A number of attempts have been reported in controlling or suppressing chaos in lasers since lasers are the practical systems aimed to operated in stable or periodic mode. On the other hand, laser chaos has been found to be applicable in high speed secure communication based on synchronization of chaos. Thus, chaos in laser systems has technological importance also.

Semiconductor lasers are most applicable in the fields of optical communications among various kinds of laser due to many reasons such as their compactness, reliability, modest cost and the opportunity of direct modulation. They show chaos and other instabilities under various physical conditions such as direct modulation and optical or optoelectronic

feedback. It is desirable for semiconductor lasers to have stable and regular operation. Thus, the understanding of chaos and other instabilities in semiconductor lasers and their control is highly important in photonics.

This thesis presents analytical and numerical results from studies based on the multiple quantum well laser rate equation model. We address the problem of controlling chaos produced by direct modulation of laser diodes. We consider the delay feedback control methods for this purpose and study their performance using numerical simulation. Besides the control of chaos, control of other nonlinear effects such as quasiperiodicity and bistability using delay feedback methods are also investigated.

A number of secure communication schemes based on synchronization of chaos semiconductor lasers have been successfully demonstrated theoretically and experimentally. The current investigations in these field include the study of practical issues on the implementations of such encryption schemes. We theoretically study the issues such as channel delay, phase mismatch and frequency detuning on the synchronization of chaos in directly modulated laser diodes. It would be helpful for designing and implementing chaotic encryption schemes using synchronization of chaos in modulated semiconductor lasers. The thesis consists of six chapters. The content of each chapter is described briefly as follows.

**Chapter 1** is an introductory chapter, which describes the basic concepts of nonlinear dynamics and chaos. A short description of the development of chaos theory is given. The fundamental properties and necessary conditions for the existence of chaos are described and chaotic behavior of discrete and continuous dynamical systems is illustrated for the logistic map and the Lorenz system respectively. The main routes to chaos are also discussed. The necessary computational tools used in numerical studies of chaotic system are presented. A brief outline of laser chaos is also presented. The concepts of control and synchronization of chaos are also given.

**Chapter 2** is a review on the physics and engineering aspects of multiple quantum well lasers. This chapter brings out a detailed plan on the modeling of such systems and various material properties and physical phenomena that controls their working.

**Chapter 3** describes the effect of direct modulation on the dynamics of multiple quantum well lasers. This chapter gives the results of various modulation schemes employed and demonstrates some new results in the dynamics of multiple quantum well lasers. Main

result of the chapter is results on the observation of chaos in the system when multitone modulation scheme is introduced.

**Chapter 4** deals with the occurrence of multistability in directly modulated multiple quantum well lasers. Hysteresis and bistability are numerically demonstrated using the bifurcation diagrams drawn by the method of continuous time simulation. Possible causes and applications of these phenomena are discussed in this chapter. Also discussed here is the observation of the crisis phenomenon in the working of such lasers.

**Chapter 5** shows the significance of feedback delay time in the suppression instabilities are discussed in this chapter along with the observation of chaos in the system when suitable modulation and feedback conditions are met. The chapter explore the feasibility of using built-in feedback methods to control the laser dynamics.

**Chapter 6** summarises the results obtained. A brief discussion on the possible future works in the area of nonlinear dynamics of multiple quantum well lasers are also discussed in this chapter.



## *Acknowledgement*

I am extremely thankful to my supervising guide Prof. V. M. Nandakumaran, who has been the constant source of knowledge and wisdom throughout my research life in Cochin University. I am indebted to his inspiration and valuable suggestions, keeping in mind the exact role of a researcher in society.

I would like to express my gratitude for the Council for Scientific and Industrial Research (CSIR) of India for supporting my research during the period from September 2002 to February 2007 in the form of Junior and Senior Research Fellowships.

I have deep admiration and gratitude for the faculty of International School of Photonics who stood for the growth and success of my career in ISP. I would like to thank Prof. V. P. N. Nampoore, the Director of ISP, who always encouraged all our pursuit for excellence in the chosen walk of life. I would always look back in admiration for the support and enthusiasm shared by Prof. C. P. Garihavallabhan, Emeritus Professor of ISP and Director of CELOS, who had a place amongst the young generation of ISP. I would like to express my sincere gratitude for Prof. P. Radhakrishnan, Professor and former Director of ISP, who stood for our cause and shared his personal appreciation. I am thankful to Mr. Kailasnath, Lecturer, who has been more like a friend than faculty during my stint there in the School.

There are none closer to express deep gratitude and heartfelt wishes than my group members and close friends Mr. Manu Punnen John and Dr. Rajesh S. I am indebted to both of them for the help and encouragement during the entire course of my research life in ISP and their inputs and exchange of ideas were invaluable in to my work. Thanks are due to my colleagues and friends in my research group Dr. Bindu M. Krishna and Ms. Parvathi. I would also like to thank Dr. Prasanth Ravindran, who has been a source of knowledge and inspiration.

Throughout my life in and out of my research career, there were always many people who stood there for me to help and encourage and to share the burdens. I would like to thank Mr. Vimu V. Namboodiri, Dr. Rajesh M, Mrs. Sheeba Rajesh, Dr. Santhi Annie Joseph, Dr. Pramod Gopinath, Dr. Thomas Lee S, Dr. Jyotsna Ravi, Dr. Deepthy Menon, Dr. Aneesh Balakrishnan, Mr. Abraham Scaria, Dr. Sajjan D. George, Mr. K. T. Umikrishnan, Mr. Hresh M. S., and Mr. Ajiunsha R. S.

Life in ISP was a really marvelous experience and exchange of ideas I have had. I thank

to all my friends in ISP, Dr. Binoy Paul, Dr. Bindu V., Dr. Geetha K., Sr. Ritty J. Nedumpara, Mr. Dann V. Joseph, Mr. Thomas K Johny, Mr. Lyjo K. Joseph, Mr. Sajeev D., Ms. Litty Irimpan, Ms. Parvathi R., Ms. Dilna Sreenivasan, Ms. Lekshmi Sasidhar, Ms. Jayasrec V. K., Ms. Rekha George, Dr. Pravitha Ramanand, and Mr. Jibu Kumar. All the present batch of researchers in ISP has been really supportive and friendly to me. I thank them all.

Life would not have been better without my friends in CUSAT especially those from the departments of Physics, Biotechnology and Chemistry. I would always remember my days with them forever. Also there are a few friends abroad, especially Mr. Bijilash Babu in Dublin, Mr. Anosh Joseph, in Syracuse whom I found as sources of constant support.

Last, but not the least, there is always the personal support that we all look forward to. I am extremely fortunate to have a few friends who were always there with support and inspiration. I have no real words to express my gratitude to Mr. Santoy John, his wife Sonia, and Ms. Nisha Treesa Joseph for their relentless support and friendship.

Thanks are due to my colleagues in Government College Madappally and Government College Kasaragod, where I spent my time putting theory to practice since February 2007.

Above all I salute my parents and my wife Sindhu for their endless support for my chosen walk of life!

**Jijo P. U.**

### *List of Publications*

- M. P. John, **P. U. Jijo** and V. M. Nandakumaran, *Effect of a fluctuating parameter mismatch and the associated time-scales on coupled Rössler systems*, *Pramana - J. Phys.*, Vol. 72, No. 3, pp. 495 - 503 (2009).
- **J. P. Ulahannan**, M. P. John, and V. M. Nandakumaran, *Bistability and Hysteresis in the Dynamics of Directly Modulated Multiple Quantum Well Lasers*, in *Laser Science*, OSA Technical Digest (CD) (Optical Society of America, 2007), paper JWC43.
- **Jijo P. U.**, M. P. John, and V. M. Nandakumaran, *Static and Dynamical Modelling Approaches to Nanostructures and Devices*, Proc. of National Conference on Current Trends in Material Science (CTMS-07), February 25-27 (2007), Chengannur, India.
- M. P. John, **P. U. Jijo** and V. M. Nandakumaran, *Effect of a fluctuating parameter in the synchronization of a chaotic system*, Proc. of National Conference on Current Trends in Material Science (CTMS-07), February 25-27 (2007), Chengannur, India.
- **Jijo P. U.**, M. P. John and V. M. Nandakumaran, *Optoelectronic feedback induced chaos in MQW laser diodes*, Proc. of Photonics 2006, 8th Intl. Conference on Optoelectronics, Fibre Optics and Photonics, December 13-16 (2006), Hyderabad, India.
- R. Prasanth and **P. U. Jijo**, *Acceptor State Fluorescence Quenching of Nanoparticle FRET*, Proc. of Photonics 2006, 8th Intl. Conference on Optoelectronics, Fibre Optics and Photonics, December 13-16 (2006), Hyderabad, India.
- M. P. John, **P. U. Jijo** and V. M. Nandakumaran, *Fast fluctuations do not destroy synchronization*, *Nonlinear Systems and Dynamics*, pp. 103-105. Allied Publishers (India), February 2006. Proc. of National Conference on Nonlinear Systems and Dynamics (NCNSD-06), Chennai, India.
- **P. U. Jijo**, M. P. John and V. M. Nandakumaran, *Significance of parameter fluctuation rates in coupled directly modulated semiconductor laser systems*, Proc. of Intl. Conf. on Optoelectronics and Lasers (ICOL - 2005), December 11 - 15 (2005), Dehradun, India.

- M. P. John, **P. U. Jijo** and V. M. Nandakumaran, *Effect of parameter fluctuations in coupled directly modulated semiconductor lasers*, Proc. of Photonics 2004, 7th Intl. Conference on Optoelectronics, Fibre Optics and Photonics, December 9-11 (2004), Cochin, India.
- **P. U. Jijo**, M P John, S. Rajesh and V. M. Nandakumaran, *Control of chaos and noise induced instabilities in a Duffing oscillator with amplitude modulated feedback*, Proc. of Perspectives in Nonlinear Dynamics, satellite meeting of the 22nd IUPAP International Conference (STATPHYS 22), 4-9 July (2004), Bangalore, India.

# Contents

<b>Preface</b>	<b>v</b>
<b>Acknowledgements</b>	<b>viii</b>
<b>Publications</b>	<b>xi</b>
<b>1 Introduction</b>	<b>3</b>
1.1 Nonlinear Dynamics and Chaos . . . . .	3
1.1.1 Phase Space and Phase Flow . . . . .	6
1.1.2 Poincaré Section . . . . .	7
1.1.3 Lyapunov Exponents . . . . .	9
1.1.4 Power Spectrum . . . . .	10
1.1.5 Bifurcation Diagrams . . . . .	11
1.2 Control of Chaos . . . . .	11
1.3 Synchronization of Chaotic Systems . . . . .	12
1.4 Conclusions . . . . .	13
<b>Bibliography</b>	<b>15</b>
<b>2 Nonlinear Dynamics of Multiple Quantum Well Lasers</b>	<b>19</b>
2.1 Introduction . . . . .	19
2.2 Physics of Low Dimensional Structures . . . . .	20
2.2.1 Quantum Wells . . . . .	21

2.3	Quantum Well Lasers . . . . .	23
2.4	Multiple Quantum Well Lasers . . . . .	25
2.5	Dynamics of Quantum Well Lasers . . . . .	26
2.5.1	Criteria for Modeling Quantum Well Lasers . . . . .	27
2.5.2	Carrier Transport in Quantum Well Structures . . . . .	28
2.5.3	Well-Barrier Hole Burning Model . . . . .	30
2.5.4	Nonradiative Recombination and Carrier Overflow . . . . .	32
2.5.5	Optical Cavity . . . . .	33
2.5.6	Fabry-Perot Lasers . . . . .	34
2.5.7	Distributed Feedback Lasers . . . . .	34
2.6	A Rate Equation Model for Directly Modulated MQW Laser Diodes . . . . .	36
2.6.1	Gain Calculation . . . . .	37
2.7	Scope of this Thesis . . . . .	38
	<b>Bibliography</b>	<b>39</b>
<b>3</b>	<b>Effect of Modulation on MQW Laser Dynamics</b>	<b>45</b>
3.1	Introduction . . . . .	45
3.2	Direct Modulation of MQW Lasers . . . . .	46
3.3	Sinusoidal Modulation and Frequency Response . . . . .	48
3.4	Single-Tone Modulation . . . . .	49
3.5	Two-Tone Modulation . . . . .	55
3.6	Effect of Multitone Modulation . . . . .	58
3.7	Routes to Chaos . . . . .	60
3.8	Synchronization of Coupled MQW Lasers . . . . .	61
3.9	Conclusions . . . . .	66
	<b>Bibliography</b>	<b>66</b>
<b>4</b>	<b>Multistability and Hysteresis in MQW Laser Dynamics</b>	<b>71</b>

4.1	Introduction . . . . .	71
4.2	Bistability in Directly Modulated Lasers . . . . .	72
4.3	Multistability in Directly Modulated MQW Laser . . . . .	72
4.4	Bistability and Hysteresis . . . . .	74
4.5	Coexisting Attractors and Crisis . . . . .	75
4.5.1	Bifurcation for Group Velocity Variation . . . . .	76
4.6	Control of Bistability and Hysteresis . . . . .	78
4.7	Applications of multistability . . . . .	78
4.8	Conclusions . . . . .	79
<b>Bibliography</b>		<b>79</b>
<b>5</b>	<b>Effect of Delay Feedback in MQW Lasers</b>	<b>85</b>
5.1	Introduction . . . . .	85
5.2	Laser Diode with Optoelectronic Feedback . . . . .	86
5.3	Control of Chaos Using Delay Feedback . . . . .	89
5.4	Delay Induced Chaos in MQW Laser Systems . . . . .	89
5.5	Applications of Delayed Laser Systems . . . . .	91
5.6	Conclusions . . . . .	91
<b>Bibliography</b>		<b>92</b>
<b>6</b>	<b>Conclusions and Future Prospects</b>	<b>95</b>
6.1	General Conclusions . . . . .	95
6.2	Future Prospects . . . . .	96

# Chapter 1

## Introduction

*"Wisdom begins in wonder."*– Socrates

### ABSTRACT

*Nonlinear dynamics and chaos are major topics of study in the mainstream physics and mathematics today. New techniques and dimensions of study have brought forward the necessity of analyzing physical systems using nonlinear tools. Many known physical systems exhibit nonlinear character and it cannot be avoided without deeper study and analysis. Lasers in general and semiconductor lasers in particular are known working models for studying nonlinear behaviour of systems in the quantum level. This chapter gives a brief introduction to nonlinear dynamics, chaos theory, and the quantum electronics of semiconductor lasers.*

### 1.1 Nonlinear Dynamics and Chaos

Nonlinear dynamics and chaotic behaviour have been studied over the last few decades in many systems belonging to different areas like biology, chemistry or physics [1, 2, 3, 4]. The interesting aspect of these studies is the search for universality in the behaviour of nonlinear systems and their transitions to chaos. A general approach in studying the complexity of such systems involves investigating their dynamics as some system parameters are varied. This method yields an analysis of qualitative changes, known as bifurcations, resulting in a change of the number of attractors, their type such as periodic, quasiperiodic, chaotic and/or their stability.



Nonlinear dynamics and chaos in laser systems have been studied since the late 1970s. Semiconductor lasers, which usually show only coupled light-carrier density oscillations known as relaxation oscillations, show chaotic instabilities when we add an additional degree of freedom [5].

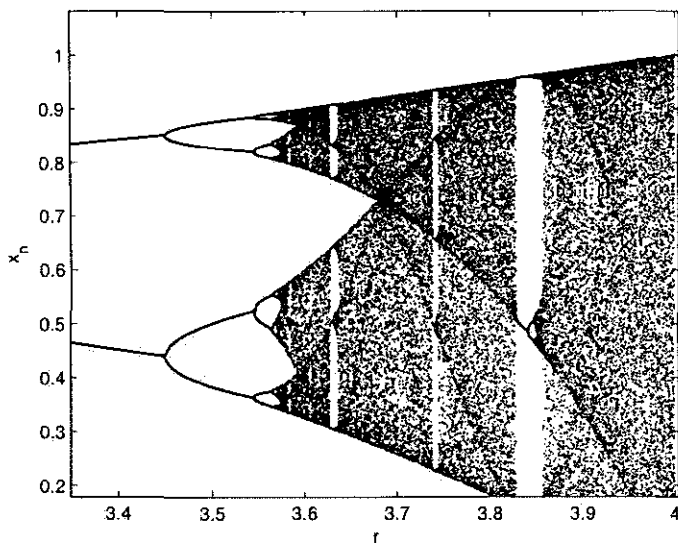


Figure 1.1: A window from the bifurcation diagram of the logistic map  $x_{n+1} = rx_n(1 - x_n)$ . Each vertical section shows the attractor for a specific value of the parameter  $r$ . The diagram displays period-doubling as  $r$  increases, eventually producing chaos beyond  $r \gtrsim 3.569$ . The periodic regions within the region  $3.569 < r < 4$  are termed as windows, for example, the window around  $r \approx 3.84$  is called a period-3 window.

A *dynamical system* has a state determined by a collection of real numbers, or more generally by a set of points in an appropriate *manifold*  $M$ . A manifold is a geometrical space and the set of points are coordinates of this space. The evolution rule of the dynamical system is a fixed rule that describes what future states follow from the current state. This rule is deterministic which means for a given time interval only one future state follows from the current state. In the case of a continuous system, the phase space evolution is said to be a *phase flow*. If  $f$  is any continuous function, then the evolution of a variable  $x$  can be given by the formula

$$x_{n+1} = f(x_n). \quad (1.1)$$

If, on the other hand, there is a discrete time ( $n$ ) evolution as in  $x_{n+1} = 2x_n \pmod{1}$ , it is referred to as a *map* rather than a *flow*. Among smooth dynamical systems, chaotic

dynamics is characterised by the presence of expanding and contracting directions for the derivative. This is a situation where the differential alone provides strong local, semi-local or even global information about the dynamics. This stretching and folding typically give rise to complicated long-term behavior in these systems. The dynamics appears in many ways effectively random, even though these systems are completely deterministic. The theory of these dynamical systems provides a rigorous mathematical foundation for this remarkable phenomenon known as deterministic chaos - the appearance of chaotic motions in purely deterministic dynamical systems. Chaotic dynamics produces several characteristic features of the orbit structure that reflect the coexistence of highly complicated long-term behavior and sensitive dependence on initial conditions on one hand with overall stability of the orbit structure on the other hand. A nonlinear dynamical system can follow different routes to chaos. Three main universal transition routes from regular to chaotic motion have been observed so far in different systems: the period-doubling or Feigenbaum route[6, 7], the intermittency or Pomcau-Manneville route[8], and the quasiperiodic or Ruelle-Takens-Newhouse route[9].

Period doubling bifurcation in a dynamical system is a bifurcation in which the system switches to a new behaviour with twice the period of the original system. The period-doubling route refers to a successive series of period-doubling bifurcations [10] that occur while changing a control parameter. A transition to chaos takes place after an infinite number of doublings follow each other with a closer spacing. The intermittency route is characterized by an increasing number of short, irregular bursts, interrupting the nearly regular motion. The mean distance between the bursts changes when we vary a control parameter. There are three different types of intermittency that can be distinguished by the statistics of the time interval between the bursts. Type-I intermittency is associated with an inverse tangent bifurcation, type-II with a Hopf bifurcation, and type-III with a period-doubling bifurcation. The quasiperiodic route corresponds to a series of Hopf bifurcations generating a new eigenfrequency each time one changes a control parameter. The first Hopf bifurcation generates a limit cycle in phase space emerging from an fixed point solution. After the second Hopf bifurcation the motion of the system in phase space takes place on a two-dimensional torus allowing periodic as well as quasiperiodic behaviour. The third Hopf bifurcation finally gives rise to the occurrence of deterministic chaos.

Though chaos is all about complexity, some of the most powerful tools used for studying chaos are rather graphical in nature and, therefore, simple to appreciate [11]. Some of these methods were developed by the great French mathematician, Henri Poincaré at the end of nineteenth century. In the following subsections, we will discuss some of those tools that are used to analyse the dynamics of systems considered in this thesis:

### 1.1.1 Phase Space and Phase Flow

The concept of phase space is a generalisation of the three dimensional coordinate system used in the *Euclidian* space [11]. The dimension of the *phase-space* depends on the degrees of freedom that the dynamical system has, and a single point in this hypothetical space represents completely the state of motion of all the variables at any instant of time. As the system evolves in time according to the laws governing it, the representative point describes a trajectory or an orbit in the phase space. Since the laws of motion are usually second order deterministic differential equations, there must be a unique trajectory through at any given phase point. It follows then that these trajectories cannot intersect or self intersect. However, they can close on themselves. This non-intersection of trajectories is the essence of the deterministic dynamics.

The phase space volume occupied by system also evolves with the evolution of the system. If the phase-space volume contracts as time progresses, the system is said to be dissipative. On the other hand, if the phase-space volume remains constant, the system is said to be conservative system. The phase-space flow can lead to various situations which, in turn, help us understand the nature of the system better. If the evolution of the phase-space volume settles down to a point and stays put there, we refer to it as being *asymptotically stable*, since the system approaches the point asymptotically. This point will be a stable equilibrium at which all motion stops. We call it then a stable *fixed point*. This, for example, in the case of a damped harmonic oscillator is the origin. The fixed point is stable because if the particle is displaced slightly away from the point, it comes back. Thus the stable fixed point is an *attractor* - it attracts trajectories in its neighbourhood, which is its domain of attraction. An under biased semiconductor laser could arguably exhibit such a situation.

Next in the hierarchy of attractors is another geometrical object, a *limit cycle*. Here the trajectory closes on itself, that is to say that the system settles down to a stable periodic oscillation, which we will observe quite often in the coming chapters in the case of directly modulated MQW laser system. It is *asymptotically stable*. In a two-dimensional phase space, the limit cycle is the only attractor other than the fixed point.

Next to the limit cycle representing a singly-periodic motion, one has a *biperiodic torus*, a doughnut-shaped attractor in a state space which is at least three-dimensional. Here the trajectory winds round in the latitudinal as well as in the longitudinal direction of the torus with frequencies  $f_1$  and  $f_2$ , say. Clearly, if the ratio  $f_1/f_2$  is rational, we have periodic motion and the trajectory eventually closes on itself. If  $f_1/f_2$  is irrational, we have a quasi-periodic motion - the trajectory comes arbitrarily close to closing on itself but never quite do so. In higher dimensions, one can have higher dimensional tori, which represents multiple

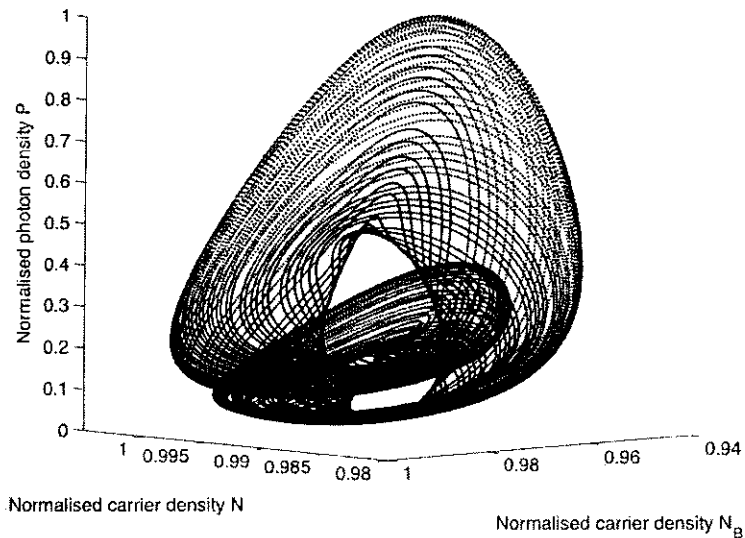


Figure 1.2: The three dimensional phase space diagram of a MQW laser system plotted using the variables  $N_B$ ,  $N$ , and  $P$ .

periodic motions.

All the above attractors correspond to regular periodic motions. A different sort of attractor that corresponds to deterministic chaos is called the *strange attractor*. It is a geometrical object of fractional dimension [4]. Thus, attractors are geometrical objects in the phase space to which the trajectories are attracted and on which they eventually lie. They have domains or *basins of attraction*. In general there may be several attractors in the phase space with their basins of attraction separated by separatrices. Together they form a landscape called the *phase portrait*. Fig. 1.2 shows the phase diagram of a multiple quantum well (MQW) laser in its three dimensional phase space. The flow corresponds to a flow in which the modulation frequencies keep an irrational ratio. The set of points that lie on the boundaries of the *basin of attraction* form a fractal set. The nature of the attractor set, whether strange attractor, a stable periodic attractor, or an unstable periodic repeller, is measured quantitatively by its Lyapunov exponents, fractal dimensions and the power spectra. We will discuss them below.

### 1.1.2 Poincaré Section

In dynamical systems, a first recurrence map or Poincaré map, named after Henri Poincaré, is the intersection of a periodic orbit in the state space of a continuous dynamical system

with a certain lower dimensional subspace, called the Poincaré section, transversal to the flow of the system[4, 12]. More precisely, one considers a periodic orbit with initial conditions on the Poincaré section and observes the point at which this orbits first returns to the section, thus the name first recurrence map. The transversality of the Poincaré section basically means that periodic orbits starting on the subspace flow through it and not parallel to it. Fig. 1.3 illustrates the method of obtaining a Poincaré section. In this, a flow is strobed every time it cuts through an imaginary plane in the phase space.

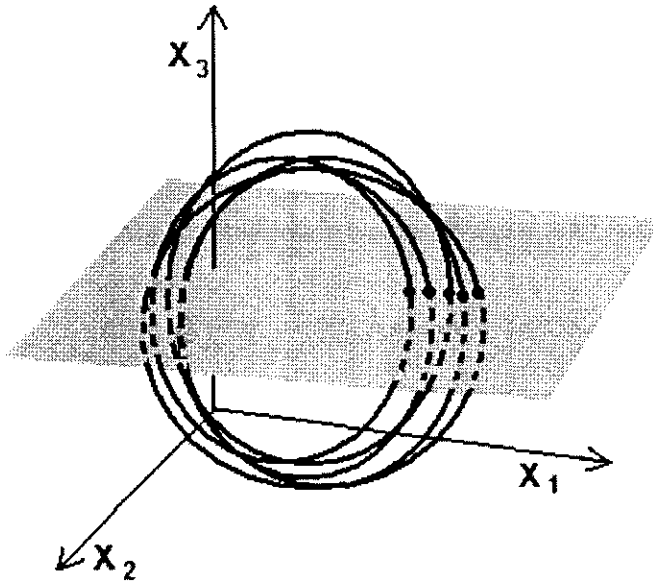


Figure 1.3: An illustration of the Poincaré section. A plane bisects the flow and strobed to reveal the complexity of the dynamics.

A Poincaré map can be interpreted as discrete dynamical systems with a state space that is one dimension smaller than the original continuous dynamical system. Because it preserves many properties of periodic and quasiperiodic orbits of the original system and has a lower dimensional state space it is often used for analyzing the original system. In practice this is not always possible as there is no general method to construct a Poincaré map.

A Poincaré map can be interpreted as discrete dynamical system with the stability of a period orbit of the original system is closely related to the stability of the fixed point of the corresponding Poincaré map. The periodic orbit  $\Upsilon$  of the continuous dynamical system is stable if and only if the fixed point  $p$  of the discrete dynamical system is stable. It is

*asymptotically stable* if and only if the fixed point  $p$  of the discrete dynamical system is *asymptotically stable*.

### 1.1.3 Lyapunov Exponents

Lyapunov exponent or Lyapunov characteristic exponent of a dynamical system is a quantity that characterizes the rate of separation of infinitesimally close trajectories. Quantitatively, two trajectories in phase space with initial separation  $\delta\mathbf{Z}_0$  diverge

$$|\delta\mathbf{Z}(t)| \approx e^{\lambda t} |\delta\mathbf{Z}_0| \quad (1.2)$$

where  $|\cdot|$  represents the modulus of the considered vectors.

The rate of separation can be different for different orientations of initial separation vector. Thus, there is a whole spectrum of Lyapunov exponents - the number of them is equal to the number of dimensions of the phase space. It is common to just refer to the largest one, i.e. to the Maximal Lyapunov Exponent (MLE), because it determines the predictability of a dynamical system. A positive MLE is usually taken as an indication that the system is chaotic. The maximal Lyapunov exponent is defined as follows:

$$\lambda = \lim_{t \rightarrow \infty} \lim_{|\delta\mathbf{Z}_0| \rightarrow 0} \frac{1}{t} \log \frac{|\delta\mathbf{Z}(t)|}{|\delta\mathbf{Z}_0|} \quad (1.3)$$

the order of the limits should be preserved to have a meaningful definition. Therefore the MLE is defined as the exponential rate of separation of a reference orbit with respect to an infinitesimally perturbed orbit averaged over an extremely long (infinite) lag of time.

For a dynamical system with evolution equation  $f^t$  in an  $n$ -dimensional phase space, the spectrum of Lyapunov exponents

$$\{\lambda_1, \lambda_2, \dots, \lambda_n\}$$

in general, depends on the starting point  $x_0$ . The Lyapunov exponents describe the behavior of vectors in the tangent space of the phase space and are defined from the Jacobian matrix

$$J^t(x_0) = \left. \frac{df^t(x)}{dx} \right|_{x_0}. \quad (1.4)$$

The  $J^t$  matrix describes how a small change at the point  $x_0$  propagates to the final point  $f^t(x_0)$ . The set of Lyapunov exponents will be the same for almost all starting points of an ergodic component of the dynamical system. If the system is conservative (i.e. there is

no dissipation), a volume element of the phase space will stay the same along a trajectory. Thus the sum of all Lyapunov exponents must be zero. If the system is dissipative, the sum of Lyapunov exponents is negative. If the system is a flow, one exponent is always zero the Lyapunov exponent corresponding to the eigenvalue of  $J$  with an eigenvector in the direction of the flow.

Generally the calculation of Lyapunov exponents [15, 16, 17, 18], as defined above, cannot be carried out analytically, and in most cases one must resort to numerical techniques. The commonly used numerical procedure estimates the  $J$  matrix based on averaging several finite time approximations of the limit defining  $J$ . One of the most used and effective numerical technique to calculate the Lyapunov spectrum for a smooth dynamical system relies on periodic Gram-Schmidt orthonormalization of the Lyapunov vectors to avoid a misalignment of all the vectors along the direction of maximal expansion [19]. For the calculation of Lyapunov exponents from limited experimental data, various methods have been proposed. Throughout this thesis, MLE were calculated numerically from the time series data [13, 14] using the software Dataplore.

Whereas the (global) Lyapunov exponent gives a measure for the total predictability of a system, it is sometimes interesting to estimate the local predictability around a point  $x_0$  in phase space. This may be done through the eigenvalues of the Jacobian matrix  $J_0(x_0)$ . These eigenvalues are also called local Lyapunov exponents. The eigenvectors of the Jacobian matrix point in the direction of the stable and unstable manifolds.

#### 1.1.4 Power Spectrum

In the time domain we investigate the covariance or correlation function of a stationary time series. Alternatively, we can study the (power) spectral density function or simply the (power) spectrum as a function of the frequency  $\omega$ . The spectrum of a stationary time series  $f(\omega)$  is the counterpart of a covariance function in frequency domain. That is, it is the Fourier transform of the covariance function  $\gamma(k)$  and vice versa:

$$f(\omega) = \frac{1}{2\pi} \sum_{k=-\infty}^{\infty} \gamma(k) e^{ik\omega} \quad (1.5)$$

and

$$\gamma(k) = \int_{-\pi}^{\pi} f(\omega) e^{ik\omega} d\omega \quad (1.6)$$

The power spectrum of the output of a laser system can be useful in revealing the underlying

dynamics and inherent periodicity of the system. For example, a chaotic state will have infinite components in the frequency spectrum and will be revealed by a power spectrum. It is quite useful in revealing the resonant frequency of the system and the sidebands.

### 1.1.5 Bifurcation Diagrams

As discussed before, number of continuous and discrete systems follow the period doubling route to chaos. For plotting the bifurcation of continuous dynamical systems, a set of values of a single variable representing the attractor must be obtained. This is usually done by the return map obtained from the Poincaré section [19] as shown in Fig. 1.3. There is another method for obtaining discrete mappings from the flows. Lorenz has constructed a one dimensional map from the three dimensional flow  $(X, Y, Z)$  by taking consecutive maxima of the variable  $Z$ . Such methods also can be used for plotting bifurcation diagrams. A laser bifurcation diagram, as will be shown in coming chapters of this thesis, can reveal the path to chaos in a laser system as we observe the system by varying its system parameters. The most common case is that of the *period-doubling bifurcation* where the orbit in the space bifurcates with a doubling of the period. Another feature of the bifurcating systems is the *intermittency* that brings unexpected richness to the system in the so-called chaotic regime. This can be understood with the help of a return map described above.

## 1.2 Control of Chaos

Controlling chaos, when it is unavoidable, exploits its hidden order—namely the many unstable periodic orbits embedded in the chaotic attractor. Chaotic dynamics then consists in a motion where the system state moves in the neighborhood of one of these orbits for a while, then falls close to a different unstable periodic orbit where it remains for a limited time, and so forth. This results in a complicated and unpredictable wandering over longer periods of time.

Control of chaos is the stabilization, by means of small system perturbations, of one of these unstable periodic orbits. The result is to render an otherwise chaotic motion more stable and predictable, which is often an advantage. The perturbation must be tiny, to avoid significant modification of the system's natural dynamics.

Several techniques have been devised for chaos control, but most are developments of two basic approaches: the OGY (Ott, Grebogi and Yorke) [20] method, and Pyragas [21] continuous control. Both methods require a previous determination of the unstable periodic orbits of the chaotic system before the controlling algorithm can be designed. In the OGY



method, small wisely chosen swift kicks are applied to the system once per cycle, to maintain it near the desired unstable periodic orbit. In the Pyragas method, an appropriate continuous controlling signal is injected into the system, whose intensity is practically zero as the system evolves close to the desired periodic orbit but increases when it drifts away from the desired orbit.

Experimental control of chaos by one or both of these methods has been achieved in a variety of systems, including turbulent fluids, oscillating chemical reactions, magneto-mechanical oscillators, and cardiac tissues [22].

### 1.3 Synchronization of Chaotic Systems

Synchronization of chaos is an area of research in nonlinear dynamics ever since it has emerged in 1980s [23, 24, 25]. Chaotic systems are known to show extreme sensitivity to the initial conditions. The phase space trajectories of two identical chaotic systems diverge exponentially and they will become totally uncorrelated after a finite time. Hence it is impossible to construct two independent chaotic systems with the same temporal evolution. However, certain techniques have been developed for synchronizing chaotic systems. Yamada *et al.* [26, 27] have shown that two identical chaotic systems are synchronized when they are coupled together by sending information between them [2]. In 1990, Pecora and Carroll [28] introduced a new synchronization scheme based on the complete replacement a variable of one of the two identical subsystems (response) by the corresponding variable of the other subsystem (drive) for synchronizing chaotic systems [29]. This method has been shown to be efficient in synchronizing many types of analogue electronic circuits [30]. However, coupling is commonly used for synchronizing other types of chaotic systems including the chaotic lasers operating in very high frequency regime.

Pecora and Carroll have shown that a chaotic system (drive system) can be synchronized with a separate chaotic system (response system) provided that the conditional Lyapunov exponents of the drive and the response systems are all negative [23, 28]. Roy *et al.* [31, 46] have demonstrated the practical viability of synchronizing laser systems. The ability to design synchronized chaotic systems has opened up opportunities for application of chaos to private communications. Chaotic switching, chaotic masking, and chaotic modulation are commonly used to achieve chaotic transmission. Chaotic switching utilizes a parameter change in the drive system, where two chaotic states are created to bear a binary signal [33]. The important issue in such a case is that two chaotic states are distinguishable when synchronised, and are indistinguishable if not synchronised. For chaotic masking, a large noise-like chaotic carrier, which is independently generated, is mixed with the signal at the

drive end to ensure privacy [34]. At the response end, the masked signal is recovered by removing the large chaotic carrier under synchronization.

Quantitatively, the extent of synchronization of lasers can be estimated by calculating the similarity function [23, 35] of the times series of the coupled systems. In the case of two coupled oscillators, the similarity function can be calculated as

$$S^2(\tau) = \frac{\langle [x_d(t - \tau) - x_r(t)]^2 \rangle}{\sqrt{\langle x_d^2(t - \tau) \rangle \langle x_r^2(t) \rangle}}, \quad (1.7)$$

where,  $x_d(t)$  is the time series signal of the drive system and  $x_r(t)$  is the same of a response system which is driven by the former.  $\tau$  accounts for any time that the drive signal takes to reach the response system. In coupled chaotic systems this function can be used to represent the nature of the dynamics in terms of the synchronization error. If  $\tau$  is set to zero, we obtain  $S(0)$ , the error in synchrony. We will discuss this further in the light of coupled multiple quantum well lasers in chapter 3.

## 1.4 Conclusions

We have discussed the general features of nonlinear dynamical systems and the emergence of chaos. Further, we have discussed different tools to measure and characterise chaos. These tools will be used in the study of the dynamics of multiple quantum well lasers about which we will describe in detail in the next chapter. This study, as we will show, is crucial in designing many optoelectronic systems with these lasers as the generators of light. As per the studies that we have discussed in the last paragraph, nonlinear behaviour in the such laser systems, especially the chaotic state, can be exploited to stabilise the lasers as well as use them for encryption. Laser chaos can therefore be useful in a tailor made circuit for communication.



# Bibliography

- [1] J. Guckenheimer, and P. Holmes, *Nonlinear Oscillations, Dynamical Systems, and Bifurcations of Vector Fields*, Springer-Verlag, New York, 1983.
- [2] E. Atlee Jackson, *Perspectives of Nonlinear Dynamics*, Cambridge University Press, New York, 1991.
- [3] J. A. York, *Chaos in Dynamical Systems*, Cambridge University Press, Cambridge, 2002.
- [4] E. Ott, *Chaos in Dynamical Systems*, Cambridge University Press, Cambridge, 2002.
- [5] H. Kawaguchi, *Bistability and Nonlinearities in Laser Diodes*, Artech House, Norwood, 1994.
- [6] M. J. Feigenbaum, "Quantitative universality for a class of nonlinear transformations", J. Stat. Phys. **19**, 25 (1978).
- [7] M. J. Feigenbaum, "The universal metric properties of nonlinear transformations", J. Stat. Phys. **21**, 69 (1979).
- [8] Y. Pomeau and P. Manneville, "Intermittent transition to turbulence in dissipative dynamical systems", Comm. Math. Phys. **74**, 189-197 (1980).
- [9] S. Newhouse, D. Ruelle, and F. Takens, "Occurrence of strange Axiom A attractors near quasiperiodic flows on  $T^m$ ,  $m \geq 3$ ", Comm. Math. Phys. **64**, 35-40 (1978).
- [10] H. D. I. Abarbanel, M. I. Rabinovich, and M. M. Sushchik, *Introduction to Nonlinear Dynamics for Physicists*, Singapore: World Scientific, 1993.
- [11] N. Kumar, *Deterministic Chaos: Complex chance out of simple necessity*, Universities Press, Hyderabad, India, 1996.
- [12] H. Goldstein, *Classical Mechanics*, Addison Wesley, 1990.
- [13] A. Wolf, J. B. Swift, H. L. Swinney, and J. A. Vastano, "Determining Lyapunov exponents from a time series,," Physica D **16**, pp. 285-317 (1985).
- [14] K. Briggs, "An improved method for estimating Liapunov exponents of chaotic times series,," Phys. Lett. A **151**, pp. 27-32 (1990).

- [15] F. Christiansen and H. H. Rugh, "Computing Lyapunov spectra with continuous Gram-Schmidt orthonormalization," *Nonlinearity* **10**, 1063-1072 (1997).
- [16] S. Habib and R. D. Ryne, "Symplectic Calculation of Lyapunov Exponents," *Phys. Rev. Lett.* **74**, pp. 70-73 (1995).
- [17] G. Rangarajan, S. Habib, and R. D. Ryne, "Lyapunov Exponents without Rescaling and Reorthogonalization," *Phys. Rev. Lett.* **80**, 3747-3750 (1998).
- [18] X. Zeng, R. Eykholt, and R. A. Pielke, "Estimating the Lyapunov-exponent spectrum from short time series of low precision," *Phys. Rev. Lett.* **66**, 3229-3232 (1991).
- [19] G. Benettin, L. Galgani, A. Giorgilli and J.M. Strelcyn; *Meccanica*, pp. 9-20 (1980); *ibidem*, *Meccanica*, pp. 21-30 (1980).
- [20] S. P. Layne, G. Mayer-Kress, J. Holzfuss, *Problems associated with dimensional analysis of electroencephalogram data*, In: *Dimensions and entropies in chaotic systems*, Springer-Verlag, Berlin, 1986.
- [21] E. Ott, C. Grebogi, and J. A. Yorke, "Controlling Chaos," *Phys. Rev. Lett.* **64**, pp. 1196-1199 (1990).
- [22] K. Pyragas, "Continuous control of chaos by self-controlling feedback," *Phys. Lett. A* **70**, pp. 421-428 (1992).
- [23] J. M. Gonzalez-Miranda, *Synchronization and Control of Chaos. An introduction for scientists and engineers*, Imperial College Press (London), 2004.
- [24] A. Pikovsky, M. Rosenblum, and J. Kurths, *Synchronization: A universal concept in nonlinear sciences*, Cambridge University Press, Cambridge, UK, 2001.
- [25] H. G. Schuster, Editor, *Handbook of Chaos Control: Foundations and Applications*, Wiley-VCH, Weinheim, 1999.
- [26] J. M. Gonzalez-Miranda, *Synchronization and Control of Chaos. An introduction for scientists and engineers*, Imperial College Press. London, 2004.
- [27] H. Fujisaka and T. Yamada, "Stability Theory of Synchronized Motion in coupled-oscillator Systems," *Prog. Theor. Phys.* **69**, pp. 32-47 (1983).
- [28] H. Fujisaka and T. Yamada, "Stability Theory of Synchronized Motion in Coupled-Oscillator Systems. II - The mapping approach." *Prog. Theor. Phys.* **70**, pp. 1240-1248 (1983).
- [29] L. M. Pecora, and T. M. Carroll, "Synchronization in chaotic systems," *Phys. Rev. Lett.* **64**, pp. 821-824 (1990).
- [30] U. Feudel, C. Grebogi, B. R. Hunt and J. A. Yorke, "Map with more than 100 coexisting low-periodic attractors," *Phys. Rev. E* **54**, pp. 71 (1996).

- [31] L. M. Pecora, T. L. Carroll, G. A. Johnson, D. J. Mar, and J. F. Heagy, “*Fundamentals of synchronization in chaotic systems, concepts, and applications*,” *Chaos* **7**, pp. 520 (1997).
- [32] G. D. VanWiggeren, and R. Roy, “*Communication with chaotic lasers*,” *Science* **279**, pp. 1198–1200 (1998).
- [33] R. Roy and K. S. Thornburg, Jr., “*Experimental synchronization of chaotic lasers*,” *Phys. Rev. Lett.* **72**, pp. 2009–2012 (1994).
- [34] K. M. Cuomo, A. V. Oppenheim, and S. H. Strogatz, “*Synchronization of Lorenz-based chaotic circuits with applications to communication*,” *IEEE Trans. Circuit Syst. II* **40**, pp. 626–633 (1993).
- [35] H. D. I. Abarbanel, M. B. Kennel, L. Illing, S. Tang, H. F. Chen, and J. M. Liu, “*Synchronization and communication using semiconductor lasers with optoelectronic feedback*,” *IEEE J. Quantum Electron.* **37**, pp. 1301–1311 (2001).
- [36] Manu P. John, P. U. Jijo and V. M. Nandakumaran, “*Effect of a fluctuating parameter mismatch and the associated time-scales on coupled Rossler oscillators*,” *Pramana* **72**, pp. 495–503 (2009).



## Chapter 2

# Nonlinear Dynamics of Multiple Quantum Well Lasers

*"We see only what we know."* - Johann Wolfgang von Goethe

### ABSTRACT

*Low dimensional structures have come a long way from being mere examples of applied quantum mechanics to widespread applications in many modern devices and instruments. Quantum well, quantum cascade and quantum dot lasers make use of the very fundamental idea of carrier confinement within dimensions that match their de Broglie wavelength. Quantum well lasers are used in many modern optoelectronic applications because of their great flexibility within the quantum limits to be integrated in various types of applications. This chapter presents the basic physics and basic features of multiple quantum well laser diodes from which the dynamic model is being developed.*

## 2.1 Introduction

Semiconductors allow the manipulation of light, the manipulation of electrical current, and their interaction within a single device, and that is why they are of great interest as optoelectronic materials of choice [1]. They can carry electrical current as well as light waves. In the next level, they can be designed to allow for the transformation of light into current and vice versa. Semiconductor lasers are the finest applications of the latter. They allow



highly efficient sources of coherent light emission and have opened a vast number of possible application of lasers.

Interaction between light and matter is ensured when an emitter or detector is constructed. Light is mostly treated using the Maxwell's equations whereas quantum theory is essential in the study of matter. The laser dynamics is understood in its totality only by using the quantum optical treatment of the various physical phenomena involved in the production of light [2, 3, 4]. A single photon traveling through a semiconductor is able to generate an identical photon by stimulating the recombination of an electron-hole pair. This photon multiplication is the key physical mechanism of lasing. Laser diodes with wavelength constraints such as vertical cavity surface emitting lasers (VCSELs) [5] and distributed feedback (DFB) laser diodes are currently of considerable interest because of their ability to be integrated in more than one dimension.

Semiconductor lasers exhibit many unique features in both functions and performances and also offer economical advantages. Therefore, by the development of semiconductor lasers, lasers, which had been a special instrument for scientific research and limited applications, acquired a position as a device for general and practical instruments. As will be outlined below, the applications of semiconductor lasers cover a wide area, including optical communications, optical data storage and processing, optical measurement and sensing, and optical energy applications.

In semiconductor microstructures of nanometer size, the behavior of electrons is strongly affected by the quantum nature of the electron and exhibits a remarkable dependence on the parameters specifying the structure. Therefore, by appropriate design of the structure parameters, one can implement artificial novel electronic properties unlike the intrinsic characteristics of the bulk materials [3, 6]. Recent advanced techniques for crystal growth have enabled precise fabrication of such quantum structures, and these quantum structures have offered very effective and attractive possibilities for improvement in semiconductor laser performances [7, 8]. This chapter presents the fundamental theory of the quantum well (QW) as the most important quantum structure and the optical amplification by stimulated emission in it.

## 2.2 Physics of Low Dimensional Structures

It is the marvel of modern technological advances that the principles of quantum mechanics and quantum optics found applications in daily life through the successful fabrication of devices such as multiple quantum well lasers and quantum cascade lasers. The progress of solid state physics and materials science in the last three decades is characterized by the

gradual displacement of bulk crystals by thin films, multi-layered structures and similar low dimensional structures as the main objects of study. In these systems, most electronic properties are considerably different and a number of new, so-called size effects occur. The most dramatic change of properties takes place in quantum size structures where carriers are confined in a region with characteristic size of the order of the *de Broglie* wavelength. In this case the quantum mechanical laws come into action, changing the most fundamental characteristic of an electron system - its energy spectrum.

Quantum dots, wires, and wells are semiconductor structures that have carrier confinement - of both electrons and holes - in three, two and one dimensions, respectively. Although each of these structures reveal a world of study itself, we will stick on to the quantum well structures as they are the ones that find application in modern systems and devices that works on the principles of optoelectronics.

### 2.2.1 Quantum Wells

The *de Broglie* wavelength of electrons in a very thin (less than a few tens of nanometers) semiconductor film structure is comparable with the thickness of the film. In such a structure, electrons exhibit interesting electric and optical characteristics dissimilar to those in bulk semiconductors and ordinary double heterostructures (DHs). The most fundamental semiconductor quantum heterostructure is a single quantum well (SQW), which consists of a very thin layer of a semiconductor sandwiched between two layers of a semiconductor having a bandgap energy larger than that of the thin layer. The conduction- and valence-band edges of this structure form potential wells, as shown in Fig. 2.1.

Once miniaturization reaches the quantum limits in one dimension, a “two-dimensional electron gas” is created, which we shall call “quantum well” (QW). In such structures, under the influence of external fields and scatterers, such as photons, impurities, etc., only two, rather than three, components of carrier momentum can change. As a result, the carrier behaviour reminds one of that of a two-dimensional gas, even though the system has finite extent along the confining coordinates.

A quantum well in our context refers to a well like potential formed from a semiconductor heterostructures such as epitaxially grown thin layers of *GaAs* and *AlGaAs* [1, 9, 10, 11, 12]. Such wells have two-dimensional density of electron states for low-energy electrons. Such wells often form the active region of a semiconductor laser diode. The small volume of the quantum well reduces the current needed to achieve lasing and offers higher differential optical gain compared to bulk laser diodes.

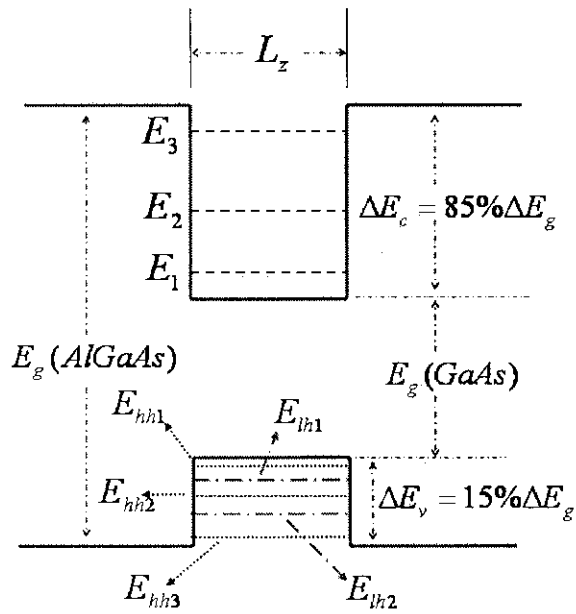


Figure 2.1: Square well potential that is typical of *AlGaAs–GaAs–AlGaAs* quantum-well heterostructure. For well thickness  $L_z \lesssim \lambda_{dB}$ , size quantization occurs and results in a series of discrete energy levels marked by the bound state energies of a finite square well. A potential well exists in both the conduction and valence bands giving rise to a series of bound states  $E_n$  for the electrons,  $E_{hhn}$  for heavy holes and  $E_{lhn}$  for light holes.

## 2.3 Quantum Well Lasers

Quantum well lasers with reduced dimensionality offer lower threshold currents, large gain and lower temperature stability than conventional double heterostructure lasers [4]. The two-dimensional character of the charge carrier gas causes a change in the density of states (DOS), the fundamental origin of improved operation characteristics like low threshold currents and lower temperature sensitivity. Use of quantum well(s) as an active layer allows implementation of quantum well lasers offering performances better than those of ordinary DH lasers. However, mere reduction in the active layer thickness of a DH laser to form a SQW or MQW structure does not lead to realization of high performances, since the resultant quantum well (QW) is too thin in comparison with the optical wavelength to ensure strong optical confinement, and therefore a high effective gain for the guided wave cannot be attained. Another problem is that it is not easy to attain a high efficiency of carrier injection in MQW structures having many heterojunctions, and the carriers injected in the thin QW may leak, thereby reducing the effective carrier injection efficiency. To overcome these problems and to implement high-performance quantum well lasers, various improved structures have been developed. They are separate-confinement heterostructures (SCHs), consisting of the QW active layer for carrier confinement and a refractive index structure for optical confinement outside it, and their modifications.

The most important factor influencing the laser characteristics is the change in the density of states due to size quantization. If in a bulk semiconductor the density of states near the band edge is small, then in a quantum size structure it does not vanish near the edge, but instead remains equal to  $m/\pi\hbar^2$ . Because of this fact, the conditions for population inversion in two-dimensional systems can be met more easily than in three-dimensional systems [12].

This has resulted in some particular applied results. The design of lasers with a size-quantized active region has enabled stationary laser generation at room temperature as well as decrease in the threshold current of the injection lasers reaching extremely low values of less than  $50 \text{ A/cm}^2$ .

The different energy dependence of the density of states changes not only the value but also the temperature dependence of the threshold current. The temperature dependence becomes weaker, which results in the possibility of CW laser generation not only at room temperature, but at temperatures several tens of centigrade higher.

Another important peculiarity of quantum well lasers is the possibility of frequency tuning. The minimal energy generated quanta is equal to

$$\hbar\omega = E_g + E_{Q1}^c + E_{Q1}^h, \quad (2.1)$$

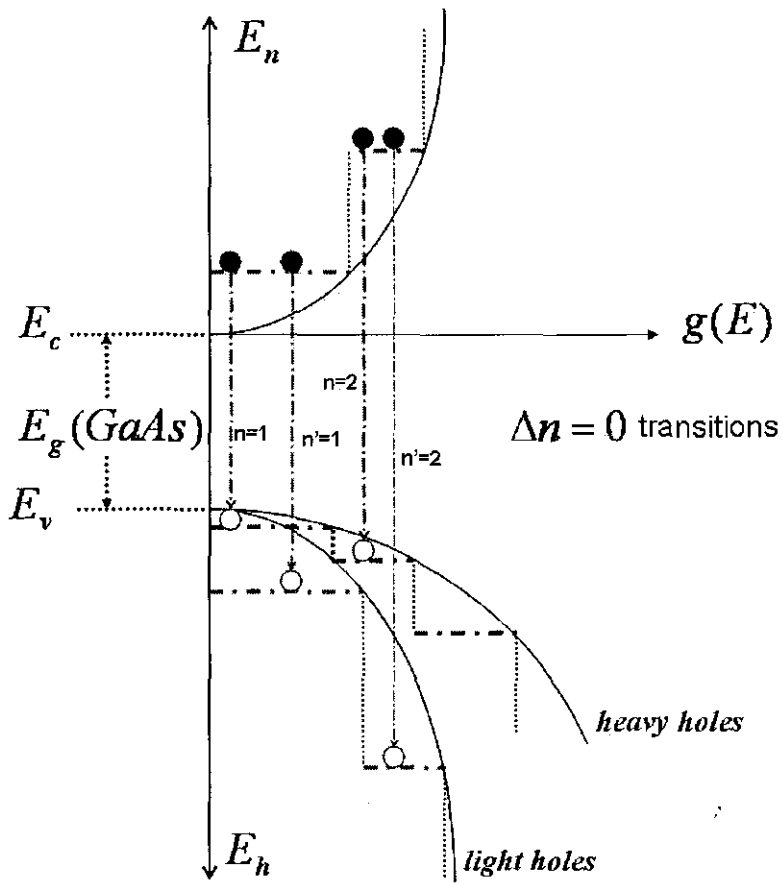


Figure 2.2: Density of state for electrons  $E_n$  and  $E_h$  for a  $AlGaAs - GaAs$  quantum-well heterostructure. The half parabolas that originate from the conduction and valence band edges represent the densities of states for bulk structures. The step-like states are characteristic of the two-dimensional electron (hole) gas in the quantum-well structure. Inter-band recombination transitions ( $\Delta n = 0$ ) occur from a bound state in the conduction band  $E_n$  to a bound state in the valence band  $E_{h'n}$  or  $E_{lh'n}$ .

and can be changed by changing the film thickness  $L_z$ , which determines the energy separation of the quantum states in the electronic and hole-like state. According to quantum mechanics we have  $E_{Q1} \simeq \hbar^2/2m_e^*L_z^2$ .

The density of states in the  $k$ -plane is  $\rho_{e,h}(k)dk = kdk/2\pi^2$  and can be converted into an energy density with  $dE = \hbar^2k/m_{e,h}^*dk$ . In the transverse direction each quantum state (energy  $E_{Qi}^{e,h}$ , for quantum number  $i$ ) contributes with the density  $\pi/L_z$ ,

$$\rho_{e,h}(E)dE = \sum_i \frac{m_{e,h}^{*i}}{\hbar^2 L_z} \Theta(E - E_{Qi}^{e,h}). \quad (2.2)$$

The *theta function* has the values  $\Theta(x) = 1$  for  $x > 0$  and  $\Theta(x) = 0$  for  $x \leq 0$ . Also, the effective masses  $m_{e,h}^{*i}$  may depend on the quantum number. The density of state grows step-like, as shown in FIG. 2.2, in a quantum well every time the energy reaches a new transverse quantum state. There it has exactly the value corresponding to the bulk material.

Typical quantum wells are rather shallow, which causes the wave function to penetrate into the barrier region [3, 1]. The distance of the energy levels shrinks with lower barriers; however, the parabolic dependence on effective mass is maintained. The actual potential widths  $\Delta E_c$  and  $\Delta E_v$  of semiconductor wells are critical parameters in the device simulations but they often are not exactly known.

## 2.4 Multiple Quantum Well Lasers

Very often, many-layered heterostructures with large number of periodically repeated similar wells are grown instead of a single well. Depending on the thickness of the wide-gap layers, these structures can be divided into two types. For energy barrier thickness  $L_z \geq 100\text{\AA}$ , the tunnel transparency of barriers is low, neighbouring wells do not influence each other and the effect of each well are simply added. Such structures, called multiple quantum well structures (MQW), are used for amplification of the effects observed. At smaller barrier energy thickness the energy spectrum of the system changes. The possibility of inter-well tunnelling transition leads to the transformation of quantum size levels into bands, as takes place for atomic levels in crystals. This results in the formation of completely new structures called superlattices. Their properties differ from single quantum wells and they are used to make detectors and sources such as the quantum cascade laser.

Multiple quantum well (MQW) laser diodes are widely used in many applications because of their superior performance characteristics over bulk laser diodes. The modified density of states due to confinement in a quantum well laser causes lower threshold currents since

fewer states per charge carrier are available, which can consequently be filled with lower currents. Typically threshold current densities of  $5 - 100 \text{ Acm}^{-2}$  are achieved. The lower threshold indirectly improves again the temperature sensitivity since there is less excess heat generated in the heterostructures.

The differential gain of a MQW laser is larger than that for the double heterostructure (DH) lasers since the electrically dissipated powers growing with the current causes a lower reduction of the gain. Also, the threshold condition depends less strongly on the temperature. For conventional DH lasers the transparency threshold grows with  $T^{2/3}$ , in quantum well lasers only in proportion to  $T$ . The characteristic temperatures according to the empirical relation [4]:

$$I_{th} = I_0 \exp\left(\frac{T - T_0}{T_0}\right) \quad (2.3)$$

are about  $200K$ .

## 2.5 Dynamics of Quantum Well Lasers

To understand the operation of a semiconductor laser diode, we need to develop a model. A general model is obtained by setting up the Maxwell-Bloch equations[10, 13], an attempt to model the laser dynamics using a semi-classical approach. Lang and Kobayashi [14] formulated the theoretical framework to study semiconductor lasers with optical injection. However, the simplest and one of the most effective approach is to use rate equations. The standard multimode rate equation for semiconductor lasers is based on the approximation that modal field shapes depend on the instantaneous value of the time-dependent dielectric function. This is known as the adiabatic approximation [15]. It will break down if the inverse of the modulation frequency approaches the photon round-trip time in the cavity. [16]. Multimode rate equation model can be, further, simplified by assuming that the laser operates in a single mode and that all photons are confined to the particular mode. This model, which is much simpler, is very effective in predicting the laser output behaviour and connects physical concepts with engineering realities very well.

Depending upon the basic assumptions that we use before modeling, the rate equation model can be single mode or multi-mode equations. If we assume that there can be lasing into only one optical mode of frequency  $\omega_s$ , we can utilize this fact to make our model more compact. In this case our calculations will not incorporate any variation in optical gain, optical loss, or carrier density along the longitudinal ( $z$ ) axis. This lumped-element model, further, assume that the conduction-band and valence-band electrons have the same density

and that they are thermalised so that they may be characterized by a single temperature as we have discussed in section 2.3. Further, we will adopt simple but effective approximations for gain, spontaneous emission, and nonradiative recombination. When considering the rate equations one needs to be very careful to define the parameters used because it is easy to become confused and make an error. The challenge is to find the exact role of each parameter and variable used, and never to omit some quantity of importance.

### 2.5.1 Criteria for Modeling Quantum Well Lasers

One of the earliest models for the multiple quantum well structures were developed by Rideout *et al.* [17] based on the well barrier (W-B) hole burning model. Nagarajan *et al.* [18] have developed a two-level ambipolar rate equation extension of the W-B hole burning model. Successive works found that the two-level model is inadequate to model the system very well and McDonald *et al.* [19] developed the full three-level ambipolar rate explicitly considering the gateway states. The work was an extension of two-level models proposed earlier.

The cavity photon density, photon lifetime, and the differential gain are considered to be the critical factors in the design of high-speed semiconductor lasers. In addition, a gain compression term,  $\epsilon$ , whose physical origins have been attributed to various phenomena such as spectral hole burning [20], transient carrier heating [21], and cavity standing wave dielectric grating [22], has been used together with rate equations for the carrier and photon density in the cavity to model the modulation dynamics of semiconductor lasers. Following this procedure, high-speed laser design meant designing lasers with tight optical mode confinement for higher photon densities, short cavity length for shorter photon lifetimes, and quantum well active areas which could in addition to be strained or *p* doped for higher differential gain.

In addition to the set of criteria listed above, it is also critically important to minimize the threshold carrier density to maximize the differential gain, and reduce the carrier transport times across the separate confinement heterostructure and the barrier layers, in order to maximize the modulation bandwidth of a quantum well laser. It has been shown that  $\epsilon$  of comparable magnitude as in lasers with bulk active areas is adequate to model the dynamics of quantum well lasers [18]. Carrier transport factors, low confinement factor, and low differential gain all contribute in reducing the modulation bandwidth of the quantum well lasers. Thus, it is imperative that transport properties have a significant effect on the modulation dynamics of quantum well lasers. The dynamics of the laser is dominated by the transport times of the slower carrier type when electrons and holes are injected from the



opposite ends of the separate confinement heterostructure.

In the case of an LED, the carrier relaxation time  $\tau = 1/(b + c)$  gives the average time required for electrons in the excited state to decay to the ground state through processes of spontaneous emission (the “b” term) and nonradiative collisions (the “c” term) [2]. The population decays according to  $e^{-1/\tau}$ . The laser modulation rate is of the order of  $\nu = 1/\tau = 1 \text{ GHz}$ . In a semiconductor laser the stimulated emission forces the carrier to recombine in addition to the carrier relaxation. Stimulated emission process in a semiconductor laser lowers the carrier lifetime and thereby effectively increase the modulation rate.

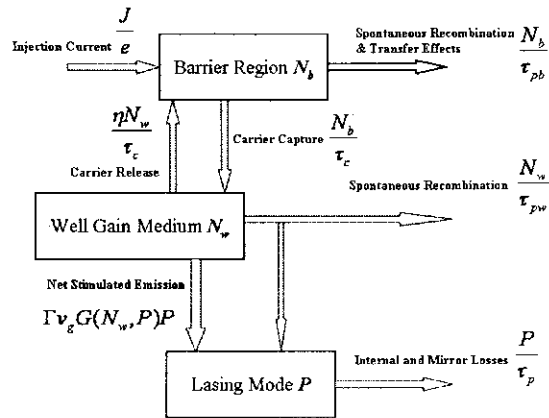


Figure 2.3: Conservation chart for the W-B hole burning model indicating the dominant rate processes for the W-B model.  $\tau_{pb}$  and  $\tau_{pw}$  stands for the carrier leakage times from the barrier and well, respectively.

## 2.5.2 Carrier Transport in Quantum Well Structures

A great deal of experimental work has been done to study carrier transport in QW lasers. This work consists mostly of time-resolved photoluminescence experiments, pump probe experiments, and modulation response measurements [23]. These experiments are designed to study the high-speed dynamics of carriers in QW lasers. Of key interest in this field are transport times across the heterostructure and carrier capture rate into the QW's as these two factors play a fundamental role in the high-speed characteristics of QW laser devices.

Electrical current flow in semiconductors is mainly dominated by drift and diffusion of electrons and holes. Drift current is generated by an electric field which is proportional to

the conductivity of electrons and holes. Diffusion current is driven by the concentration gradient of electrons  $\nabla n$  and holes  $\nabla p$ . It is proportional to the diffusion coefficient  $D_n$  and  $D_p$  respectively [1].

The phenomenological description of lasing in a semiconductor laser is complete once the carrier density  $n$  is related to the pump parameter, the current density  $J$ . This is accomplished through a rate equation that incorporates all the mechanisms by which the carriers are generated and drift inside the active region. In general, the continuity equations for both electrons and holes should be considered. The two are interrelated because of charge neutrality, and it suffices to consider one rate equation for for electrons. In its general form, the carrier–density rate equation is [1, 13, 24]

$$\frac{\partial n}{\partial t} = D(\nabla^2 n) + \frac{J}{qd} - R(n). \quad (2.4)$$

The first term accounts for carrier diffusion, and  $D$  is the diffusion coefficient. The second term governs the rate at which the carriers, electrons or holes, are injected into the active layer because of the external pumping. The electron and hole populations are assumed to be the same to maintain charge neutrality. In the second term,  $q$  is the magnitude of the electron charge and  $d$  is the active-layer thickness. Finally, the last term  $R(n)$  takes into account the carrier loss due to various recombination processes, both radiative and nonradiative. A rigorous derivation of Eqn. 2.4 has to be based on the density-matrix approach.

In order to apply the rate equation analysis to quantum well lasers, the photon lifetime  $\tau_p$ , the photon density  $S$ , and output power  $P$  must be expressed by using the device parameters of quantum well lasers. The threshold gain  $g_{th}$  of a DFB laser calculated is given in the form of the net gain for the guided mode. The threshold gain  $G_{th}$  for use in the rate equations is expressed in the form of a temporal material gain  $G$ , and  $g_{th}$  and  $G_{th}$  are correlated to each other by [3]

$$g_{th} = \frac{\Gamma G_{th}}{v_g} - \alpha_{int}, \quad (2.5)$$

where  $\Gamma$  is the confinement factor and  $\alpha_{int}$  the internal loss. Group velocity of the guided mode is represented by  $v_g$ . The optical wave in the laser cavity (waveguide) can be written as

$$E(x, y, z; t) = E(x, y)E(z)e^{-i\omega t}e^{-\gamma t}, \quad (2.6)$$

where  $E(z)$  is the component in the direction of propagation. This equation indicates that the power in the resonator decays with time in a form of  $\exp(-2\gamma t)$ . If there is no optical

power source, the optical wave can exist only in such a form that the power stored in the resonator in the past is consumed and attenuates with time. We define the photon lifetime  $\tau_p$  as  $2\gamma = 1/\tau_p$ , the time for which the power in the resonator decays to  $1/e$  times the initial value, and is an important parameter for the rate equation analysis of semiconductor lasers [3].

### 2.5.3 Well-Barrier Hole Burning Model

It is also found that the conventional single mode rate equations fail to explain the resonance characteristics profoundly, because of non inclusion of factors such as spatial and spectral inhomogeneities. Hence well barrier hole burning model is introduced to incorporate the effects contributing to non linear gain [25]. MQW bistable lasers are normally analysed by numerically solving the single mode rate equations [26]. The modulation response of semiconductor lasers is determined by an intrinsic dynamic resonance in the nonlinear photon-carrier interaction, and the conventional single-mode (S-M) rate-equation model predicts improved resonance characteristics with enhanced differential gain. On that basis alone, lasers containing single QWs, many uncoupled QWs, and strained QWs should show progressive levels of improvement. However, so far such expectations have neither been realized nor verified satisfactorily, inasmuch as the resonance frequencies and damping rates inferred from recent parasitic-free experiments vary widely [27]. Evidently, factors such as spatial and spectral inhomogeneities not taken fully into account by the conventional model affect the resonance characteristics profoundly.

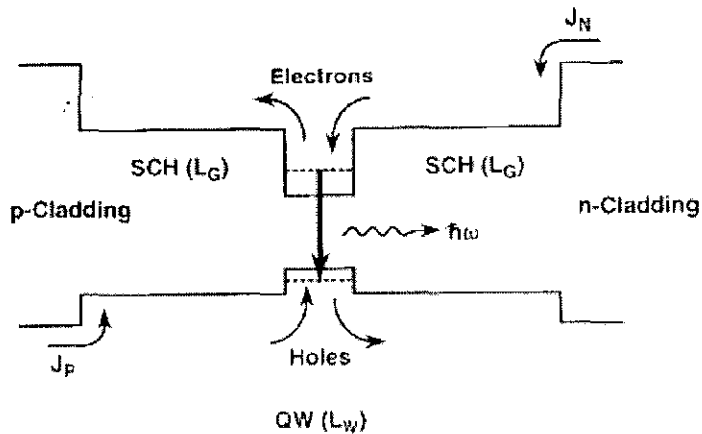


Figure 2.4: Schematic diagram of perpendicular carrier transport in a prototype *InGaAs-GaAs* QW laser illustrating the capture and release processes for electrons and holes. The potential profile shows the relative positions of the *n*- and *p*-*AlGaAs* cladding layers, the *GaAs* SCH layers of thickness  $L_G$ , and the *InGaAs* QW layer of thickness  $L_W$ .

The well-barrier hole burning model, proposed to explain observed large damping in certain QW lasers, incorporates certain features of the spatial inhomogeneities in perpendicular carrier transport (i.e., transport along the growth axis of the quantum wells). As Fig. 2.4 illustrates schematically, after injection, electrons and holes diffuse and drift through the separate-confinement-heterostructure (SCH) region to within a few hundred Angstroms of the QW where, among other possibilities, they may be captured quantum mechanically by the QW's. At the high injection levels required for lasing, the densities of electrons and holes in excess of equilibrium values are approximately equal, and the diffusion-dominated regions spread away from the contacts throughout the entire intrinsic region. Thus jointly, these excess densities play the role of an effective mobile carrier density for ambipolar transport (with ambipolar-averaged rate constants) across the p-i-n region of the device. W-B hole burning is argued to result from the buildup of this mobile carrier density in the SCH regions during capture and release of carriers by the quantum wells.

The W-B model treats the carriers in the barriers (i.e., in the continuum states of the SCH regions) and wells (i.e., in the localized subband states of the wells) as separate species with average densities,  $N_B$ , and  $N_W$ , respectively, and focuses attention on the capture process. The transport and trapping dynamics of carriers across semiconducting heterostructures are not yet fully understood [28].

The W-B model postulates that the photon-carrier resonance results from the coupled nonlinear interaction between a photon reservoir of density  $S$  and two carrier reservoirs: a collector with density  $N_b$ , and a gain reservoir of density  $N_B$ , and a gain reservoir of density  $N_W$ . As suggested by the conservation chart in Fig. 2.3, the collector receives carriers remotely from the pump current source, loses carriers to the environment by spontaneous recombination in the barrier region, and supplies carriers as needed to the gain reservoir. The gain reservoir captures and releases carriers from and to the collector reservoir, and loses carriers by spontaneous emission into the lasing mode, as well as by spontaneous recombination to the environment. The photon reservoir loses photons by internal and mirror losses in the lasing cavity. The gain medium and photon reservoir interact via stimulated absorption and emission. We emphasize two significant features of the W-B model: that the well region is the only gain medium; and that the model supports three phase-space dimensions (associated with two carrier densities and the photon density) *vis-a-vis* the two dimensions of the S-M model. Since the well region is the only gain medium, the carriers in the barrier region interact only indirectly with the lasing mode via their coupling to carriers in the wells.

The conservation chart (Fig. 2.3) contains the essential rate processes for the nonlinear rate equations described below.

### 2.5.4 Nonradiative Recombination and Carrier Overflow

Decay mechanisms through which electrons in a given energy state can decay out of that state are broadly divided into two categories corresponding to the *intraband* and *interband decay* mechanisms [13]. *Intraband processes* in a semiconductor laser constitute of electron-electron scattering and the electron-phonon scattering, and occur at fast time scale of  $\sim 0.1$  ps. By contrast, *interband processes* occur at a time scale of few nanoseconds; they consist of radiative recombination leading to spontaneous and stimulated emissions as well as nonradiative recombination. In long wavelength semiconducting lasers an important source of nonradiative recombination is the *Auger process*, as discussed in this section.

Some of the injected minority carriers are consumed in the active layer by the nonradiative recombination without photon emission. This gives rise to a factor that causes the internal quantum efficiency for spontaneous emission to deteriorate. Although the nonradiative recombination includes recombination due to lattice defects and recombination due to impurities, and also recombination at the interfaces of the heterostructure, it is negligibly small for ordinary lasers that use high-quality crystals. More important and essential nonradiative recombination is that caused by the Auger processes [1, 13, 29]. Collision of two electrons and one hole resulting in recombination of one electron and the hole, and excitation of another electron with the energy released by the recombination up to a higher level in the conduction band, and collision of two heavy holes with one electron resulting in similar recombination and excitation. The excited carriers give energy to the crystal lattice in the form of heat and return to the unexcited level. Since both energy conservation and momentum conservation must hold also for the Auger process, recombination occurs with carriers at energies apart from the band edge. Accordingly, the recombination rate  $R_A$  exhibits a remarkable temperature dependence and bandgap energy dependence;  $R_A$  is larger for a narrow bandgap and a high temperature. Since the process is a collision of three particles, the carrier density dependence of  $R_A$  can be phenomenologically written as [3]

$$R_A \approx C_n n^2 p + C_p n p^2 \approx C n^3, \quad (2.7)$$

where  $C_n$ ,  $C_p$ , and  $C$ , are constants with  $n \approx p$ . While the Auger recombination is usually negligibly small for lasers for short-wavelength emission, it is an important factor that significantly affects spontaneous emission in lasers for long-wavelength emission. The Auger recombination can be reduced by using strained quantum well structures.

Another important factor that causes the emission efficiency to deteriorate is the overflow of minority carriers injected in the active layer into the region opposite to the injection side, which gives rise to additional current without contribution to the laser action. The

magnitude of the overflow current can be evaluated by calculating the carrier density at the boundary between the active and barrier regions under the assumption that the quasi-Fermi level is continuous across the boundary, and solving the carrier diffusion equation in the barrier region with the use of the boundary value. The overflow is larger for lower barrier heights and higher temperatures. The current consists of diffusion current and drift current with the ratio dependent on the thickness and the resistivity of the barrier region. In many lasers the overflow can be suppressed to a negligible value by appropriate design. For short-wavelength lasers where it is difficult to assure sufficient barrier height, and for laser operation at elevated temperatures, the overflow can be an important factor that limits the performances.

### 2.5.5 Optical Cavity

We exploit the existence of optical gain in a semiconductor to make a laser diode. One might imagine constructing a  $p-n$  diode out of a direct band-gap semiconductor such as *GaAs* or *InGaAsP*. When forward-biased to pass a current,  $I$ , electrons are injected into the conduction band and holes into the valence band. The optically active region of the semiconductor is where the electrons and holes overlap in real space, so that vertical optical transitions can take place in the momentum space ( $k$ -space) [11]. If the density of carriers injected into the active region is great enough, then it satisfies the Bernard-Duraffourg condition [30] that the separation in quasi-chemical potentials electronic states at upper and lower energy states must be greater than the photon energy for net optical gain to exist. This implies that optical gain exists for light at some wavelength in the semiconductor. There is, however, more to designing a useful device. Among other things, we would like to ensure that a high intensity of lasing light emission occurs at a specific wavelength.

Typical value of gain for an optical mode in a semiconductor laser diode is not very large ( $\sim 500 \text{ cm}^{-1}$ ), and therefore, in order to precisely control emission wavelength, one typically places the active semiconductor in a high-Q optical cavity. This cavity has the effect of storing light at a particular wavelength, allowing it to interact with the gain medium for a longer time. In this way, relatively modest optical gain may be used to build up high light intensity in a given optical mode. Electrons contributing to the injection current  $I$  are converted into lasing photons that have a single mode and wavelength. The efficiency of the conversion process is enhanced if only one high-Q optical-cavity resonance is in the same wavelength range as semiconductor optical gain.

### 2.5.6 Fabry-Perot Lasers

In our MQW laser models, the most widely employed cavity structures are the Fabry-Perot optical cavity, which is arguably the simplest, and the distributed feedback (DFB) cavity employing periodic stacks of dielectric mirrors. The former consists of an index-guided active region placed within a Fabry-Perot optical resonator. Assuming that the photons travel normal to the two mirror planes and in the  $z$ -direction, the expression for the spectral range of corresponding longitudinal optical resonances will be

$$\Delta\omega = \frac{c\pi}{L_c n_r}, \quad (2.8)$$

where  $n_r$  is the refractive index of the dielectric,  $L_c$  is the length of the cavity, and  $c$  is the speed of light in vacuum. The mode confinement factor  $\Gamma$  is calculated from the spatially varying dielectric constant in the cavity,  $\epsilon(x, y)$ , which is obtained as a solution of the time independent Maxwell's equations assuming no free charge and an electromagnetic wave traveling in the  $z$ -direction:

$$\nabla^2 E + \epsilon(x, y)k_0^2 E = 0. \quad (2.9)$$

by assuming that  $\epsilon(x, y)$  varies slowly in the  $x$ -direction compared with the  $y$ -direction and by adopting the effective index approximation. Finally, one can definitely say that it is the cavity formation that makes a laser different from a light emitting diode (LED). Multiple round trips are necessary to approach steady-state laser characteristics that are independent of laser injection current [11].

### 2.5.7 Distributed Feedback Lasers

In many applications, such as optical communications and measurements, semiconductor lasers that maintain stable and pure single-mode oscillations even under high-speed modulation are required. FabryPerot (FP) lasers cannot satisfy this requirement. Therefore, various types of dynamic single mode semiconductor lasers have been developed. Such lasers are mainly classified into distributed feedback (DFB) and distributed Bragg reflector (DBR) lasers, which maintain stable single-mode oscillation even under high-speed modulation [3]. They are suitable for monolithic integration and accomplishing advanced functions and performances. We have, therefore, mostly used the MQW lasers with DFB configuration in our studies leading to this thesis.

We can achieve dynamic single-mode oscillation by giving the oscillation threshold gain a sharp mode selectivity to prevent oscillation of modes except for a single mode. One of the

simplest methods is to combine a FP laser with an external mirror, thereby constructing of a composite resonator consisting of the two facet mirrors and the third external mirror. One of the laser waveguide FP modes that coincides with one of the resonance frequencies for the facet and the external mirror oscillates [31].

If we integrate a grating with sharp wavelength selectivity as a feedback element in a semiconductor laser waveguide, dynamic single-mode lasers can be implemented without spoiling the compactness of semiconductor lasers [32, 33, 34]. This type of semiconductor laser is classified as a distributed feedback (DFB) laser using a grating within the active section (carrier injection section), and a distributed Bragg reflector (DBR) laser using a grating outside the active section. Although the fabrication of these lasers requires advanced techniques, they can offer excellent performances including dynamic single-mode oscillation. The DFB and DBR configurations are suitable for implementing advanced devices such as wavelength-tunable lasers. They do not require facet mirrors, and this unique feature facilitates monolithic integration of lasers and other optical elements, such as photodetectors and passive elements, in a semiconductor waveguide. With these advantages, DFB and DBR lasers are the most important components for implementation of various photonic integrated circuits. All the above mentioned features make us to concentrate more on DFB lasers available in modern laser systems vital to long distance optical communication.

We can see that DFB lasers have specified device parameters more than those of FP lasers, and the operating characteristics have complex dependencies on them. As presented above, the oscillation condition for DFB lasers is significantly different from that of FP lasers. They have unique longitudinal mode characteristics and oscillate in a single longitudinal mode. However, many of the operating characteristics are common to those of FP lasers, as they are described by rate equations similar to those of FP lasers.

Also, for ordinary single-quantum-well and multiple-quantum-well structures, the TE gain is significantly larger than the TM gain. Strained quantum wells can be designed so as to have a larger gain for a TE mode or a TM mode. Therefore, DFB lasers with a high polarization extinction ratio can be implemented by using a SCH structure with a quantum well active region and an appropriately designed grating.

We can see that quantum well DFB lasers having a high relaxation oscillation frequency and a small line width enhancement factor ( $\alpha_e$ ), in particular, single-mode high-speed modulation above 10 GHz is possible [20], and frequency chirping is small. Because of these excellent characteristics, quantum well DFB lasers are most suitable as a light source for high-speed optical fiber communications.



## 2.6 A Rate Equation Model for Directly Modulated MQW Laser Diodes

In a multiple quantum-well (MQW) laser the carrier density is not generally the same in each quantum-well (QW). The distribution of carriers in the QW's can profoundly affect device operation and is crucial to the understanding of MQW devices [35, 36, 37, 38, 39, 40]. The carrier distribution in MQW devices has been studied both experimentally and theoretically in the past [38, 39, 40].

Based on all the details above, we choose the three level multiple quantum well laser model proposed by Bennet *et al.* [41] which is a modified version of the model put forward by Nagarajan *et al.* [18]. Carrier densities in the core (barrier) region ( $N_c$ ) and the well region ( $N_w$ ) influence the photon number density  $N_p$  in the active region as according to the following set of equations:

$$\frac{dN_c}{dt} = \frac{\Gamma_q I}{eV} - \frac{N_c}{\tau_c} + \frac{\Gamma_q N_w}{\tau_e} \quad (2.10)$$

$$\frac{dN_w}{dt} = \frac{N_c}{\Gamma_q \tau_c} + N_w \left[ \frac{1}{\tau_n} + \frac{1}{\tau_e} \right] - v_g G(N_w, N_p) N_p, \quad (2.11)$$

$$\frac{dN_p}{dt} = \left[ \Gamma v_g G(N_w, N_p) - \frac{1}{\tau_p} \right] N_p + \Gamma \beta B N_w^2, \quad (2.12)$$

where  $\Gamma_q$  is the fraction of the MQW region filled by the quantum wells.  $\Gamma$  is the mode confinement factor of the laser, defined as

$$\Gamma = \frac{\int_{-L_z/2}^{L_z/2} |E|^2 dz}{\int_{-\infty}^{\infty} |E|^2 dz} \approx \frac{L_z}{W_{mode}}, \quad (2.13)$$

where  $L_z$  (usually  $< 100 \text{ \AA}$ ) is the height of the active region, and  $W_{mode}$  is the width of the EM mode [10]. When the optical mode is effectively confined to the active region, the gain scales as  $L_z^{-1}$ , which is due to the fact that as the optical density, for a fixed total power, in guided mode, goes as  $L_z^{-1}$ , so the stimulated emission emission rate and hence the gain scale similarly. As long as  $\Gamma \sim 1$ , that is most of the mode energy is in the active region, the gain  $G(N_w, N_p)$  is inversely proportional to the active region thickness  $L_z$ .

### 2.6.1 Gain Calculation

We have observed that a precise theory for conventional double heterostructure lasers, which explains many of the observed properties well, has been developed taking into account the electronic intraband relaxations. Such a theory is necessary for quantum well lasers as well, since the intraband relaxation is particularly important for quantum well lasers with narrow gain spectrum since the gain spectrum is broadened due to this intraband relaxation. The gain  $G(N_w, N_p)$  is obtained by careful theoretical analysis as trial and error optimization of the multi-quantum-well(MQW) laser structure is both costly and time consuming since there are innumerable possible combinations of optical confinement structure, well width, well number, and cavity length, only a few of which lead to useful devices [42]. The linear gain of quantum-well lasers, taking into account the effects of the intraband relaxation can be written as [42, 43]

$$g(h) = \frac{Z_0 m_r}{\mu \pi \hbar^2 L_z} \sum_{n, n'} \int_{E_{cn} + E_{vn'} + E_g}^{\infty} \langle R_{ch}^2 \rangle \frac{(f_c - f_v) \Delta E d E_{ch}}{(E_{ch} - \hbar \omega)^2 + \Delta E^2} \quad (2.14)$$

where  $Z_0 = (\mu_0/\epsilon_0)^{1/2}$  is the free space impedance,  $\tau = h/\Delta E$  is the intra-band scattering time,  $E_{ch} = E_c - E_v$  is the transition energy,  $E_{cn}$  and  $E_{vn'}$  are the  $n^{th}$  and  $n'^{th}$  energy levels of the electron and hole quantum wells, respectively, and  $f_c$  and  $f_v$  are the corresponding Fermi factors.  $L_z$  is the well width,  $R_{ch}$  is the interband matrix element (set to zero for  $n \neq n'$ ),  $\langle x \rangle$  denotes the average of  $x$  taken over the polar angle  $\phi$ ,  $\mu$  is the effective refractive index, and  $E_g$  is the semiconductor band gap. The Fermi levels are calculated assuming bimolecular recombination and equal carrier concentrations ( $n = p$ ), i.e., assuming current density  $J = e L_z B_{eff} n^2$ . Using the above equation, we can calculate the gain of a single well as a function of frequency and current and apply to the MQW laser model for optimization.

The most important design parameter of the MQW laser is the number of wells. The optimum number depends on the required gain at threshold. If the total active width is small (less than - 1000 Å) and a separate confinement heterostructure (SCH) is used, then numerical calculations show that the optical confinement factor  $\Gamma$  is approximately proportional to the total number of wells. We therefore use this as the starting point of our model, and make the explicit assumption that  $J$  is directly proportional to the number of wells for a limited range of conditions, which we shall later define. Based on these assumptions, the function  $G(N_w, N_p)$  is deduced from Eqn. 2.14 as [41, 42]

$$G(N, P) = \frac{G_0}{(1 + \epsilon P)} \ln \frac{N}{N_0}, \quad (2.15)$$

where  $\epsilon$  is the nonlinear gain compression factor.  $N_0$  is the transparent carrier density, and

$G_0$  is the gain parameter dependent on the well structure. The carrier recombination rate  $R(N)$  is expressed by the truncated power series fit to inverse differential carrier lifetime ( $1/\tau_n = \partial R/\partial N$ ) measurements by [3, 19]

$$R(N) = AN + BN^2 + CN^3, \quad (2.16)$$

where A, B, and C are the mono-molecular, bi-molecular and Auger recombination coefficients which we discussed in preceding sections.

In conclusion, we have discussed the basic physics and related device parameters that leads to a successful model in studying the multiple quantum well structures. It is shown that transport mechanisms in the structure play an important role in the carrier-photon coupling within the cavity and their dynamics. The basic rate equation model for the QW laser and the need for the well-barrier hole burning model have been discussed in detail. A detailed account of the parameters involved in the laser rate equation model with due emphasis on their physical origin, and their role in determining the dynamic features of the laser, which is the major topic of discussion of this thesis will be presented in the coming chapters. We have also presented the justification in choosing the DFB configured MQW laser because of its advantages over F-P lasers.

## 2.7 Scope of this Thesis

As we have discussed in this chapter, laser diodes represent a key element in the field of optoelectronics. For all applications, information is either transmitted, stored or read out. The performance of these systems depends to a great deal on the performance of the laser diode with regard to its modulation and noise characteristics. Since the modulation and noise characteristics of laser diodes are of vital importance to optoelectronic systems, the work in the thesis mostly concentrate on the modulation characteristics of the modern day laser system made up of multiple quantum well structures. A second interest in these less studied systems arises due to their potential application in one of the modern findings in communication, that is chaotic encryption.

In a chaotic modulation scheme, the chaotic oscillator in the drive end is directly modulated by the information signal. We have investigated the possibilities of using the directly modulated MQW lasers for such communication scheme. We will make use of different modulation schemes such as single-tone (STM), two-tone (TTM), and multi-tone modulation (MTM), by injecting one, two and  $N$  sinusoidal carriers, respectively [41, 44].

Communication with light waves with chaotic fluctuations of intensity has been considered

in recent years by several researchers [45, 48, 46, 47]. The natural masking of information by chaotic fluctuations has served as a practical motivation for the research. Great interest also exists in understanding the basic mechanisms by which information can be encoded and decoded through the use of synchronized chaotic systems. We will discuss the synchronization of coupled MQW laser in chapter 3 along with the discussion of its nonlinear dynamics.

Bistable lasers have always been looked as means of optical computing elements and memory systems [15]. We explore the nature of multistability in directly modulated multiple quantum well lasers in chapter 4.

Also interesting is the role of feedback in the dynamics of multiple quantum well lasers. It is shown in chapter 5 that feedback can act as means of controlling instabilities as well as generate chaos in the system. The possibility of integrating an optoelectronic feedback circuit to the laser control circuit makes these possibilities more attractive.



# Bibliography

- [1] J. Priprek, *Semiconductor Optoelectronic Devices: Introduction to Physics and Simulation*, Academic Press, San Diego, 2003.
- [2] M. A. Parker, *Physics of Optoelectronics*, Taylor and Francis, Boca Raton, 2005.
- [3] T. Suhara, *Semiconductor Laser Fundamentals*, Marcel Dekker, New York, 2004.
- [4] D. Meschede, *Optics, Light and Lasers*, Wiley-VCH Verlag GmbH and Co. KGaA, Weinheim, 2004.
- [5] R. S. Geels, S. W. Corzine, and L. A. Coldren, "InGaAs vertical-cavity surface-emitting lasers," *IEEE J. Quantum Electron.* **27**, pp. 1359–1367 (1991).
- [6] C. Weisbuch and B. Vinter, *Quantum Semiconductor Structures*, Academic Press, New York, 1991.
- [7] W. Tsang, "Heterostructure semiconductor lasers prepared by molecular beam epitaxy," *IEEE J. Quantum Electron.* **QE-20**, 1119–1132 (1984).
- [8] P. S. Zory, Jr (ed.), *Quantum Well Lasers*, Academic Press, New York, 1993.
- [9] N. Holonyak, Jr., R. M. Kolbas, R. D. Dupuis and P. D. Dapkus, "Quantum-well heterostructure lasers," *IEEE J. Quantum Electron.* **QE-16**, pp. 170–186 (1980).
- [10] A. Yariv, *Quantum Electronics*, John Wiley & Sons, New York, 1989.
- [11] A. F. J. Levi, *Applied Quantum Mechanics*, Cambridge University Press, Cambridge, 2003.
- [12] A. Shik, *Quantum Wells: Physics and Electronics of Two-Dimensional Systems*, World Scientific, Singapore, 1998.
- [13] G. P. Agrawal and N. K. Dutta. *Long-Wavelength Semiconductor Lasers*, Van Nostrand Reinhold, New York, 1993.
- [14] R. Lang and K. Kobayashi, "Suppression of the relaxation oscillation in the modulated output of semiconductor lasers," *IEEE J. Quantum Electron.* **QE-12**, pp. 194–199 (1976).
- [15] H. Kawaguchi. *Bistability and Nonlinearities in Laser Diodes*. Artech House, Norwood, 1994.

- [16] G. A. Baraff and R. K. Smith, "Nonadiabatic semiconductor laser rate equations for the large-signal, rapid-modulation regime," *Phys. Rev. A* **48**, pp. 043808 (2000).
- [17] W. Rideout, W. F. Sharfin, E. S. Koteles, M. O. Vassel, and B. Elman, "Well-barrier hole burning in quantum-well lasers," *IEEE Photon. Technol. Lett.* **3**, pp. 784-786 (1991).
- [18] R. Nagarajan, T. Fukushima, S. W. Corzine, and J. E. Bowers, "Effects of carrier transport on high-speed quantum well lasers," *Appl. Phys. Lett.* **59**, pp. 1835-1837 (1991).
- [19] D. McDonald and R. F. O'Dowd, "Comparison of two- and three-level rate equations in the modeling of quantum-well lasers," *IEEE J. Quantum Electron.* **31**, pp. 1927-1934 (1995).
- [20] K. Uomi, T. Tuchiya, H. Nakano, M. Aoki, M. Suzuki, and N. Chinone, "High-speed and ultralow-chirp 11.55 $\mu\text{m}$  multiquantum well  $\lambda/4$ -shifted DFB lasers," *IEEE J. Quantum Electron.* **QE-27**, pp. 1705-1713 (1991).
- [21] A. P. DeFonzo, and B. Gomatam, "Gain nonlinearities in semiconductor lasers and amplifiers," *Appl. Phys. Lett.* **56**, pp. 61-613 (1990).
- [22] J. Eom, and C. B. Su, "Observation of positive and negative nonlinear gain in an optical injection experiment: Proof of the cavity standing-wave-induced nonlinear gain theory in 1.3 $\mu\text{m}$  wavelength semiconductor diode lasers," *Appl. Phys. Lett.* **54**, pp. 1734-1736 (1989).
- [23] N. Tessler and G. Eisenstein, "On carrier injection and gain dynamics in quantum well lasers," *IEEE J. Quantum Electron.* **29**, pp. 1586-1595 (1993).
- [24] M. Yamada and Y. Suematsu, *IEEE J. Quantum Electron.* **QE-15**, pp. 743 (1979); *J. Appl. Phys.* **52**, pp. 2653 (1981).
- [25] M. O. Vassel, W. F. Sharfin, W. C. Rideout, and J. Lee, "Competing effects of well-barrier hole burning and nonlinear gain on the resonance characteristics of quantum-well lasers," *IEEE J. Quantum Electron.* **29**, pp. 1319-1329 (1993).
- [26] H. Uenohara, R. Takahashi, Y. Kawamura, and H. Iwamura, "Static and dynamic response of Multiple quantum well voltage controlled bistable laser diodes," *IEEE J. Quantum Electron.* **32**, pp. 873-883 (1996).
- [27] W. F. Sharfin, J. Schlafer, W. Rideout, B. Elman, R. B. Lauer, J. LaCourse, and F. D. Crawford, "Anomalously high damping in strained InGaAs-GaAs single quantum well lasers," *IEEE Photon. Technol. Lett.* **3**, pp. 193-195 (1991).
- [28] S. Morin, G. Cocorullo, F. G. Della Corte, H. L. Harnagel, and Schwoeeger, "Capture of photoexcited carriers in a single quantum well with different confinement structures," *IEEE J. Quantum Electron.* **27**, pp. 1669-1675 (1991); and references therein.
- [29] N. K. Dutta and R. J. Nelson, "The case for Auger recombination in  $\text{In}_{1-x}\text{Ga}_x\text{As}_y\text{P}_{1-y}$ ," *J. Appl. Phys.*, vol. **53**, pp. 74-76 (1982).

- [30] M. G. A. Bernard and G. Duraffourg, "Laser conditions in semiconductors," *Phys. Stat. Solidi* **1**, pp. 699-703 (1961).
- [31] K-Y. Liou, C. A. Burrus, R. A. Linke, I. P. Kaminow, S. W. Granlund, C. B. Swan, and P. Besomi, "Single-longitudinal-mode stabilized graded-index-rod external coupled-cavity laser," *Appl. Phys. Lett.*, **45**, pp. 729-731 (1984).
- [32] H. Kogelnik and C. V. Shank, "Coupled-Wave theory of distributed feedback lasers," *J. Appl. Phys.* **43**, pp. 2327 (1972).
- [33] M. Nakamura, A. Yariv, H. W. Yen, S. Someck, and H. L. Garvin, "Laser oscillation in epitaxial GaAs waveguides with corrugation feedback," *Appl. Phys. Lett.* **23**, pp. 224-225 (1973).
- [34] S. Wang, "Principles of distributed feedback and distributed Bragg-reflector lasers," *IEEE J. Quantum Electron.* **QE-10**, pp. 413-427 (1974).
- [35] H. Yamazaki, A. Tomita, and M. Yamaguchi, "Evidence of nonuniform carrier distribution in multiple quantum well lasers," *Appl. Phys. Lett.* **71**, pp. 767-769 (1997).
- [36] J. F. Hazell, J. G. Simmons, J. D. Evans, and C. Blaauw, "The effect of varying barrier height on the operational characteristics of 1.3- $\mu\text{m}$  strained-layer MQW lasers," *IEEE J. Quantum Electron.* **34**, pp. 2358-2363 (1998).
- [37] A. Champagne, R. Maciejko, and T. Makino, "Enhanced carrier injection efficiency from lateral current injection in multiple-quantum-well DFB lasers," *IEEE Photon. Technol. Lett.* **8**, pp. 749-751 (1996).
- [38] G. B. Morrison, D. M. Adams, and D. T. Cassidy, "Extraction of gain parameters for truncated well gain coupled DFB lasers," *IEEE Photon. Technol. Lett.* (1999).
- [39] M. J. Hamp, D. T. Cassidy, B. J. Robinson, Q. C. Zhao, D. A. Thompson, and M. Davies, "Effect of barrier height on the uneven carrier distribution in asymmetric multiple-quantum-well InGaAsP lasers," *IEEE Photon. Technol. Lett.* **10**, pp. 1380-1382 (1998).
- [40] M. J. Hamp, D. T. Cassidy, B. J. Robinson, Q. C. Zhao, and D. A. Thompson, "Nonuniform carrier distribution in asymmetric multiple-quantum-well InGaAsP laser structures with different numbers of quantum wells," *Appl. Phys. Lett.* **74**, pp. 744-746 (1999).
- [41] S. Bennett, C. M. Snowden and S. Iezekiel, "Nonlinear dynamics in directly modulated multiple-quantum-well laser diodes," *IEEE J. Quantum Electron.* **33**, pp. 2076-2083 (1997).
- [42] P. M. A. Mc Ilroy, A. Kurobe, Y. Uematsu, "Analysis and application of theoretical gain curves to the design of multi-quantum-well lasers," *IEEE J. Quantum Electron.* **QE-21**, pp. 1958-1963 (1985).
- [43] M. Asada, A. Kameyama, Y. Suematsu, "Gain and intervalence band absorption in quantum-well lasers," *IEEE J. Quantum Electron.* **QE-20**, pp. 745-753 (1984).



- [44] C. Juang, S. T. Huang, C. Y. Liu, W. C. Wang, T. M. Hwang, J. Juang, and W. W. Lin, "*Subcarrier multiplexing by chaotic multitone modulation*," IEEE J. Quantum Electron. **41**, pp. 1213-1223 (1998).
- [45] L. M. Pecora, T. L. Carroll, G. A. Johnson, D. J. Mar, and J. F. Heagy, "*Fundamentals of synchronization in chaotic systems, concepts, and applications*," Chaos **7**, pp. 520 (1997).
- [46] G. D. VanWiggeren, and R. Roy, "*Communication with chaotic lasers*," Science **279**, pp. 1198-1200 (1998).
- [47] R. Roy and K. S. Thornburg, Jr., "*Experimental synchronization of chaotic lasers*," Phys. Rev. Lett. **72**, pp. 2009-2012 (1994).
- [48] K. M. Cuomo, A. V. Oppenheim, and S. H. Strogatz, "*Synchronization of Lorenz-based chaotic circuits with applications to communication*," IEEE Trans. Circuit Syst. II **40**, pp. 626-633 (1993).

## Chapter 3

# Effect of Modulation on MQW Laser Dynamics

*"Every great advance in science has issued from a new audacity of imagination."*

- John Dewey

### ABSTRACT

*Direct modulation of semiconductor lasers make them highly useful in optical communication. From a dynamical perspective, the modulation adds another degree of freedom which make the laser vulnerable to coherence collapse and chaotic oscillations. Multiple quantum well lasers have high bandwidth and allows high frequency small signal modulation with signals in the order of GHz. In this chapter we present the results of our rigorous numerical analysis of the modulation response of the directly modulated multiple quantum well laser.*

### 3.1 Introduction

It is now well established that the modulation response of semiconductor lasers for optical communications is determined by an intrinsic dynamic resonance in the photon-carrier interaction. The competition between various dominating frequencies of oscillation within the laser cavity can lead to various situations such as periodic oscillation, quasiperiodicity, multistability and hysteresis, and chaos. The semiconductor laser dynamics, in general, is

well studied and depending on whether gives self pulsating, bistable or non self pulsating output, the laser dynamics can follow various routes to chaos [1, 2, 3].

## 3.2 Direct Modulation of MQW Lasers

It is well understood today that the direct modulation of the semiconductor laser adds the necessary degree of freedom that makes the laser chaotic [1, 2]. This is due to the finding that chaotic behaviour arises in a single mode laser when its losses are periodically modulated with a frequency comparable to the relaxation oscillation frequency. Kawaguchi [4] showed that a self-pulsating laser with a sinusoidal current modulation shows period-doubling bifurcation and chaos. Lee *et al.* showed that the directly modulated laser diode, which does not have self-pulsation, with the modulation frequency of the injection current comparable to the relaxation frequency, exhibits a period-doubling route to chaos as the modulation current is increased [5]. This is observed in the absence of any other disturbance such as external feedback and relies simply on the photon-electron resonances and their interaction with the modulation frequency.

Our attempt in this chapter is to understand the response of a directly modulated multiple quantum well laser diode to various modulation schemes. We choose a  $\lambda/4$  shifted DFB *InGaAsP – InGaAs* MQW laser diode for our study based on the reasons cited in chapter two. The laser has 16 quantum wells (QW's) with lengths of  $350\mu m$ . The thicknesses of the well and barrier regions were  $70 \text{ \AA}$  and  $100 \text{ \AA}$ , respectively, and the active regions had widths of  $1.3 \mu m$ . The laser has a threshold current of  $19 mA$  and emission wavelength  $1.53 \mu m$ . The emission wavelength of the laser has a detuning of approximately  $30 nm$  from the material gain peak. The laser has a  $3 - dB$  modulation bandwidth of  $11.3 GHz$  at  $100 mA$  and  $D$  [6] and  $K$  [7] factors of  $3.96 GHz/mW$  and  $0.42 ns$ , respectively. The  $K$  factor refers to the Petermann factor, which sums up the existence of excessive noise in radiation modes, leading to enhancements in intrinsic laser line widths and spontaneous emission rates [8].  $P$  is a factor dependent on the waveguide dimensions when we write the resonance frequency,  $f_r$ , as a function of laser output power per facet,  $P$ , as:

$$f_r \approx DP^{1/2} \quad (3.1)$$

The value of  $D$  determines the differential gain coefficient  $G_0$ , and the laser output powers. Spatially averaged carrier densities in the barrier region ( $N_B$ ) and the well region ( $N$ ) influence the photon number density ( $P$ ) in the active region according to the following set modified equations from the set of equations obtained in section 2.6 [9, 10]:

Table 3.1: Parameters Used in Rate Equation Analysis and Their Description

Parameter	Value	Description
$V$	$5.1 \times 10^{-17} m^3$	Active region volume
$\Gamma$	0.22	Mode confinement factor
$\Gamma_q$	0.66	Fractional volume of Quantum Wells
$\tau_p$	1.3 ps	Photon lifetime
$\tau_c$	20 ps	Carrier decay time (Barrier to Well)
$\tau_e$	191 ps	Carrier decay time (Well to Barrier)
$\beta$	$10^{-6}$	Spontaneous emission factor
$G_0$	$141107 m^{-1}$	Gain parameter
$N_0$	$2.41 \times 10^{24} m^{-3}$	Transparent carrier density
$\epsilon$	$3.24 \times 10^{-23} m^3$	Gain compression coefficient
$A$	$10^8 s^{-1}$	Mono-molecular Recombination Coefficient
$B$	$10^{-16} m^3 s^{-1}$	Bi-molecular Recombination Coefficient
$C$	$3 \times 10^{-41} m^6 s^{-1}$	Auger Recombination Coefficient
$v_g$	$7.5 \times 10^7 ms^{-1}$	Group velocity
$I_{th}$	19 mA	Threshold Current

$$\frac{dN_B}{dt} = \frac{\Gamma_q I}{eV} - \frac{N_B}{\tau_c} + \frac{\Gamma_q N}{\tau_e} \quad (3.2)$$

$$\frac{dN}{dt} = \frac{N_B}{\Gamma_q \tau_c} + N \left[ \frac{1}{\tau_n} + \frac{1}{\tau_e} \right] - v_g G(N, P) P, \quad (3.3)$$

$$\frac{dP}{dt} = \left[ \Gamma v_g G(N, P) - \frac{1}{\tau_p} \right] P + \Gamma \beta B N^2, \quad (3.4)$$

where  $I$  is the injected current,  $e$  is the electron charge,  $\Gamma_q$  is the fraction of the MQW region filled by the quantum wells and  $\Gamma$  is the mode confinement factor as calculated using the effective index method for the quantum well structure,  $v_g$  is the group velocity and  $\tau_p$  is the photon lifetime in the well region.

We have used following expression for the nonlinear gain of the laser  $G(N, P)$  [11] is modelled as the same given in equation 2.15. The carrier recombination rate  $R(N)$  is expressed by the truncated power series fit to inverse differential carrier lifetime ( $1/\tau_n - \partial R/\partial N$ ) measurements [12] given by equation 2.16 discussed in chapter 2.

### 3.3 Sinusoidal Modulation and Frequency Response

In principle, direct modulation at a gigabit rate is expected to be feasible. However, the practical rate of pulse modulation has been limited to below several hundred megahertz, owing to the serious distortion of the output waveform caused by the relaxation oscillation of the light intensity. The typical repetition frequency  $\omega_r$  of the intensity spikes is a few gigahertz, with the spike height decreasing exponentially with the time constant of a few nanoseconds. The optical gain varies with the carrier density causing the number of lasing modes, and hence the width of the spectral envelope to increase. In order to attain practical rates of direct modulation in the gigahertz range, it therefore appears essential to suppress relaxation oscillations in the modulated output of semiconductor lasers.

Since the main application of semiconductor lasers is as a source for optical communication systems, the problem of the high-speed modulation of their output by the high data rate information is one of great technological importance [13]. A unique feature of semiconductor lasers is that, unlike other lasers that are modulated externally, the semiconductor laser can be modulated directly by modulating the excitation current. This is especially important in the view of the possibility of the monolithic integration of the laser and the modulation electronic circuit.

In Eqn. 3.2, the laser is modulated directly using a source of injection current

$$I = I_b + \sum_k I_k \sin(2\pi f_k t), \quad (3.5)$$

where  $I_b$  is the bias current and  $I_k$  is the modulation current amplitude for frequencies  $f_k$  [2]. In the present study, we have biased the laser above the threshold current value of 19 mA. It is ensured that the laser never goes below the threshold even when the modulation amplitude  $I_k$  is increased.

The QW's have one conduction subband so that the relationship between the carrier density and the junction voltage  $V_j$  can be approximated as [14]

$$N \approx kT \frac{m_c}{\pi \hbar^2 L_z} \ln \left[ 1 + \exp\left(\frac{eV_j - E_{ph}}{kT}\right) \right] \quad (3.6)$$

where  $m_c$  is the electron effective mass,  $L_z$  is the QW width, and  $E_{ph}$  is the photon energy. We have then numerically solved the dynamical equations (Eqs. 3.2-3.4) using the fourth order *Runge-Kutta* scheme. The parameters used for the study is given in Table 3.1 which are adapted from literature [10, 12, 15] citing experimental values. The photon density and other variables after vanishing the transients are recorded. We have used the normalised

values of variables to obtain the phase space diagrams. Power spectral density of the laser output is plotted on a logarithmic scale using the Fast Fourier Transform (FFT) algorithm for a better picture of the output frequency spectrum.

It is observed that the phase space trajectory of the system starting from a typical initial condition converges to the attractor (it can be periodic or chaotic) within a finite time. For small signal modulation the laser output depends on the ratio of modulation frequency to the laser excitation frequency [3]. Our estimations show that large detuning corresponds to trajectories in the phase space lying on a two-dimensional torus. It is observed that a rational ratio of frequencies lead to closed trajectories lying on the torus, irrational ratio to a never repeating, and a multitone modulation with a set of incommensurate frequencies lead to chaotic trajectory.

We have seen before that the relaxation oscillation frequency  $\omega_R$  and the damping factor  $\Gamma_R$  depend upon the laser structure and the choice of the operation point. Using the steady-state photon density given by  $S_0 = \tau_p (J - J_0)/dq$ , we obtain an approximate expression for  $\omega_R$ :

$$\omega_R^2 \approx \frac{\Gamma G_N S_0}{\tau_p} = \frac{\Gamma G_N (J_0 - J_{th})}{dq}. \quad (3.7)$$

The above expression shows that  $\omega_R$  is dominated by the effective differential gain  $\Gamma G_N$  and the volume density of the injection current. The damping factor  $\Gamma_R$ , on the other hand, is mainly determined by the carrier lifetime  $\tau_s$ . When the output power increases, the attenuation becomes faster owing to the enhanced stimulated emission.

We next consider a case where the injection current density is modulated by a small sinusoidal signal of frequency  $\omega$ . Kawaguchi showed that a self-pulsating laser diode with a sinusoidal current modulation shows period-doubling bifurcation and chaos [4]. Soon after, Lee *et al.* showed that the directly modulated laser diode, which does not have self-pulsation, with the modulation frequency of the injection current comparable to the relaxation oscillation frequency, exhibits a period-doubling route to chaos as the modulation index of current is increased [5].

### 3.4 Single-Tone Modulation

Laser diodes are known to be susceptible to nonlinear behaviour caused by unintentional optical feedback. Therefore, so as to study the nonlinear dynamics resulting from direct modulation of the laser alone, optical feedback into the laser can be minimised by the use of an optical isolator.

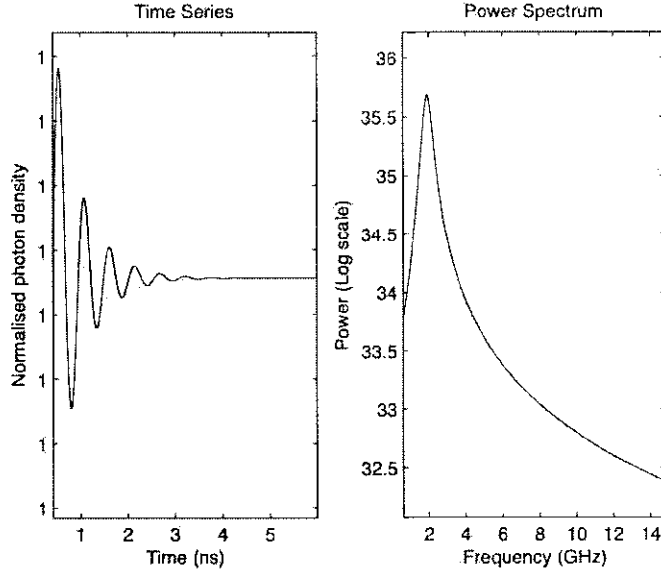


Figure 3.1: MQW laser output for a bias current  $22\text{ mA}$  just above threshold current of  $19\text{ mA}$  without any input modulation. The time series is plotted by normalising the photon density. Both diagrams show the relaxation oscillation within the laser cavity.

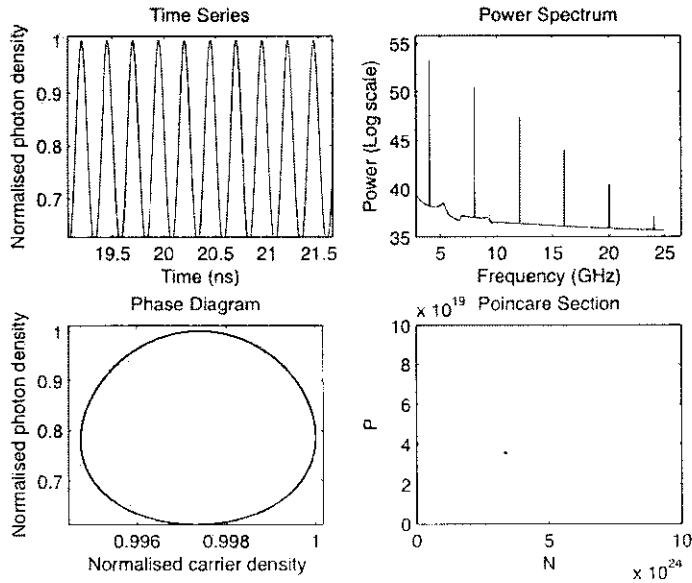


Figure 3.2: Laser dynamics with a single tone modulation of frequency  $4.01\text{ GHz}$ . Bias current is  $23\text{ mA}$  and  $I_m = 5\text{ mA}$ . The periodic times series is also revealed by the closed single loop obtained in the phase space diagram. This is also revealed by the Poincaré section with the single flow. The power spectrum shows the resonant oscillation at  $4.01\text{ GHz}$  and its harmonics.

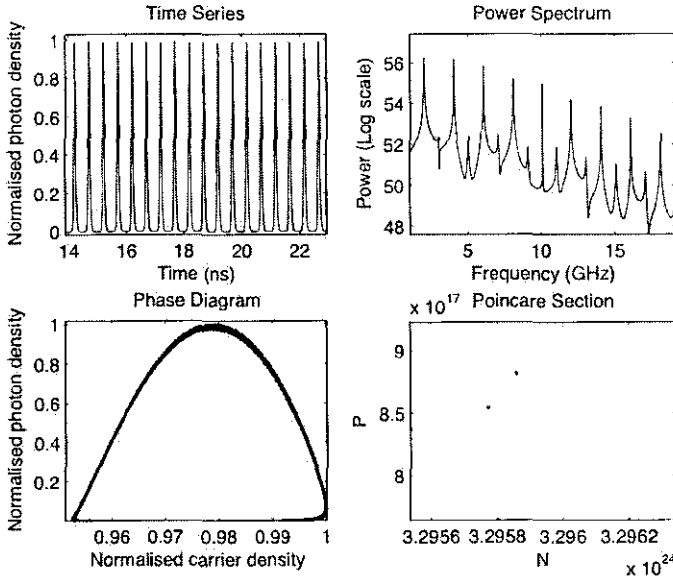


Figure 3.3: Laser dynamics with a single tone modulation of frequency  $2.01\text{GHz}$ . Bias current is  $23\text{mA}$  and  $I_m = 5\text{mA}$ . The laser output shows pulsating output and the power spectrum shows sub-harmonic bifurcation.

When the laser diode was biased just above the threshold, it exhibited a weak resonance peak with a broad pedestal in the power spectrum. Such a laser without any sinusoidal modulation is damped as seen in Fig. 3.1. We have modulated the laser with a single frequency of  $4.0\text{GHz}$  by setting  $k = 1$  in Eqn. 3.15, and as shown in Fig. 3.2, resonance sets in and the laser output is regular and periodic. The power spectrum shows sub-harmonic bifurcations exhibited by the laser in this state. The laser output, when modulated with a frequency below the relaxation frequency ( $4\text{GHz}$  in the present case), shows several sub harmonics with single tone modulation as shown in Fig. 3.3 for a modulation with  $2.01\text{GHz}$ . The calculations in the figure and similar figures used throughout the thesis illustrate phase diagrams and Poincaré sections calculated for the same time scale but the phase diagrams are plotted on a normalised scale for the sake of convenience. Poincaré sections are plotted showing the relevant region in the picture where the phase trajectories cross the plane of intersection. Therefore, Poincaré sections in different illustrations in this chapter and subsequent chapters may show different scales. The output in this case is a pulsating one and we show that the MQW laser can be used to generate ultrashort pulses by suitably selecting the modulating frequency [16]. Our results so far indicate that we can modulate the MQW laser with a suitable modulation frequency to achieve sinusoidal and pulsating outputs, in which the latter is highly useful in digital communication.



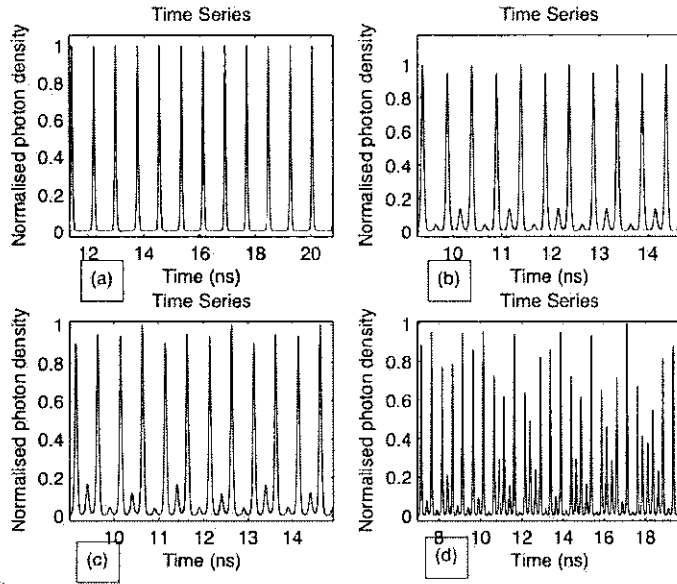


Figure 3.4: Waveforms of multiperiodic pulsing in MQW laser: (a) regular periodic pulsing obtained by scale modulation ( $m = 0.02$ ), (b) period 2 state (c) period 4 state, (d) chaotic state.

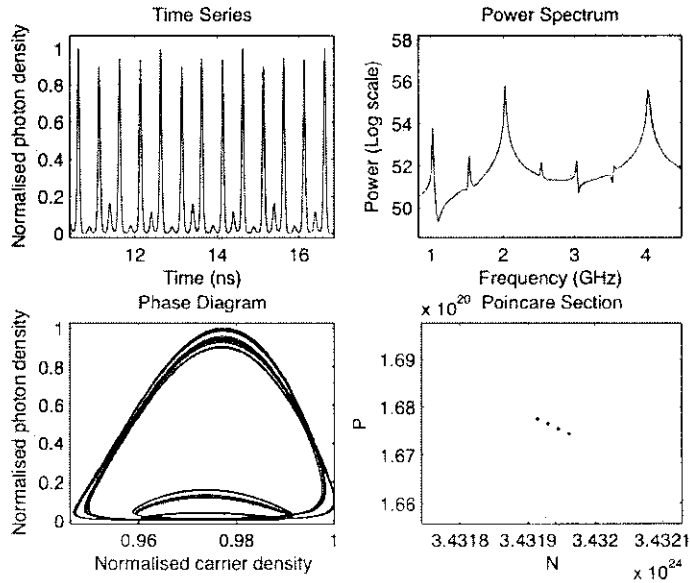


Figure 3.5: Dynamic features of the laser in a period 4 state shown in figure 3.4. The time series shows four distinct pulses and the power spectrum show their frequencies at  $1\text{ GHz}$ ,  $1.5\text{ GHz}$ ,  $2\text{ GHz}$  and  $4\text{ GHz}$ . The spike at  $3\text{ GHz}$  is the harmonic of the  $1.5\text{ GHz}$  oscillation. The Poincaré section is scaled to the portion of the phase space where the plane bisects the flow and it clearly shows the four distinct periodicities.

We have then kept the modulation frequency at  $f_k = 4.0 \text{ GHz}$  and varied the modulation depth ( $m = I_k/I_b$ ) and found that the laser output follows a period-doubling route to chaos. This is shown in Fig. 3.4(a)-(d), where we have plotted the time series corresponding to period-1, period-2, period-4, and chaotic states, respectively. The periodic time series is obtained for a small scale modulation of  $m = 0.02$ . Period-2 is obtained for  $m = 0.5625$ , period-4 is obtained for  $m = 0.6391$ , and the chaotic state is obtained for  $m = 0.7$ . Fig. 3.5 shows the laser output in a period-4 state where there are four stable states repeating regularly in time. There are peaks at every integer multiples of the fundamental frequency. In addition to the main peak at  $f_k$  in the spectra, the period-4 output in the figure shows four peaks at the values  $f_k/4, f_k/2, 3f_k/4$ . Period-doubling route to chaos has been observed by many researchers [2] for directly modulated bulk and QW self pulsating lasers. When modulated with a frequency above the natural relaxation frequency, the output will exhibit a shift in relaxation frequency towards the resonant frequency. For small signal modulation the laser output depends on the ratio of modulation frequency to the laser excitation frequency as shown in the following section.

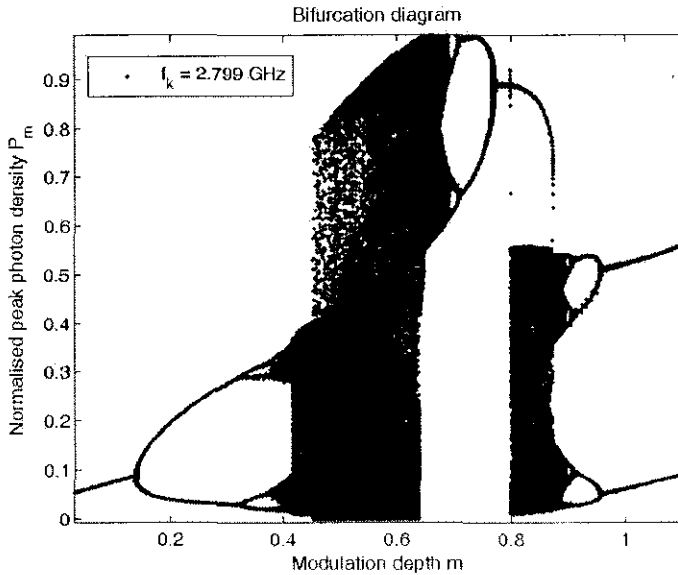


Figure 3.6: Laser bifurcation diagram for various modulation depths showing the period-doubling route to chaos. The biasing current is  $22 \text{ mA}$ .

A bifurcation diagram of the laser is shown in Fig. 3.6, where the peak photon density (normalised) is plotted against various modulation depths ( $m = I_k/I_b$ ). It can be seen from the figure that the laser follows a period-doubling route to chaos very quickly when the modulation current is increased by keeping the modulation frequency at  $f_k = 2.799 \text{ GHz}$ .

This is the first reported work on the occurrence of chaos in the MQW laser system for such small values of modulation current [16, 17]. To verify this, we have simulated the system for a modulation depth of 0.46 and a modulation frequency of 2.799 GHz and have found that the system goes into a chaotic state as illustrated by figure 3.7. To verify the chaotic state of the system quantitatively, we have calculated the maximal Lyapunov exponent (MLE) of the system using the software Dataplore. Parameters of the MLE are the embedding dimension  $m$ , the number  $M$  of neighbours taken into account in phase space, and the degree  $pd$  of the fitting polynomial. While calculating the MLE, we have made use of the following values for these parameters:  $m = 3$ ,  $M = 35$  and  $pd = 2$ . The embedding dimension has been fixed after evaluating the number of false neighbours which we obtained as less than 2. The program first digitises the time series and then gives MLE in terms of the amount of binary information created per second when sampling the data. In the present case the MLE found to be equal to  $2.6084 \times 10^{11}$  bits/s, which is quite large due to the large number of photons created within the laser cavity per second. In the periodic and non-chaotic oscillations, the MLE has been calculated and found to be nearly zero. To understand more about the nature of chaos in MQW system, we have studied the response of the system under various modulation frequencies and modulation depths as will be discussed in following sections.

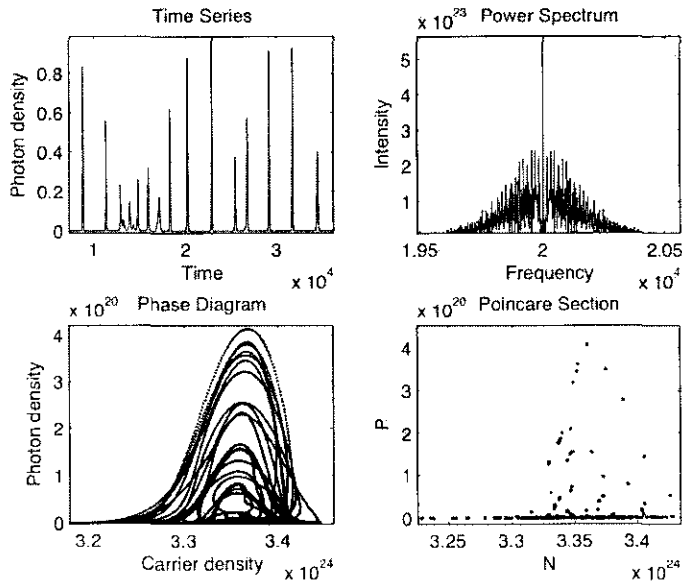


Figure 3.7: Laser chaos with a single tone modulation at frequency 2.799 GHz for modulation depth  $m = 0.46$ . (a) Time series of the laser, (b) Power spectrum plotted on the absolute scale with frequency shifting, (c) Phase diagram and (d) Poincaré section showing the never repeating flow that cuts through the bisecting plane.

### 3.5 Two-Tone Modulation

In the case of current modulation, two cases can be distinguished:

1. The modulation frequency is of the same order or higher than the laser relaxation oscillation frequency. A period-doubling route to chaos is predicted in bulk lasers in such a situation [18].
2. The modulation frequency is either of the order of the round-trip frequency of the laser photons within the resonator or amounts to a rational fraction  $p/q$  of the round-trip frequency. In this case frequency locking following the hierarchy of a Farey tree [19, 20] and quasiperiodicity is expected and has been observed [3].

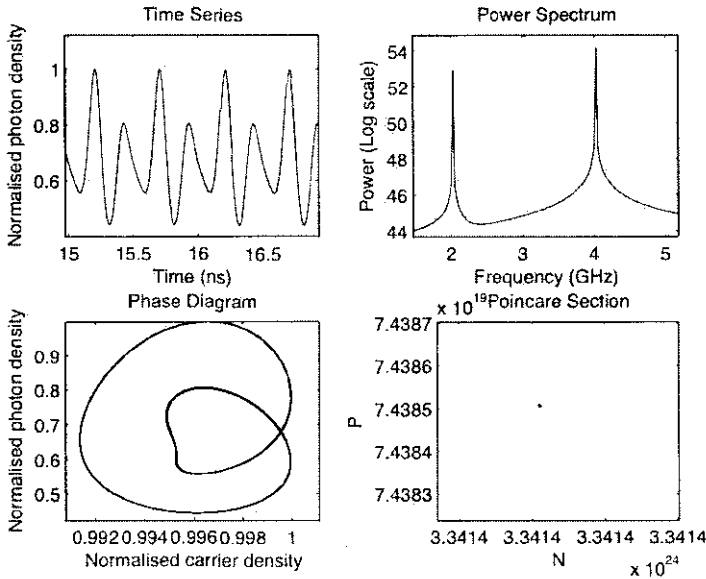


Figure 3.8: The period 1 loop with double peak resulting from a two-tone modulation of 2.0 GHz and 4.0 GHz. The two frequencies are harmonics and therefore the Poincaré section shows only a single flow.

Large detuning of one of the modulating frequencies with another corresponds to trajectories in the phase space lying on a bi-periodic torus. On such a torus there are two possibilities for the combination of modulation frequencies. They can be held at a rational ratio  $f_m/f_{res} = p/q$  which gives a closed curve on the torus, or the ratio can be an irrational value resulting in an open trajectory.

We have chosen the combination of frequencies to be 2.0 GHz and 4.0 GHz. For a biasing current of 22mA and modulation amplitudes of 2mA each, it is observed from Fig. 3.8 that

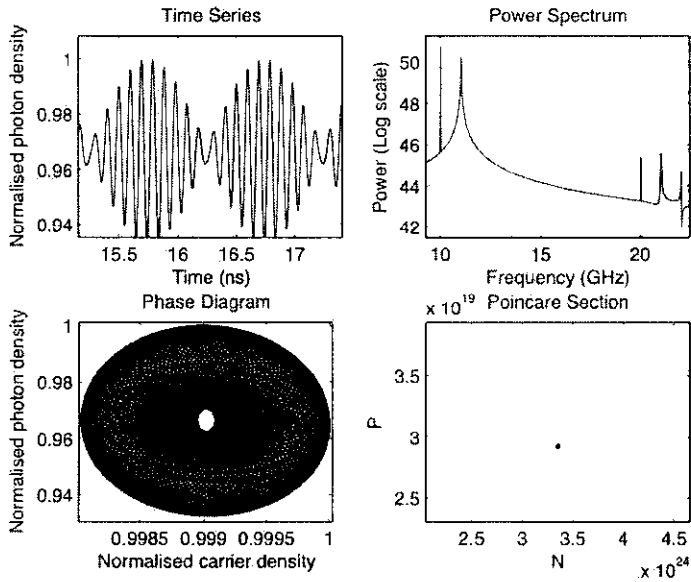


Figure 3.9: Dynamics features of the laser resulting from a two-tone modulation of  $10.0\text{ GHz}$  and  $11.01\text{ GHz}$ . Irrational ratio of the frequencies results in the chirp visible in the time series. The phase space diagram shows that the trajectories lie on a bi-periodic torus. Biasing current is  $22\text{ mA}$  and modulation current is  $3\text{ mA}$  each for the two frequencies.

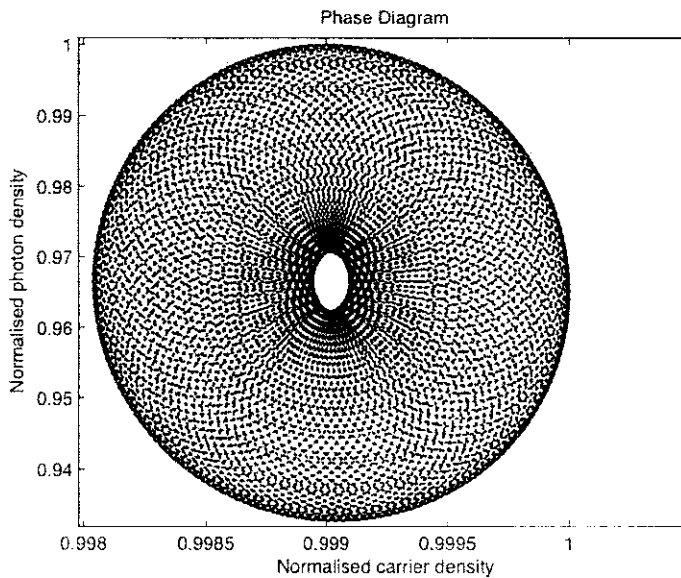


Figure 3.10: The bi-periodic torus shown in figure 3.9.

the phase space trajectories form a closed trajectory. This is in accordance with the same results obtained bulk semiconductor laser cavity with a set of two modulation frequencies with a rational ratio  $p/q$  between them [3]. Next we have chosen two higher values  $10.0\text{ GHz}$  and  $11.01\text{ GHz}$  retaining the biasing conditions and the results, as shown in Fig. 3.9, show the chirped output due to the frequency detuning. The corresponding phase diagram is shown as enlarged in Fig. 3.10 clearly shows that trajectories close in on the bi-periodic torus. It is seen from this result that the MQW laser show a variation from the bulk semiconductor laser in exhibiting the frequency locking effects on the dynamics.

Next, we have then chosen two values  $2.4721\text{ GHz}$  and  $4.0\text{ GHz}$  which have a ratio equal to the golden mean  $\sigma_g = 0.61803399\dots$ . The result is obtained in torus as seen in Fig. 3.11. We have then increased the bias current to  $25\text{ mA}$  and modulation current values to  $3\text{ mA}$  each and the result as shown in Fig. 3.12 shows that the laser has a chaotic dynamics. The maximal lyapunov exponent (MLE) for the system is  $1.8931 \times 10^{11}\text{ bits/s}$ . This is a significant result which shows that the laser takes a torus-breaking route to chaos. When the ratio of frequencies is rational, the frequency locking happens and the laser output is periodic. The light output is quasiperiodic when  $p/q$  lies between these locked states.

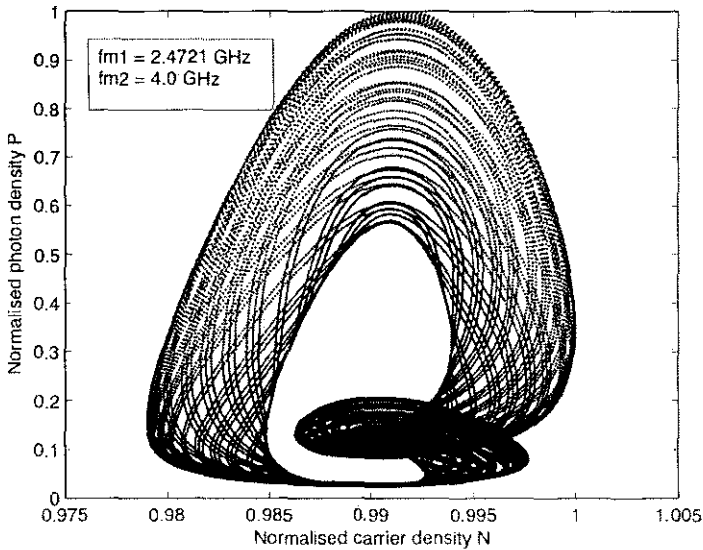


Figure 3.11: The torus resulting from a two-tone modulation with two frequencies having a golden mean ratio ( $\sigma_g = 0.61803399\dots$ ). Biasing current is  $22\text{ mA}$  and modulation current is  $3\text{ mA}$ .

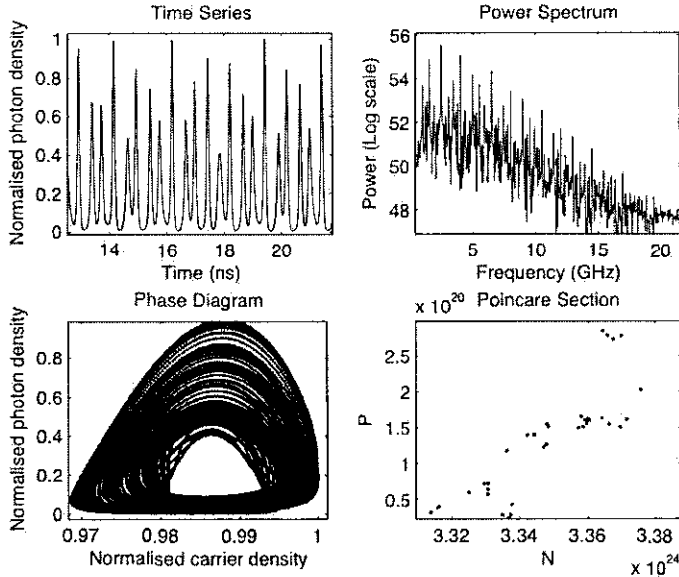


Figure 3.12: Two tone chaos resulting from a choice of two frequencies  $2.4721\text{ GHz}$  and  $4.0\text{ GHz}$  having golden mean ratio. The biasing current is increased to  $25\text{ mA}$  from the previous result shown in figure 3.11.  $MLE = 1.8931 \times 10^{11}\text{ bits/s}$ .

### 3.6 Effect of Multitone Modulation

We then look to see the possibility of introducing more than two frequencies in the modulation spectrum. This we term as multitone modulation and as a first step, we have modulated the laser with a combination four frequencies, viz.  $2.0\text{ GHz}$ ,  $4.0\text{ GHz}$ ,  $6.0\text{ GHz}$ , and  $8.0\text{ GHz}$ . Fig. 3.13 shows the resulting dynamics where the laser output contains all the harmonics with a two-periodic loop in the phase diagram. When the frequencies are  $2.4721\text{ GHz}$ ,  $4.01\text{ GHz}$ ,  $8.79\text{ GHz}$ , and  $11.17\text{ GHz}$  to have a non-integer ratio among themselves, it is observed that the laser system has a chaotic trajectory as given by (Fig. 3.14). The MLE for this system is equal to  $4.6673 \times 10^{11}\text{ bits/s}$ . We have verified this result for several combination of such frequencies under stable biasing conditions for the laser [21].

The importance of this result arises when we consider the fact that researchers have demonstrated the viability of using directly modulated semiconductor lasers under multitone modulation for synchronized chaotic communication [22, 23]. We, therefore, propose that a MQW laser with multitone modulation is a suitable choice for chaotic masking and encryption. The challenge is, however, to achieve chaotic synchronization among such laser systems which we have achieved and will be discussed in section 3.8.

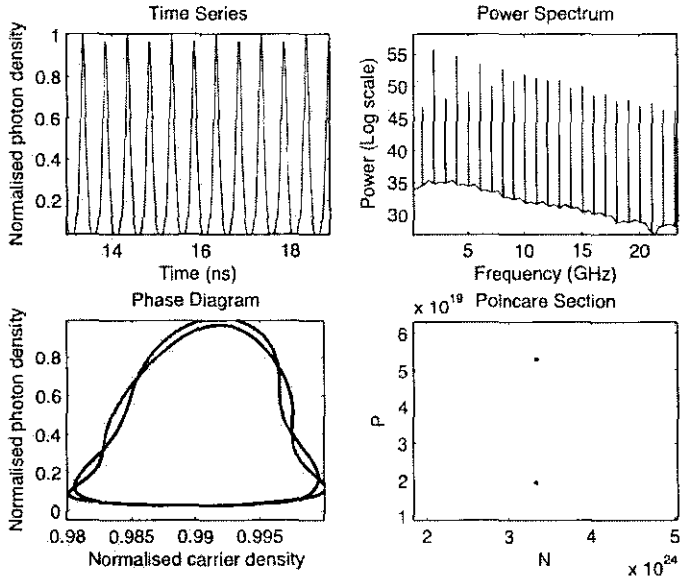


Figure 3.13: Effect of a multitone resonant modulation with frequencies 2.0 GHz, 4.0 GHz, 6.0 GHz, and 8.0 GHz. The biasing current is 22 mA and modulation amplitude is 1.5 mA each. The power spectrum and the Poincaré section both show the two harmonic frequencies.

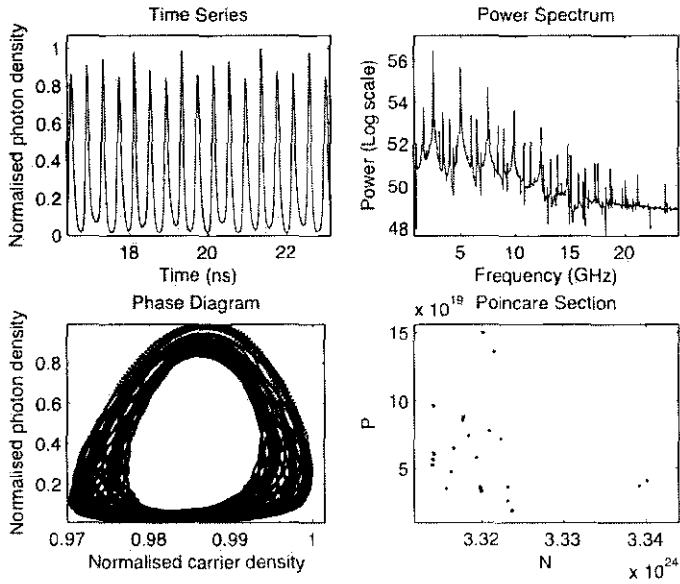


Figure 3.14: Chaotic state of the laser when modulated by a set of four frequencies. The biasing current is 22 mA and modulation amplitude is 1.5 mA each. All the four diagrams indicate the chaotic state of the laser and the  $MLE = 4.6673 \times 10^{11}$  bits/s.



### 3.7 Routes to Chaos

In the first chapter we have discussed the various routes for a transition to chaos. Semiconductor lasers can be modulated externally by either an optical injection or by a direct current modulation. Depending upon the type of modulation, various groups working on the semiconductor laser physics field have shown that there are at least three possible routes to chaos in a semiconductor lasers [3, 24]. It has been shown that a optically injected laser follows the torus breaking, bi-periodic torus breaking and intermittency routes to chaos [3]. In the case of a directly modulated system, an irrational detuning between modulating frequencies can make the laser quasiperiodic and further, this can lead to chaos as shown in the previous section.

In our studies there are features of the period doubling which were common to semiconductor lasers. Our analysis show that the multiple quantum well laser also exhibits these two situations depending on the working conditions of the laser diode. The upper and lower modulation frequency limits of the period-doubling regions follow one and two times the relaxation frequency of the laser, respectively. At frequencies close to the relaxation frequency of the laser, it was found that there was an optimum value of power under which the subharmonic of the modulation frequency had the greatest magnitude. In addition, our analysis of the frequency modulation response of the laser has shown that the dynamics follow a torus-breaking route to chaos when subjected to multitone modulation.

Comparing the behaviour of the MQW DFB laser with that of the bulk DFB laser, it would seem that although period tripling was found in both lasers, the MQW laser is less susceptible to nonlinear behavior. This is because in contrast to the bulk laser neither period quadrupling nor chaos were observed in the MQW laser. However, the range of modulation frequencies over which period doubling occurs in the MQW laser is much greater than that reported in the bulk laser. The range of modulation frequencies over which period doubling occurred in the bulk laser was between 2 and 4 *GHz* in comparison to a range of between 4 and 18 *GHz* in the MQW laser. The greater range of frequencies over which period doubling occurred in the MQW laser is due to the greater *D* factors [25] found in this type of laser resulting in greater relaxation frequencies. The DFB laser has higher relaxation damping and such lasers are less susceptible to bifurcations [26]. This could be one of the main reasons for the absence of experimental observation of chaos in MQW DFB lasers, though simulations show the possibility of chaos in these systems.

The rate equations used in this study include well-barrier hole burning effect [27]. The gain compression factor represents the additional well-barrier transport which is another mechanism for gain compression. This can affect the occurrence of chaos by damping the

relaxation oscillation, and is one of the differentiators between chaos exhibited by MQW and bulk lasers.

### 3.8 Synchronization of Coupled MQW Lasers

Two directly modulated semiconductor lasers can be coupled optoelectronically. In principle this means addition of a fraction of the output of the drive laser to the injection current of the remote laser. We consider the synchronization of two unidirectionally coupled semiconductor lasers separated by a considerable distance [28]. A current signal proportional to the difference between the photon density of the drive laser corresponding to a past state and the present photon density of the response laser can be obtained from the differential amplifier by adjusting its gain. This signal can be represented by the expression  $C[P_1(t - \tau) - P_2(t)]$ , where  $\tau$  is the delay and  $C$  is the coupling strength. Our aim is to synchronize the response system to the earlier state of the drive system and the feedback is designed in such a manner that the feedback signal vanishes when the synchronization is achieved. This is a common method of coupling that has been used in many synchronization schemes. Such a method has been used for synchronization of chaos in lasers with delayed optoelectronic feedback and in directly modulated semiconductor lasers [29].

The coupled system can be modelled by adding a fraction of the time delayed out of one laser to the injection current of the second. We have made use of the same MQW rate equation model described in equations 1.2 - 1.4 to model two similar laser diodes. The lasers are then simulated to run under similar and dissimilar operating conditions such as modulation frequencies and other parameters such as modulation current strength. We model the drive laser diode (LD1) as follows:

$$\frac{dN_{B1}}{dt} = \frac{\Gamma_q I_1}{eV} - \frac{N_{B1}}{\tau_c} + \frac{\Gamma_q N_1}{\tau_e}, \quad (3.8)$$

$$\frac{dN_1}{dt} = \frac{N_{B1}}{\Gamma_q \tau_c} + N_1 \left[ \frac{1}{\tau_n} + \frac{1}{\tau_e} \right] - v_g G(N_1, P_1) P_1, \quad (3.9)$$

$$\frac{dP_1}{dt} = \left[ \Gamma v_g G(N_1, P_1) - \frac{1}{\tau_p} \right] P_1 + \Gamma \beta B N_1^2, \quad (3.10)$$

where the suffix 1 to the variables and parameters indicate LD1 and the injection current,  $I_1$  for direct modulation with a set of frequencies  $f_k$  can be represented as

$$I_1 = I_{b1} + \sum_k I_k \sin(2\pi f_k t). \quad (3.11)$$

Functions and variables are taken as the same given under section 3.2. The response laser diode (LD2), which, apart from the current and modulation with a set of frequencies  $f_i$ , is driven by a fraction of the photocurrent fed from the output of LD1 is modelled as:

$$\frac{dN_{B2}}{dt} = \frac{\Gamma_q I_2}{eV} - \frac{N_{B2}}{\tau_c} + \frac{\Gamma_q N_2}{\tau_e}, \quad (3.12)$$

$$\frac{dN_2}{dt} = \frac{N_{B2}}{\Gamma_q \tau_c} + N_2 \left[ \frac{1}{\tau_n} + \frac{1}{\tau_e} \right] - v_g G(N_2, P_2) P_2, \quad (3.13)$$

$$\frac{dP_2}{dt} = \left[ \Gamma v_g G(N_2, P_2) - \frac{1}{\tau_p} \right] P_2 + \Gamma \beta B N_2^2, \quad (3.14)$$

where injection current  $I_2$  with the coupling term will be

$$I_2 = I_{b2} + \sum_i I_i \sin(2\pi f_i t) + C[P_1(t - \tau) - P_2(t)], \quad (3.15)$$

where, as explained before, the delay time factor  $\tau$  accounts for the channel delay between the two laser systems.

Three important factors to be considered while studying the coupled laser system are the initial phase difference of the modulating signals, the channel delay and the detuning between the modulating frequencies of the systems. Our aim in this section is to show that multiple quantum well lasers are suitable choice for chaotic synchronization and subsequent secure communication using chaotic encryption and decryption with the help of synchronization. In this regard, we consider the laser systems to be identical, that is, they have the same design parameters and physical features as given in Table 1.3. We have biased both lasers with the same current amplitude of  $I_{b1} = I_{b2} = 5 \text{ mA}$ . We have then simulated the coupled system with zero initial phase difference and zero channel delay.

The results are shown in figure 3.15, where the two lasers achieve synchronization under a three tone modulation at frequencies 2.01 GHz, 4.02 GHz and 6.04 GHz. The biasing current is  $I_{dc} = 22 \text{ mA}$  and modulation amplitude is  $2 \text{ mA}$  for each frequency. The coupling strength has been set to  $1.4e - 004$  which is chosen to match with the mean photon number density of the drive laser. The modulation frequencies were chosen so as to drive the laser diode into a high periodic state as can be seen from the time series in figure 3.15. The synchronization error is calculated by taking the absolute difference between the two laser outputs and is of the order of  $10^{-3}$ . It can be seen that the error fluctuations decrease exponentially with time and finally converge as seen in the figure. To verify the results quantitatively, we have calculated the similarity function  $S(\tau)$ , discussed in section 1.3 which is modified for the

coupled MQW laser system as follows:

$$S^2(\tau) = \frac{\langle [P_d(t - \tau) - P_r(t)]^2 \rangle}{\sqrt{\langle P_d^2(t - \tau) \rangle \langle P_r^2(t) \rangle}}, \quad (3.16)$$

where the variables  $P_d$  and  $P_r$  represent the output power of drive laser (LD1) and the response laser (LD2). In the present case, we have calculated the similarity function  $S(0)$  by setting  $\tau = 0$ . The value of  $S(0)$  is very close to zero in the case of highly level synchronised systems. In the present case of the coupled system,  $S(0) = 0.0031$  which is very close to zero and, therefore, indicate a very strong synchronization between the coupled lasers.

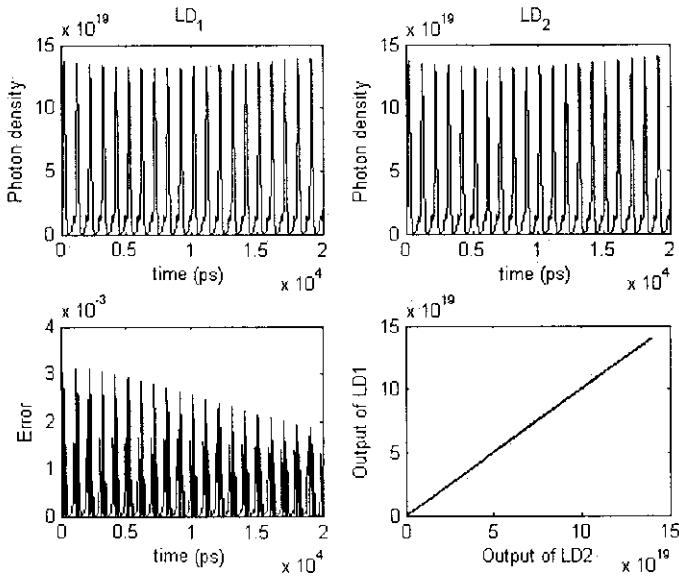


Figure 3.15: State of coupled lasers: (a) Time series of the drive laser diode LD1 modulated with three tones at  $2.01GHz$ ,  $4.02GHz$  and  $6.04GHz$ . (b) Time series of the driven system LD2 with the same modulation. (c) The synchronization error as a function of time. (d) The phase diagram showing perfect synchronization indicated by the straight line. The coupling strength  $C = 1.4 \times 10^{-4}$  and  $S(0) = 0.0031$ .

Next, we have studied the synchronization between the coupled systems when both of them are in a chaotic state. For this, we have studied the system with various coupling strengths under a two-tone modulation scheme in which both the lasers were modulated with the same set of frequencies  $2.4721 GHz$  and  $4.01 GHz$  with zero phase shift and the same biasing and modulation currents as before. This modulation scheme was adopted because of its suitability in driving the lasers to a chaotic state as observed in section 3.5. The largest lyapunov exponent (MLE) of the drive laser has been calculated and is equal to  $2.9437 \times 10^{10} bits/s$ . When the coupling strength is set to  $C = 0.0066$ , we have found that

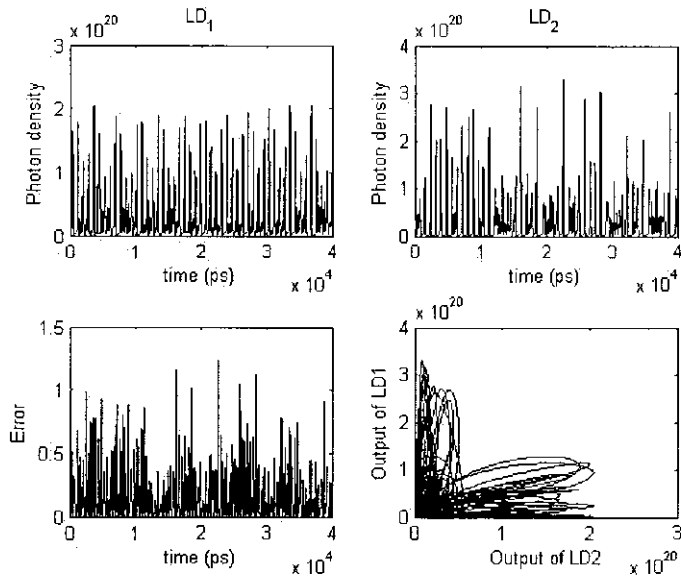


Figure 3.16: State of two coupled chaotic lasers in out of synchronization: (a) Time series of the drive laser diode LD1 modulated with three tones at  $2.4721\text{GHz}$  and  $4.01\text{GHz}$ . (b) Time series of the driven system LD2 with the same modulation as the drive laser. (c) The synchronization error as a function of time. (d) The phase diagram indicating the lack of synchronization at a coupling strength of  $C = 0.0066$  and  $S(0) = 1.46$ .

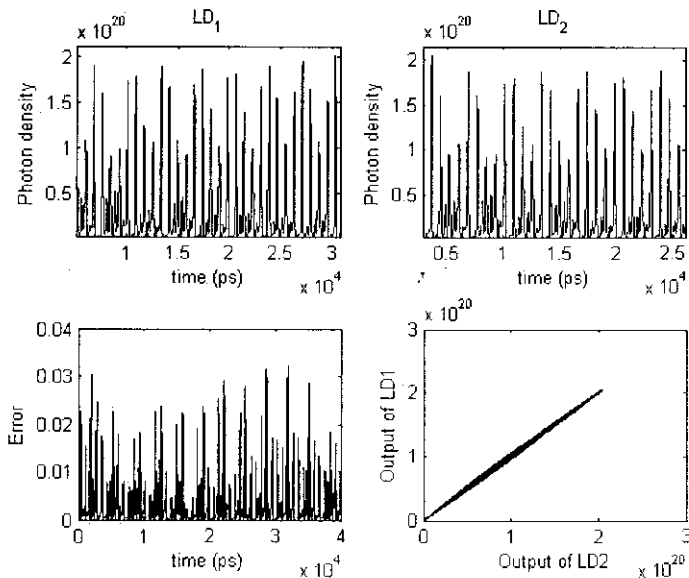


Figure 3.17: State of two coupled chaotic lasers in synchrony: (a) Time series of the drive laser diode LD1 modulated with three tones at  $2.4721\text{GHz}$  and  $4.0\text{GHz}$ . (b) Time series of the driven system LD2 with the same modulation as the drive laser. (c) The synchronization error as a function of time. (d) The phase diagram indicating good synchronization  $C = 0.0078$ . The similarity function  $S(0) = 0.0338$  is two orders smaller than the situation in 3.16.

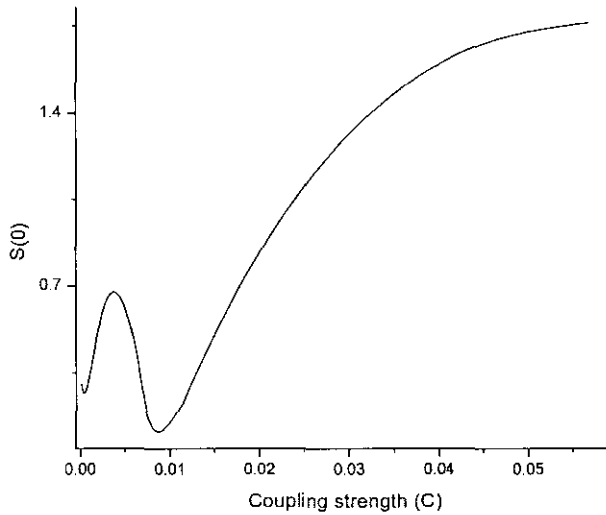


Figure 3.18: The similarity function  $S(0)$  for vs coupling strengths  $C$  of two coupled chaotic MQW lasers modulated at 2.4752 GHz and 4.01 GHz with a modulation current of 6 mA. The synchronization is robust around  $C = 0.01$

the two lasers are out of synchrony as illustrated in figure 3.16. The similarity function is very higher compared to the previous case and we have a large mismatch from linearity in the phase diagram shown in the figure. The synchronization error,  $S(0) = 1.4600$  in this case and is very high compared to the previous value. To verify this, the coupling between the two lasers is set to  $C = 0.0078$  and a state of synchronization is achieved as shown in figure 3.17. The level of synchronization in this situation is very high and quantitatively, the low value of  $S(0) = 0.0338$  shows that the two lasers have very good synchronization between them. This conclusion is supported by the two time series and error plots in figure 3.17. The error is very small and is closer to zero. Thus, we have shown that two chaotic MQW lasers can be synchronised by choosing the optimum value of coupling between them and this can be easily tuned electronically in a practical system by employing a control circuit.

To analyse the nature of the synchronization with respect to various coupling strengths, we have calculated the similarity function for different coupling strengths and the results are illustrated in figure 3.18. The figure shows that the system achieve good synchronization for coupling a coupling strength  $C = 1 \times 10^{-3}$  and then goes out of synchronization. Further, when we increase the coupling strength, the systems achieve robust synchronization near  $C = .01$ . The synchronization is most stable when  $C = 0.0078$ . Altogether, the diagram shows the regions of robust synchronization achieved between the two coupled lasers under

the particular modulation and biasing schemes.

In conclusion, we have achieved synchronization between coupled MQW laser diodes and verified the results graphically and quantitatively by calculating the similarity function. Our results show that there is an optimum value for coupling strength which can achieve perfect synchrony under a fixed modulation scheme. This can be suitably chosen to satisfy the device engineering parameters and conditions. Our studies so far in this section has shown that the MQW laser diode makes a very good choice for chaotic synchronization when two or more lasers are coupled with suitably chosen coupling strengths and modulation parameters.

### 3.9 Conclusions

The nonlinear dynamical phenomena exhibited by a MQW laser diode when studied using the existing rate equation models. Chaos in the system has been studied and characterised with the help of times series analysis, phase space diagrams, power spectra, Poincaré section, and quantitatively by calculating the maximal Lyapunov exponent. We have shown that the MQW laser follows a period-doubling route to chaos which has been known to exist in directly modulated semiconductor lasers. This result shows that the laser can be chaotic for small values of modulation depths. In addition, we show that the laser phase space trajectory lies on a two-torus when subjected to multi-tone modulation. The periodicity with which the trajectories close on the surface of the torus is determined by the number of tones in the modulation spectrum and their ratios. Thus we show that the MQW laser to follow a torus-breaking route to chaos. Further, we have shown that a suitable choice of the frequencies and amplitudes in a multitone modulation scenario could make the laser generate periodic, quasiperiodic, and chaotic outputs. This result has been exploited further in achieving synchronization between coupled MQW laser systems modulated under various frequency conditions. Thus we have shown that the MQW laser system can achieve optimum synchronization when modulated under desired operating conditions such as periodic, quasiperiodic and chaotic oscillations. We have thus established that the MQW laser diode that we have modelled in this work is a suitable candidates for being used as a source of light for chaotic synchronization which will ensure data masking and encryption.

# Bibliography

- [1] G. P. Agrawal and N. K. Dutta. *Long-Wavelength Semiconductor Lasers*, Van Nostrand Reinhold, New York, 1993.
- [2] H. Kawaguchi, *Bistability and Nonlinearities in Laser Diodes*, Norwood, USA: Artech House, 1994.
- [3] J. Sacher, D. Baums, P. Panknin, W. Elsässer, and E. O. Göbel, “*Intensity instabilities of semiconductor lasers under current modulation, external light injection, and delayed feedback*,” *Phys. Rev. A* **45**, pp. 1893–1905 (1992).
- [4] H. Kawaguchi, “*Optical bistability and chaos in a semiconductor laser with a saturable absorber*,” *Appl. Phys. Lett.* **45**, pp. 1264–1266 (1984).
- [5] C.-H. Lee, T.-H. Yoon, and S.-Y. Shin, “*Period doubling and chaos in a directly modulated diode*,” *Appl. Phys. Lett.* **46**, pp. 95–97 (1985).
- [6] J. E. Bowers, B. R. Hemenway, A. H. Gnauck, and D. P. Wilt, “*Highspeed InGaAsP constricted-mesa lasers*,” *IEEE J. Quantum Electron.* **QE-22**, pp. 833-844 (1986).
- [7] R. Olshansky, P. Hill, V. Lanzisera, and W. Powazinik, “*Frequency response of 1.3  $\mu\text{m}$  InGaAsP high speed lasers*,” *IEEE J. Quantum Electron.* **QE-23**, pp. 1410-1418 (1987).
- [8] K. Petermann, “*Calculated spontaneous emission factor for double heterostructure injection lasers with gain induced waveguiding*”, *IEEE J. Quantum Electron.* **QE-15**, 566-570 (1979).
- [9] R. Nagarajan, T. Fukushima, S. W. Corzine, and J. E. Bowers, “*Effects of carrier transport on high-speed quantum well lasers*,” *Appl. Phys. Lett.* **59**, pp. 1835-1837 (1991).
- [10] S. Bennett, C. M. Snowden and S. Iezekiel, “*Nonlinear dynamics in directly modulated multiple-quantum-well laser diodes*,” *IEEE J. Quantum Electron.* **33**, pp. 2076-2083 (1997).
- [11] P. W. A. McIlroy, A. Kurobe, and Uematsu, *Analysis and application of theoretical gain curves to the design of multi-quantum-well lasers*, *IEEE J. Quantum Electron.* **QE-21**, pp. 1958-1963, Dec. 1985.
- [12] D. McDonald and R. F. O’Dowd, “*Comparison of two- and three-level rate equations in the modeling of quantum-well lasers*,” *IEEE J. Quantum Electron.* **31**, pp. 1927-1934 (1995).



- [13] A. Yariv, *Quantum Electronics*, John Wiley & Sons, New York, 1989.
- [14] C. P. Seltzer, L. D. Westbrook, and H. J. Wickes, "The 'Gain-Lever' effect in InGaAsP/InP multiple quantum well lasers," *IEEE J. Quantum Electron.* **31**, pp. 283-289 (1995).
- [15] A. D. Vandermeer and D. T. Cassidy, "A rate equation model of asymmetric multiple quantum-well lasers," *IEEE J. Quantum Electron.* **41**, pp. 917-924 (2005).
- [16] J. P. Ulahannan, M. P. John, and V. M. Nandakumaran, "Bistability and Hysteresis in the Dynamics of Directly Modulated Multiple Quantum Well Lasers," in *Laser Science, OSA Technical Digest (CD)* (Optical Society of America, 2007), paper JWC43.
- [17] J. P. Ulahannan, M. P. John, and V. M. Nandakumaran, "Chaos and Quasiperiodicity in Directly Modulated MQW Lasers," (revised article to be communicated to *IEEE J. Quantum Electron.*).
- [18] C.-H. Lee, T.-H. Yoon, and S.-Y. Shin, "Period doubling and chaos in a directly modulated laser diode," *Appl. Phys. Lett.* **46**, pp. 95-97 (1985).
- [19] J. Farey, "On a curious property of vulgar fractions," *Phil. Mag. London* **47**, pp. 385 (1816).
- [20] R. Devaney, "The Mandelbrot set and the Farey Tree, and the Fibonacci sequence," *Amer. Math. Monthly* **106**, pp. 289-302 (1999).
- [21] J. P. Ulahannan, M. P. John, and V. M. Nandakumaran, "Chaos and Quasiperiodicity in Directly Modulated MQW Lasers", (communicated to *IEEE J. Quantum Electron.*).
- [22] C. Juang, S. T. Huang, C. Y. Liu, W. C. Wang, T. M. Hwang, J. Juang and W. W. Lin, "Subcarrier multiplexing by chaotic multitone modulation," *IEEE J. Quantum Electron.* **39**, pp. 1321-1326 (2003).
- [23] C. Juang, T. M. Hwang, J. Juang and W. W. Lin, "A synchronization scheme using self-pulsating laser diodes in optical chaotic communication," *IEEE J. Quantum Electron.* **36**, pp. 300-304 (2000).
- [24] B. Krauskopf, S. Wicczorek, and D. Lenstra, "Different types of chaos in an optically injected semiconductor laser," *Appl. Phys. Lett.* **77**, pp. 1611-1613 (2000).
- [25] M. C. Tatham, I. F. Lealman, C. P. Seltzer, L. D. Westbrook, and D. M. Cooper, "Resonance frequency, damping and differential gain in 1.55  $\mu\text{m}$  multiple quantum well lasers," *IEEE J. Quantum Electron.* **28**, pp. 408-414 (1992).
- [26] T. H. Yoon, C. H. Lee, and S. Y. Shin, "Perturbation analysis of bistability and period doubling bifurcations in directly-modulated laser diodes," *IEEE J. Quantum Electron.* **25**, pp. 1993-2000 (1989).
- [27] M. O. Vassel, W. F. Sharfin, W. C. Rideout, and J. Lee, "Competing effects of well-barrier hole burning and nonlinear gain on the resonance characteristics of quantum-well lasers," *IEEE J. Quantum Electron.* **29**, pp. 1319-1329 (1993).

- [28] V. Bindu and V. M. Nandakumaran, “*Chaotic encryption using long wavelength directly modulated semiconductor lasers,*” *J. Optics A- Pure & Appl. Optics* **4**, 115-119 (2002).
- [29] H. D. I. Abarbanel, M. B. Kennel, L. Illing, S. Tang, H. F. Chen, and J. M. Liu, “*Synchronization and communication using semiconductor lasers with optoelectronic feedback,*” *IEEE J. Quantum Electron.* **37**, pp. 1301-1311 (2001).



## Chapter 4

# Multistability and Hysteresis in MQW Laser Dynamics

*"Truth is what stands the test of experience."* - Albert Einstein

### ABSTRACT

*Optical bistability is a promising tool for all optical communication and computing systems. There are various examples where lasers are tailor made to produce bistable outputs. In this chapter we present some of the results showing the bistable behaviour of directly modulated multiple quantum well laser systems. The systems under consideration are not intrinsically bistable, but we show that they can exhibit bistability and hysteresis under suitable modulation conditions.*

### 4.1 Introduction

Optical bistability [1] in semiconductor lasers has received much attention because of its potential application in optical switching and signal processing. It is well established that the presence of an unpumped absorber in the laser cavity can lead to bistability [2]. Introducing quantum wells in the active regions of gain and absorber sections could significantly improve the switching speed and controllability of hysteresis characteristics [3].

Many processes in nature do not possess only one long term asymptotic state or attractor, but are rather characterized by a large number of coexisting attractors for a fixed set of

parameters. This implies that which attractor is eventually reached by a trajectory of the system depends on the initial condition [4, 5]. Several nonlinear systems such as chemical oscillators [6, 7, 8], nonlinear electronic circuits [9, 10], passive optical resonators [11, 12, 13, 14] and lasers [6, 15, 16, 17, 18] show this phenomena, known as multiple *bistability* or *multistability*. Multistable dynamical systems have important applications as pattern recognition and memory storage devices [11, 10, 14]. A well studied case is the bistability associated with a subcritical Hopf bifurcation.

Bistability is a case where two distinct states corresponding to the same set of parameters of a system are stable. Multiple bistability is defined as two or stable output states existing for one input power level. Bistability in driven nonlinear oscillators are usually observed in association with the hysteresis effect. A well known example is the hysteresis observed in the driven double well Duffing oscillator. A similar effect has been reported in directly modulated semiconductor lasers [19]. In this chapter we numerically demonstrate the multistability and hysteresis in the MQW laser dynamics controlled by both current and frequency modulations, and how to control and make use of the bistable conditions.

## 4.2 Bistability in Directly Modulated Lasers

An important dynamical behaviour exhibited by directly modulated laser systems is multistability [19], in which two or more stable states coexist, and bistability is a usual phenomenon [2, 20]. Multistability is usually accompanied by hysteresis effect in directly modulated laser systems. Multistability is an undesirable effect in a laser that is supposed to operate in a regular dynamical state.

However, it is shown that majority of the attractors are periodic, the chaotic component of the dynamics is in the chaotic saddles embedded in the basin boundary [21]. As a result, trajectories, starting with arbitrary initial conditions in the state space, experience periods of long chaotic transients before approaching one of the periodic attractors [22]. Therefore, because of these chaotic saddles, the trajectory is highly sensitive to the initial state. A slight change in the initial condition results in a trajectory that is attracted to a totally different periodic orbit.

## 4.3 Multistability in Directly Modulated MQW Laser

In this section, we examine the nature of multistability in the directly modulated MQW laser system and we find that the laser shows multistability and hysteresis when modulated under

different current values for certain values of the modulation frequencies. We have made use of the same dynamical model (Eqs. 3.2–3.4) as used in the previous chapter [23]. The simulation is started with arbitrarily chosen initial conditions and a minimum value of the parameter (here it is the modulation depth  $m = I_m/I_{th}$ ). The maxima of the photon density after vanishing the transients are recorded and they are used for constructing the bifurcation diagram. For obtaining the attractor points corresponding to another value of the concerned parameter, the parameter is increased slightly and the maxima of photon densities belonging to the stable state are recorded again. This process is repeated for the complete range of values of the parameter. The spectrum of values for the parameters are plotted along the  $x$ -axis as shown in Figs. 4.1-4.3. This method is called brute force approach [24] and it has an advantage. The bifurcation diagram plotted using this method (Figs. 4.1-4.3) contains only the stable attracting sets of the phase points. The laser bifurcation diagrams are plotted for various modulation frequency regimes and modulation current strengths. A current modulation index or modulation depth, is defined as  $m = I_m/I_{th}$  [25, 26, 2] for a clear indication of different stable orbits over the variation of modulation strength.

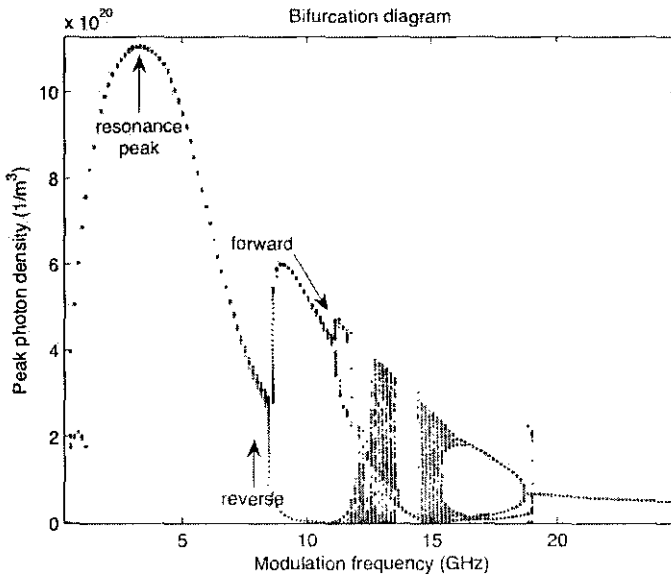


Figure 4.1: The laser bifurcation diagram for modulation frequency as a parameter under proper modulation conditions.

We have under consideration the MQW model used in the previous chapter and we have simulated the laser for a single tone modulation with a biasing current of  $22mA$  and modulation amplitude of  $5mA$ . Peak photon density for various modulation frequencies are stored and plotted against the modulation frequency (in  $GHz$ ) to obtain the bifurcation diagram

shown in Fig. 4.1. The figure shows the main resonance at the relaxation frequency of the laser, which is  $4\text{ GHz}$  based on calculations. When we increase the modulation frequency, the peak photon density follows a bifurcation route which is different when we reduce the modulation frequency from a higher value towards main resonance frequency. This is illustrated in the as forward and reverse paths in Fig. 4.1. The has a bistable output for modulation frequency range from  $8\text{ GHz}$  to  $11.5\text{ GHz}$  and thereafter it has a period-4 state. The output is chaotic for the windows  $12.5\text{ GHz} - 13.9\text{ GHz}$  and  $14.6\text{ GHz} - 15.3\text{ GHz}$ . It then follows a reverse period-doubling route.

Hysteresis is observed in the dynamics as seen in Fig. 4.1, where the output states are different for the forward path (coloured blue) and the reverse path (coloured red) for the modulation range above  $8.0\text{ GHz}$ . Below this value of modulation frequency, the laser has is monostable and has no hysteresis as is the case for high frequency modulation beyond  $19\text{ GHz}$ .

## 4.4 Bistability and Hysteresis

Further, we have simulated the laser model for a chosen modulation frequency and studied the variation in the output intensity by continuously varying the modulation depth  $m$ . Peak photon densities ( $P_m$ ) are stored first by increasing the modulation depth from zero to a value well above the threshold current of  $19\text{ mA}$  and then by decreasing the modulation depth to zero from the maximum. The bifurcation diagrams are then plotted using these values and are shown in Fig. 4.2. The upper part of the loop in the diagram shows the forward path and the lower part shows the reverse path. The bifurcation diagram corresponding to the modulation frequency  $1.2\text{ GHz}$  shows the bistable nature of the system along with hysteresis, where the laser output traces back to the initial point through a different path when the modulation current is lowered from a higher value.

Sudden jumps seen in the bifurcation diagram (Fig. 4.2) corresponding to the values 0.06 and 0.12 of modulation depth are associated with the pulse position bistability and hysteresis shown by the MQW laser and is the pitchfork bifurcation bistability [2]. In Fig. 4.3, we observe that the hysteresis nature grows out and become chaotic when the modulation frequency values are increased. In Fig. 4.3(a), the laser is simply bistable, and at the same time shows hysteresis.

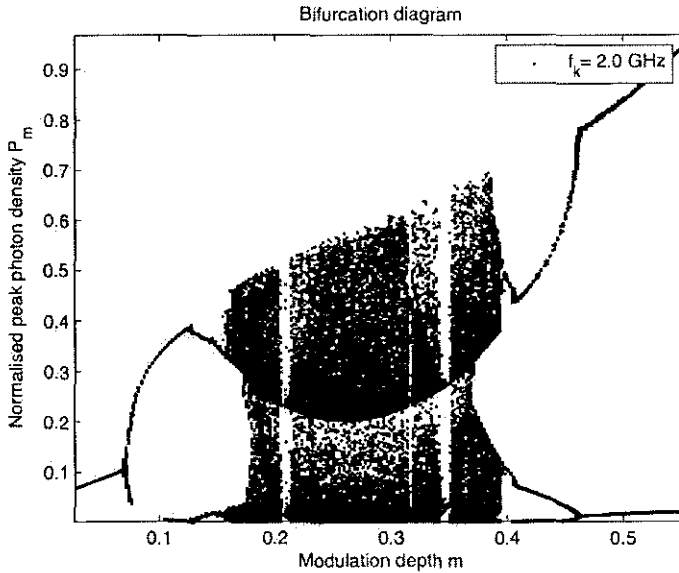


Figure 4.2: The laser bifurcation diagram for various modulation indices showing period doubling and reverse period doubling: Maxima of normalized photon density versus modulation depth.

## 4.5 Coexisting Attractors and Crisis

It is observed in Fig. 4.3 that from the bistable state at a modulation of  $1.20 \text{ GHz}$ , the laser becomes chaotic for a value  $f = 2.1327 \text{ GHz}$  (Fig. 4.3(b)). In this case, for modulation indices between 0.2 and 0.4, it can be seen that the chaotic attractor disappears and this is the crisis [29] situation in which the chaotic attractor collides with coexisting unstable fixed point and disappears. This is the first time that the crisis phenomenon has been reported in the MQW laser dynamics [27, 28]. Further, as the frequency reaches higher values the attractor reappears for the same modulation indices as shown distinctively in Fig. 4.3(c) and Fig. 4.3(d). Thus we have shown that the modulation current amplitude has a significant role in controlling the dynamics of the multiple quantum well laser.

We thus have shown that a variety of types of multistability exists in the MQW laser system - a stationary state coexisting with another stationary state, a stationary state with a limit cycle, a stationary state with a chaotic attractor, a limit cycle with another limit cycle, and a limit cycle with a chaotic attractor [27].



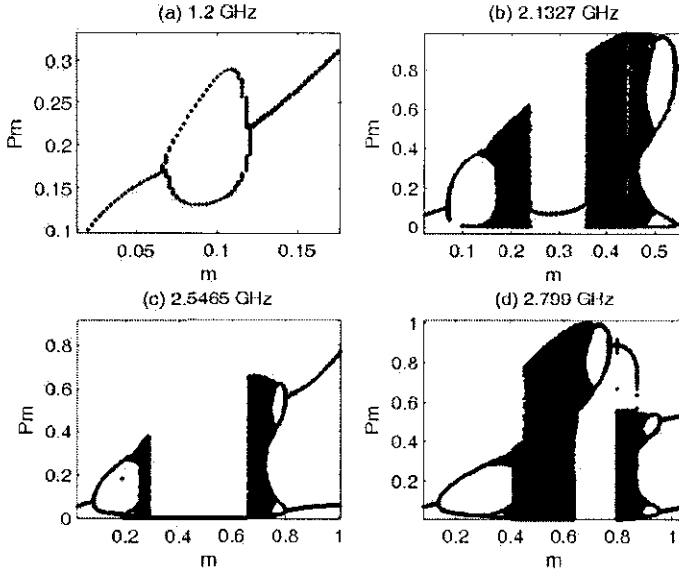


Figure 4.3: The laser bifurcation diagram against various modulation indices obtained for different modulation frequencies.

#### 4.5.1 Bifurcation for Group Velocity Variation

Interestingly, we have obtained a bifurcation diagram for the optical output power when the group velocity of photons is varied within a small range of values around the experimental value of  $v_g = 7.5 \times 10^7 m/s$ , taken from literature [30]. The bifurcation diagram is shown in Fig. 4.4, where the laser power output is plotted against a spectrum of possible values for the group velocity  $v_g$ . Fig. 4.5 shows the dynamical features of the laser when the group velocity value is fixed as  $8.7 \times 10^7 m/s$ . This value is taken from the bifurcation diagram in Fig. 4.4 and it can be seen that the laser output follows a period-2 state when group velocity is increased to such a large value.

We can explain this result as follows: the change in group velocity in this context is the same as changing differential gain and this would affect the relaxation oscillation frequency ( $f_r$ ). Changing the bias current is equivalent to changing the carrier density and we can see from Eqn. 2.16 that the differential gain is related to the carrier density. This is due to the fact that carrier-induced refractive index change in the quantum-well laser cavity leads to gain antiguiding [31]. Therefore, a change in bias current (modulation depth) would change  $f_r$  and therefore the group velocity changes. This is why there is a similarity between changing the bias current (modulation depth) and group velocity. Thus, we have shown that the carrier transport in the MQW laser cavity has a significant role in determining the output

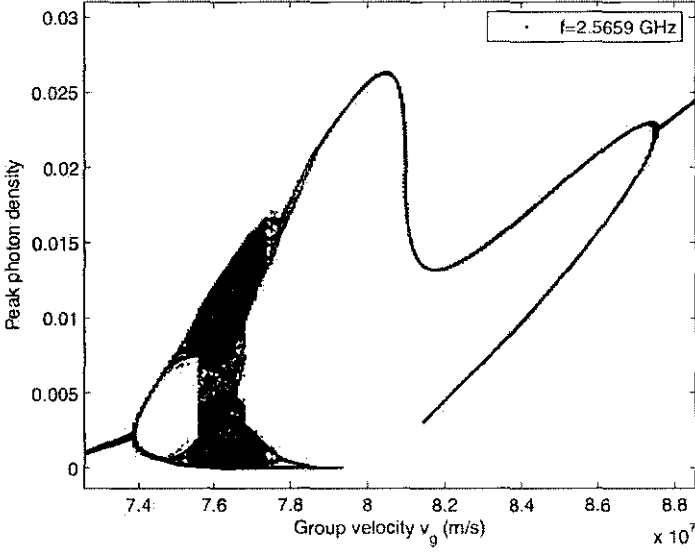


Figure 4.4: Bifurcation diagram for the variation of group velocity in the active region.

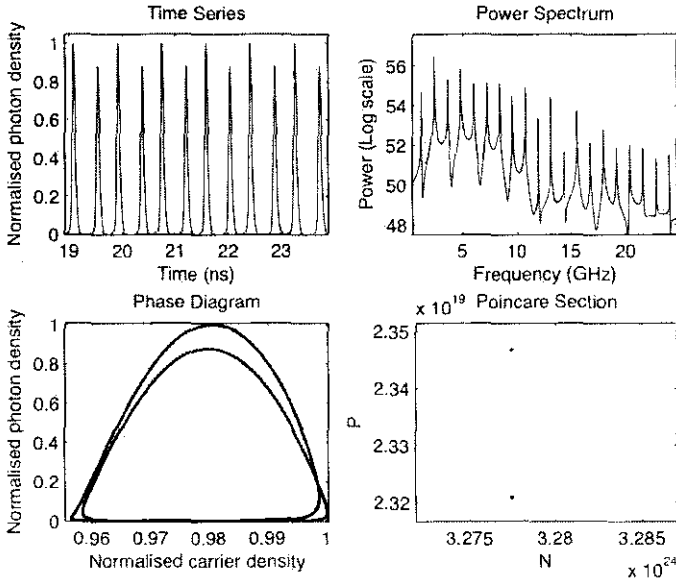


Figure 4.5: Features of the laser output dynamics corresponding to a group velocity value  $v_g = 8.7 \times 10^7$  m/s.

state as well as relaxation frequency values. This justifies the selection of the differential gain parameter model adopted in the MQW laser model. It should be noted that a considerable change in the group velocity is not desirable for the smooth working of the laser as it may induce undesirable output conditions.

## 4.6 Control of Bistability and Hysteresis

We have numerically demonstrated the early reported hysteresis and bistability in directly modulated multiple quantum well lasers. In standard applications, a semiconductor laser is expected to work in a monostable condition, where the laser phase space trajectory approaches, asymptotically, a stable periodic orbit and remains there for the entire operating period. Such working conditions demand that the laser should be prevented from going into multistable states [2].

In this situation, we consider the possible methods for controlling bistability in modulated laser diodes. Several methods for controlling bistability in lasers have been reported earlier [32, 33]. However, most of these schemes are not aimed at eliminating the bistability completely but to allow the system to switch from one of the stable states to the other. Pisarchik and Kuntsevich has proposed a control scheme based on periodic perturbation to the selected state [34]. They have numerically shown that such a scheme would suppress the bistability completely. It is important to mention that the perturbation is external in nature. However, we consider the direct delay feedback for suppressing the bistability. This method has been shown to be efficient in completely eliminating subharmonic generation and chaos in directly modulated laser diodes. The main advantage of this scheme is that no external signal is used as the perturbation. The numerical results regarding the suppression of chaos using this method is given in the following chapter.

## 4.7 Applications of multistability

Multistable dynamical systems have important applications as pattern recognition and memory storage devices [11, 10, 14]. Optical multistability demonstrated in passive *GaAlAs* waveguides and later in hybrid electro-optic devices [2] find use in digitizing incoming light pulses. Apart from that flat input-output curve make multistable devices suitable for optical limiting. In the field of digital communication, a multistable laser diode, when controlled properly, can be used to represent multilevel optical logic. Optical multistable devices are compatible with *multiple-valued* logic. The potential benefits of multiple-valued logic are increased speed and reliability, higher information storage density, decreased size, reduced

cost and power requirements. The main advantage of using a multistable MQW laser is that only a few optical beams are required for signal transmission.

## 4.8 Conclusions

In conclusion, our analysis of the laser parameter space reveals multistability and hysteresis in MQW laser dynamics. Instabilities in the laser output observed for different group velocity values points to the role of transport in the laser dynamics. Also, chaotic oscillations under multi-tone modulation would make the laser a prospective choice for multi-channel secure communication if two such lasers can be synchronized. Suitable selection of modulation frequency can drive the laser in the desirable working condition suitable of ultrafast pulse generation and communication. The results give some direction to the study of synchronized laser systems used for communication. The results in this direction could help better maneuverability if one wishes to use multiple quantum well lasers in secure optical communication. A more detailed analysis is needed to understand the role of noise and other conditions that may lead to the absence of chaos in a laboratory observation.



# Bibliography

- [1] H. M. Gibbs, F. A. Hopf, D. L. Kaplan, and R. L. Shoemaker, “*Observation of chaos in optical bistability*,” *Phys. Rev. Lett.* **46**, pp. 474–477 (1981).
- [2] H. Kawaguchi, “*Optical bistability and chaos in a semiconductor laser with a saturable absorber*,” *Appl. Phys. Lett.* **45**, pp. 1264–1266 (1984).
- [3] H. Uenohara, R. Takahashi, Y. Kawamura, and H. Iwamura, “*Static and dynamic response of Multiple quantum well voltage controlled bistable laser diodes*”, *IEEE J. Quantum Electron.* **32**, pp. 873–883 (1996).
- [4] U. Feudel and C. Grebogi, “*Multistability and the control of complexity*,” *Chaos* **7**, pp. 597–604, 1997.
- [5] U. Feudel, C. Grebogi, B. R. Hunt, and J. A. Yorke, “*Map with more than 100 coexisting low-period periodic attractors*,” *Phys. Rev. E* **54**, pp. 71–81 (1996).
- [6] M. Brambilla, F. Battipede, L. A. Lugiato, V. Penna, F. Prati, C. Tamm, and C. O. Weiss, “*Transverse laser patterns. I. Phase singularity crystals*,” *Phys. Rev. A* **43**, pp. 5090–5113 (1991).
- [7] F. Prengel, A. Wacker, and E. Scholl, “*Simple model for multistability and domain formation in semiconductor superlattices*,” *Phys. Rev. B* **50**, pp. 1705–1712 (1994).
- [8] P. Marmillot, M. Kaufmann, and J.-F. Hervagault, “*Multiple steady states and dissipative structures in a circular and linear array of three cells: Numerical and experimental approaches*,” *J. Chem. Phys.* **95**, pp. 1206–1214 (1991).
- [9] J. Kastrup, H. T. Grahn, and E. Scholl, “*Multistability of the current-voltage characteristics in doped GaAs-AlAs superlattices*,” *Appl. Phys. Lett.* **65**, pp. 1808–1810 (1994).
- [10] J. Foss, F. Moss, and J. Milton, “*Noise, multistability, and delayed recurrent loops*,” *Phys. Rev. E* **55**, pp. 4536–4543 (1997).
- [11] K. Ikeda and K. Matsumoto, “*High-dimensional chaotic behavior in systems with time-delayed feedback*,” *Physica D* **29**, pp. 223–235 (1987).

- [12] K. Ikeda, "Multiple-valued stationary state and its instability of the transmitted light by a ring cavity system," *Opt. Commun.* **30**, pp. 257-261 (1979).
- [13] K. Ikeda, H. Daido and O. Akimoto, "Optical Turbulence: Chaotic behavior of transmitted light from a ring cavity," *Phys. Rev. Lett.* **45**, pp. 709-712 (1980).
- [14] T. Aida and Y. Iino, "Effects of small signal injection on laser diode pumped hybrid bistable system with large delay," *Opt. Rev.* **2**, pp. 270-279 (1995).
- [15] M. Brambilla, L. A. Lugiato, V. Penna, F. Prati, C. Tamm, and C. O. Weiss, "Transverse laser patterns. II. Variational principle for pattern selection, spatial multistability, and laser hydrodynamics," *Phys. Rev. A* **43** pp. 5114-5120 (1991).
- [16] Z. Wang, W. Guo, and S. Zheng, "Quantum theory of optical multistability in a two-photon three-level  $\Lambda$ -configuration medium," *Phys. Rev. A* **46**, pp. 7235-7241 (1992).
- [17] F. T. Arecchi, R. Meucci, G. Puccioni, and J. Tredicce, "Experimental Evidence of Subharmonic Bifurcations, Multistability, and Turbulence in a Q-Switched Gas Laser," *Phys. Rev. Lett.* **49**, pp. 1217-1220 (1982).
- [18] F. T. Arecchi, R. Badiali, and A. Politi, "Generalized multistability and noise-induced jumps in a nonlinear dynamical system," *Phys. Rev. A* **32**, pp. 402-408 (1985).
- [19] C. Mayol, R. Toral, C. R. Mirasso, S. I. Turovets, and L. Pesquera, "Theory of main resonances in directly modulated diode lasers," *IEEE J. Quantum Electron.* **38**, pp. 260-269 (2002).
- [20] J. C. Celet, D. Dangoisse, P. Glorieux, G. Lythe, and T. Erneux, "Slowly passing through resonance strongly depends on noise," *Phys. Rev. Lett.* **81**, pp. 975-978 (1998).
- [21] C. Grebogi, H. Nusse, E. Ott, and J. A. Yorke, *Dynamical Systems, Lecture Notes in Mathematics*, edited by J. C. Alexander Springer-Verlag, New York, Vol. 1342, pp. 220-250 (1988).
- [22] L. Poon and C. Grebogi, "Controlling complexity," *Phys. Rev. Lett.* **75**, pp. 4023-4026 (1995).
- [23] S. Bennett, C. M. Snowden and S. Iezekiel, "Nonlinear dynamics in directly modulated multiple-quantum-well laser diodes," *IEEE J. Quantum Electron.* **33**, pp. 2076-2083 (1997).
- [24] T. S. Parker and L. O. Chua, *Practical numerical algorithms for chaotic systems*, Springer-Verlag, New York, 1989.
- [25] G. P. Agrawal, "Effects of gain nonlinearities on period doubling and chaos in directly modulating semiconductor lasers," *Appl. Phys. Lett.* **49**, pp. 1013-1015 (1986).
- [26] S. Rajesh and V. M. Nandakumaran, "Control of bistability in a directly modulated semiconductor laser using delayed optoelectronic feedback," *Physica D: Nonlinear Phenomena* **213**, pp. 113-120 (2006).

- [27] J. P. Ulahannan, M. P. John, and V. M. Nandakumaran, “*Bistability and Hysteresis in the Dynamics of Directly Modulated Multiple Quantum Well Lasers*,” in Laser Science, OSA Technical Digest (CD) (Optical Society of America, 2007), paper JWC43.
- [28] J. P. Ulahannan, M. P. John, and V. M. Nandakumaran, “*Chaos and Quasiperiodicity in Directly Modulated MQW Lasers*”, (communicated to *IEEE J. Quantum Electron.*).
- [29] C. Grebogi, E. Ott, and J. A. York, “*Chaotic attractors in crisis*,” *Phys. Rev. Lett.* **48**, pp. 1507–1510 (1982).
- [30] D. McDonald and R. F. O’Dowd, “*Comparison of two- and three-level rate equations in the modeling of quantum-well lasers*,” *IEEE J. Quantum Electron.*, vol. 31, pp. 1927–1934 (1995).
- [31] W. W. Chow and D. Depatie, “*Carrier-induced refractive-index change in quantum-well lasers*,” *Opt. Lett.*, vol. 13, pp. 303–305 (1988).
- [32] V. N. Chizhevsky and S. I. Turovets, “*Periodically loss-modulated CO<sub>2</sub> laser as an optical amplitude and phase multitrigger*”, *Phys. Rev. A*, **50**, pp. 1840–1843 (1994).
- [33] V. N. Chizhevsky, R. Corbaln, and A. N. Pisarchik, “*Attractor splitting induced by resonant perturbations*”, *Phys. Rev. E* **56**, pp. 1580–1584 (1997).
- [34] A. N. Pisarchik and B. F. Kuntsevich, “*Control of multistability in a directly modulated diode laser*”, *IEEE J. Quant. Electron.* **38**, pp. 1594–1598 (2002).





## Chapter 5

# Effect of Delay Feedback in MQW Lasers

*"Happy is he who gets to know the reasons for things." - Virgil*

### ABSTRACT

*It is known that chaotic dynamics can be controlled by stabilising unstable periodic orbits embedded in the chaotic attractors using small perturbations. Optoelectronic delay feedback is an effective tool in controlling instabilities in semiconductor laser systems. In this chapter, We show that the optoelectronic delay can control instabilities as well as induce them in multiple quantum well lasers when applied suitably.*

### 5.1 Introduction

In usual electronic systems negative feedback is used to improve either the linearity or the frequency characteristics of electronic amplifiers [1, 2]. Similarly, earlier works in the field of semiconductor lasers show that electronic feedback may also be applied to laser diodes to improve their modulation characteristics [3, 4, 5, 6, 7, 8]. If the optical frequency of the laser emission is detected, a negative electronic feedback may also be applied to stabilize the emitted optical frequency. Research work has been directed with respect to both long term stability as well as to reducing the short term fluctuations for achieving narrow laser spectra.

In most of the applications, a semiconductor laser is coupled to an environment where it is a part of a rather complex network. The dynamical behaviour of a semiconductor laser, i.e. the emitted light (phase, intensity and polarization), depends very much on the type of feedback caused by this coupling. We hold systematic studies of these dynamics based on delay-differential rate-equations. The goal is to understand the nature and origin of the various types of dynamics. Such knowledge is indispensable for successful control of the laser dynamics in complex network applications.

## 5.2 Laser Diode with Optoelectronic Feedback

Among dynamical systems capable of displaying chaotic behaviour, systems with delayed feedback are of interest since their time evolution is determined by a concurrence of a discrete step which tends to induce chaos and a continuous step which tends to smear it [9]. A laser cavity exhibiting bistability and chaos, under suitable operating conditions, is a fine physical example of such a system. The delay increases the dimensionality, and hence the complexity. It has also been shown that even small delay times affect the global dynamics of two-dimensional systems of limit cycle oscillators [10]. A delay differential equation modeling the dynamics of the system incorporating the nonlinear delay coupling can be used to analyze such a system.

The introduction of a delay in a dynamical system often leads to a change in the stability properties of the system. It is observed that short delay times lead to the creation of limit cycles via a subcritical Hopf bifurcation [11]. In our studies on the effects of nonlinear delayed feedback on MQW laser system, we are interested in two goals: (a) the introduction of dynamical complexity into the laser dynamics, and (b) the use of a delay feedback as a means by which to control the laser dynamics. Since differential delay equations, which are infinite-dimensional systems, can display great dynamical complexity in their behavior, we use a delayed feedback in a laser system, which by introducing additional dynamical complexity into the system, gives information on the dynamics of the system without delay.

We have used the same dynamical model described in previous chapters [12, 13, 14] to accommodate the optoelectronic delay feedback. A current signal proportional to the photon density of the laser delayed by a time  $\tau$  is added to the injection current to provide the direct delayed optoelectronic feedback [15]. A laser diode with optoelectronic feedback is shown schematically in Fig. 5.1. The conversion of optical signal into the electronic signal can be done by a photodiode and the necessary delay can be produced by the external transit of the light signal. The current signal obtained from the photodiode can be amplified to the required strength by using an operational amplifier and added to the input injection current

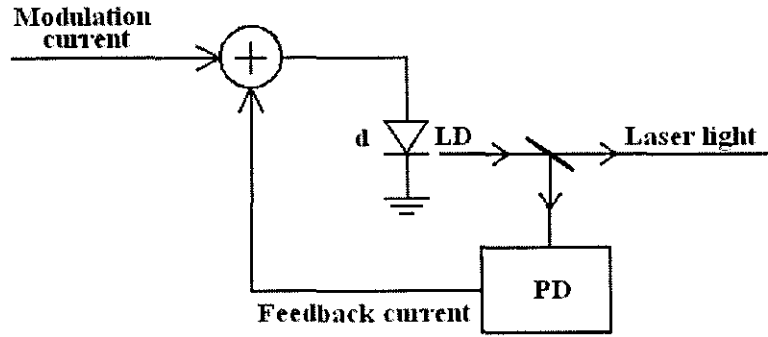


Figure 5.1: Schematic representation for a laser diode with optoelectronic feedback.

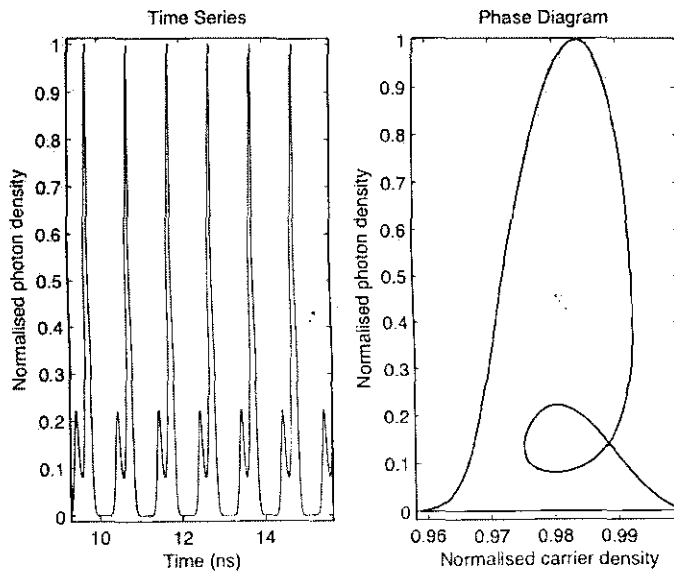


Figure 5.2: Time series and phase diagram showing unwanted pulsation (cusp) in the laser output for a modulation frequency  $2.0\text{ GHz}$ .

of the laser. The feedback signal would be proportional to the intensity of the optical signal delayed by a time  $\tau$  and hence it can be represented by  $DP(t - \tau)$ , where  $D$  is the feedback strength that is determined by the gain of the amplifier.

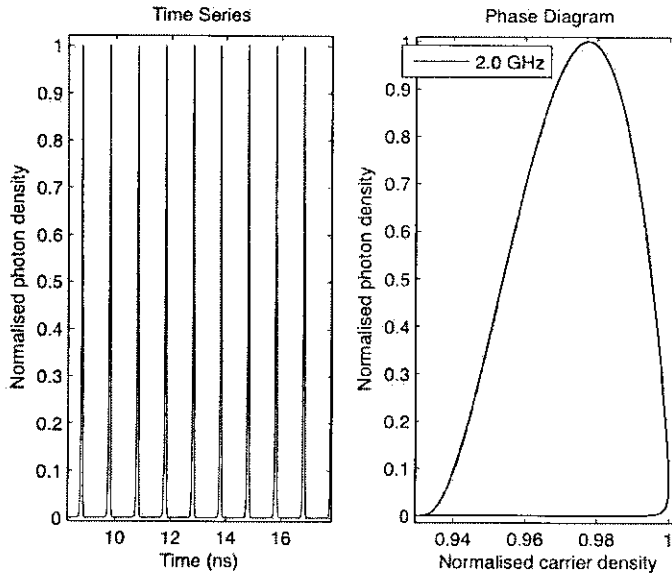


Figure 5.3: The cusp can be removed to give a highly regular output using a delay feedback of strength  $D = 1 \times 10^{-4} P_{av}$ .

Thus the expression for the injection current becomes

$$I = I_b + \sum_k I_k \sin(2\pi f_k t) + DP(t - \tau). \quad (5.1)$$

A variation of the injection current  $I(t)$  through the laser diode yields a variation of the emitted optical power and the optical emission frequency.

Instead of controlling the chaos and smoothening the waveform, the feedback is found to make the waveform more chaotic even in situations where chaos is not present in the absence of feedback. This has been verified by Juang *et al.* [16] for quantum well laser model. Our study shows that the MQW laser chaos can be controlled by both multitone modulation and feedback [17]. This in effect could make the lasers ideal choice for secure communication sources if one employs them in chaotic communication.

### 5.3 Control of Chaos Using Delay Feedback

When chosen properly, delay feedback can control instabilities in the laser system such as the unwanted pulsation in the output or certain quasiperiodic situations. We have set the laser delay strength appropriately around the value  $D = 10^{-4}P_{av}$ , where  $P_{av}$  is the mean output photon density of the laser under stable operating conditions of modulation frequency, biasing and modulation currents. The laser is modulated with a frequency of 2.0 GHz and with a modulation strength of  $I_k = 5mA$  when the laser is biased slightly above threshold. The feedback time is chosen to be 10ps and the results are shown in Figs. 5.2 and 5.3, where we have controlled the unwanted pulsation in the laser output.

When the time delay chosen is higher, of the order of  $\tau \sim 100ps$ , along with a sufficiently strong value for the feedback strength  $D \sim 5 \times 10^{-4}P_{av}$ , chaos in the laser can be controlled. We verify this result is for the a chaotic state of the laser when modulated by a set of two frequencies 2.4572 GHz and 4.0 GHz having golden mean ratio. The laser is modulated well above the bias current and the chaotic state is shown as in Fig. 5.4. This can be brought to a high periodic orbit as shown in Fig. 5.5 when we apply the delay feedback with  $D = 3 \times 10^{-4}P_{av}$  and delay time of  $\tau = 110ps$ . Thus, we show that it is possible stabilize the unstable periodic orbits in the a MQW laser system to a high periodic state. Therefore, proper delay strength and feedback time can control chaos in the laser system. In this way we can control multistability by choosing proper delay strength and time delay.

### 5.4 Delay Induced Chaos in MQW Laser Systems

Ikeda [9, 18] has shown that multistable modes of oscillation can arise in delayed feedback systems when the delay is larger than the response time of the system. We have observed chaos in the MQW laser system when the feedback strength is increased for slight variations from the chosen value of  $10^{-4}$  of the average photon density. The transitions are shown in Fig. 5.6, where the feedback strength is increased up to  $5 \times 10^{-4}$  of the average photon density while retaining the delay time at 100 ps. This can applied in the case of both single tone and multitone modulations schemes, though the chaotic transition occurs at at different points in the parameter space.

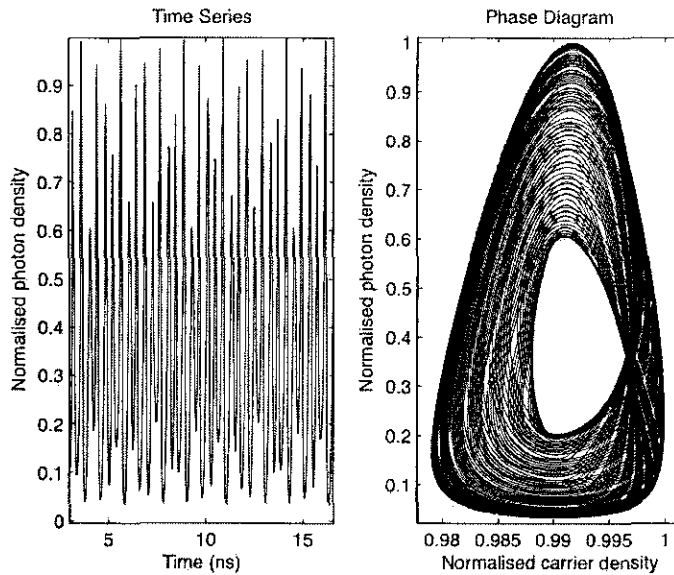


Figure 5.4: A chaotic state with two-tone modulation of  $2.4572 \text{ GHz}$  and  $4.0 \text{ GHz}$ . The maximal Lyapunov exponent (MLE) for this state is calculated as  $2.3513 \times 10^{11} \text{ bits/s}$ .

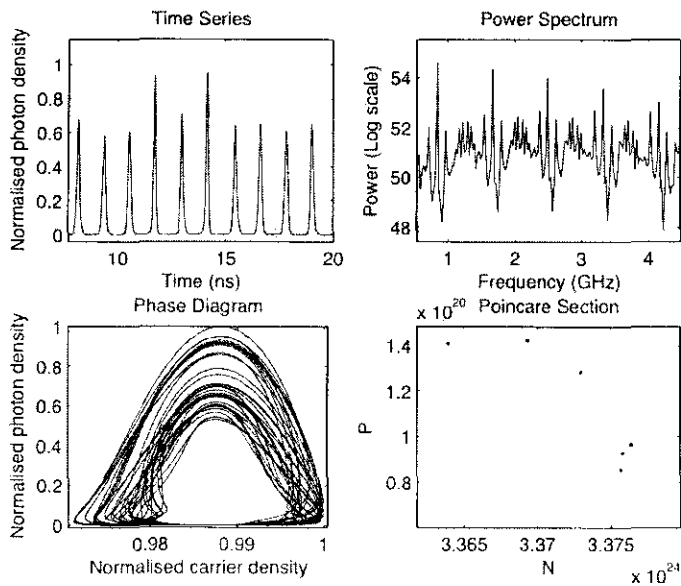


Figure 5.5: High periodic state obtained when the laser is subjected to a delay of  $D = 3 \times 10^{-4} P_{th}$  and  $\tau = 110 \text{ ps}$ .

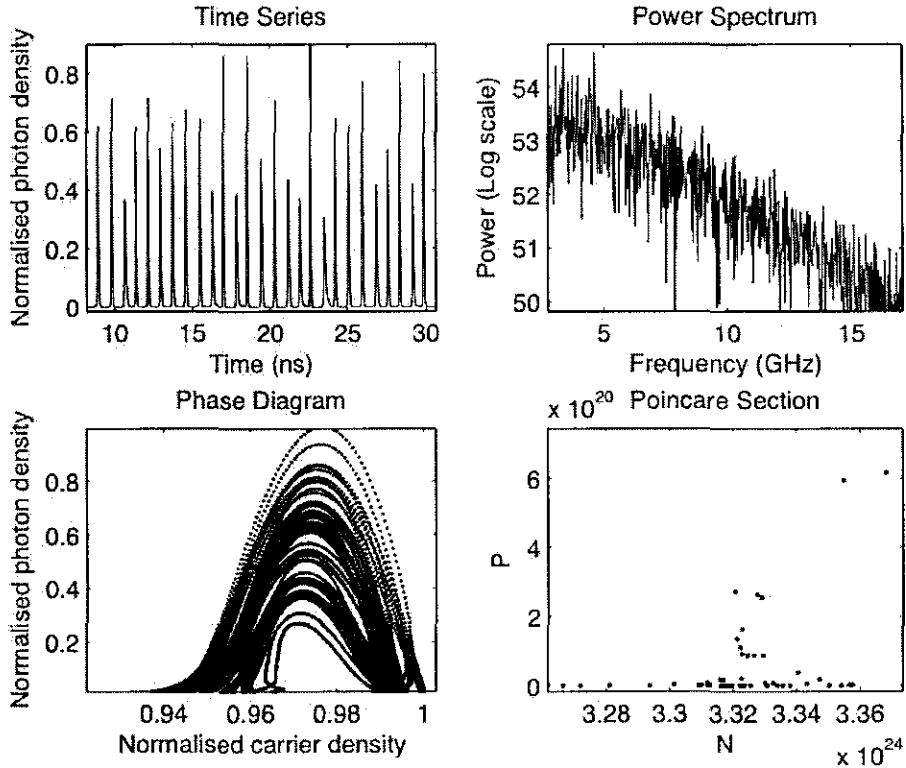


Figure 5.6: With a feedback strength of  $D = 3 \times 10^{-4} P_{on}$ , the laser goes into chaotic state with  $MLE = 2.091 \times 10^{11}$  bits/s.

## 5.5 Applications of Delayed Laser Systems

The most attractive part of the delay feedback scheme is its easy adaptation into any laser driving circuit. This could make the laser driving circuit more powerful by making it possible to control the dynamics of the laser output by using the same circuit that drives the laser. This could be a big boost for the chaotic communication schemes where the easy control over the drive laser could be an added advantage along with the chaotic encryption that the source offers when it works in the chaotic regime.

## 5.6 Conclusions

We have shown that delay feedback, when introduced optoelectronically in a directly modulated multiple quantum well laser system, can be quite decisive in determining the resultant dynamics of the laser. It is relevant to use the delay feedback in a semiconductor laser ow-



ing to various reasons, the best being its effectiveness in controlling unwanted instabilities in the laser output, as we have shown in section 5.4. The delay feedback, therefore, serve the cause of controlling chaos in the laser system. In addition to this feature, our study has shown that the optoelectronic delay can push the laser output into chaotic regimes and this is a quite important result owing to the viability of integrating such a circuit to the laser drive circuit. Thus the laser can be an ideal source for chaotic encryption and secure communication when two or more systems are used in synchrony to achieve these results.

# Bibliography

- [1] H. S. Black, "Stabilized Feedback Amplifiers," *Elec. Eng.* **53**, pp. 114-120 (1934).
- [2] K. Petermann, *Laser Diode Modulation and Noise*, Kluwer Academic Publishers, Dordrecht, 1988.
- [3] K. Pyragas, "Continuous control of chaos by self-controlling feedback," *Phys. Lett. A* **170**, pp. 421-428 (1992).
- [4] C. Mayol, R. Toral, C. R. Mirasso, S. I. Turovets, and I. Pesquera, "Theory of main resonances in directly modulated diode lasers," *IEEE J. Quantum Electron.* **38**, pp. 260-269 (2002).
- [5] J. C. Celet, D. Dangoisse, P. Glorieux, G. Lythe, and T. Erneux, "Slowly passing through resonance strongly depends on noise," *Phys. Rev. Lett.* **81**, pp. 975-978 (1998).
- [6] H. Kawaguchi, *Bistability and Nonlinearities in Laser Diodes*, Artech House, Norwood, 1994.
- [7] H. Lamela, G. Carpintero, and F. J. Mancebo, "Period tripling and chaos in the dynamic behavior of directly modulated diode lasers," *IEEE J. Quantum Electron.* **34**, pp. 1797-1801 (1998).
- [8] J. Sacher, D. Baums, P. Panknin, W. Elsässer, and E. O. Göbel, "Intensity instabilities of semiconductor lasers under current modulation, external light injection, and delayed feedback," *Phys. Rev. A* **45**, pp. 1893-1905 (1992).
- [9] K. Ikeda, H. Daido and O. Akimoto, "Successive higher-harmonic bifurcations in systems with delayed feedback," *Phys. Rev. Lett.* **49**, pp. 1467-1470 (1982).
- [10] E. Niebur, H. G. Schuster, and D. M. Kammen, "Collective frequencies and metastability in networks of limit-cycle oscillators with time delay," *Phys. Rev. Lett.* **67**, pp. 2753-2756 (1991).
- [11] T. Chevalier, A. Freund, and J. Ross, "The effects of a nonlinear delayed feedback on a chemical reaction," *J. of Chem. Phys.* **95**, pp. 308-316 (1991).
- [12] S. Bennett, C. M. Snowden, and S. Izackiel, "Nonlinear dynamics in directly modulated multiple-quantum-well laser diodes," *IEEE J. Quantum Electron.* **33**, pp. 2076-2083 (1997).

- [13] D. McDonald, and R. F. O'Dowd, "Comparison of two- and three-level rate equations in the modeling of quantum-well lasers," *IEEE J. Quantum Electron.* **31**, pp. 1927-1934 (1995).
- [14] P. W. A. McIlroy, A. Kurobe, and Uematsu, "Analysis and application of theoretical gain curves to the design of multi-quantum-well lasers," *IEEE J. Quantum Electron.* **21**, pp. 1958-1963 (1985).
- [15] S. Rajesh, and V. M. Nandakumaran, "Control of bistability in a directly modulated semiconductor laser using delayed optoelectronic feedback," *Physica D*, vol. 213, pp. 113-120, 2006.
- [16] C. Juang, S. M. Chang, N. K. Hu, C. Lee, and W. W. Lin, "Nonlinear dynamics in directly modulated multiple-quantum-well laser diodes," *Jap. J. Appl. Phys.* **44**, pp. 7827-7831 (2005).
- [17] Jijo P. U., M. P. John and V. M. Nandakumaran, "Optoelectronic feedback induced chaos in MQW laser diodes", *Proc. of Photonics 2006*, 8th Intl. Conference on Optoelectronics, Fibre Optics and Photonics, December 13-16, Hyderabad, India.
- [18] K. Ikeda and K. Matsumoto, "High-dimensional chaotic behavior in systems with time-delayed feedback," *Physica D* **29**, pp. 223-235 (1987).

## Chapter 6

# Conclusions and Future Prospects

*"Only the educated are free." - Epictetus*

### ABSTRACT

*The chapter summarises the work and presents some of the future prospects of the work.*

## 6.1 General Conclusions

The ability of semiconductor lasers to be modulated directly at high speed is among the unique features of those lasers which make them especially desirable sources for optical communication systems. Multiple Quantum Well Lasers are being widely used in many of the modern optoelectronic applications because of their large scale integrability, high speed and low threshold operation. We have modeled the MQW region of the lasers incorporating the light matter interaction phenomena involved in the generation of laser photons under the DFB and Fabry-Perot configurations.

Direct modulation with a time varying component adds an extra dimension to the laser dynamics thereby bringing in the occurrence of chaos in the light output. Our study on the effect of modulation has shown that the laser dynamics can be taken to periodic, quasi-periodic and chaotic regimes by suitably choosing the modulation depth and frequency. We

have shown that a moderate modulation depth can lead the MQW laser dynamics through a period-doubling route to chaos. We have shown qualitatively and quantitatively that a multi-tone modulation can bring chaos into the system through a quasiperiodic route by torus breaking. It is also shown that an incommensurate ratio of frequencies can result in a phase space trajectory lying on a torus with never repeating loops.

The synchronization of coupled MQW lasers have been studied and we have shown that with suitable coupling strength and modulation, we can achieve perfect synchronization between two such lasers. The results are verified with the help of time series analysis, phase space plots and quantitatively by calculating the synchronization error and similarity function. The results have been verified for different conditions.

Multistability and hysteresis phenomena are studied in the MQW laser system and we have shown that the laser output can be controlled for generating multistable outputs by suitably choosing the modulation depth. We have shown the occurrence of pulse position pitchfork bistability in the MQW laser system. The laser goes into multiple bistable states when the modulation frequency is increased. Another interesting behaviour we have observed is the phenomenon of crisis as explained in the thesis. This is the first ever reported work as far as MQW laser diode simulation studies are concerned.

Feedback mechanisms are being employed in semiconductor lasers for various purposes, from controlling chaos to stabilizing the laser output. We have analysed the role of delayed optoelectronic feedback in the MQW system and have shown that it can control unwanted pulsation and cusps in the MQW laser output. This in fact shows that multistable orbits can be controlled to be periodic with the help of a suitable feedback mechanism. We have also shown that delay can take the system to chaotic regime if we vary the delay time and feedback strength accordingly.

## 6.2 Future Prospects

Apart from their applied relevance, study of the dynamics of semiconductor lasers helps us to understand at least some of the universal features of nonlinear systems. Such a study also presents an opportunity to have a better understanding of the specific material and device level properties of the semiconductor laser. Thus, the semiconductor laser based study of nonlinear dynamics combines the aspects of material science and fundamental semiconductor physics with quantum optics and nonlinear dynamics. This is one of the reasons why we feel this area of research so exciting and promising for the future.

Multistability is an area where lot of work can be done to explore the possibility of making better devices to be used in areas such as digital communication. Much work is to be

621313 826 (0432)

J1J



T13

done in controlling the multiple stable states in the MQW laser to make them generating multilevel optical logic states. Further work in this area seems to be thrilling when we see the opportunities in integrated optics and optical computing.

Noise and fluctuations always play an important role in the dynamics of any physical system, and it has been shown to be important in the case of semiconductor lasers as well. Noise causes partial destruction of period doubling sequences, and as a result, chaos may occur with less period doublings as theoretically predicted. There have been many attempts to understand the crucial role of noise in the working of multiple quantum well lasers but a clear answer is still elusive. There is ample scope for extending the work to understand the role of noise, rapid fluctuations and random forcing the dynamics of quantum well lasers as they encounter forces at the quantum level.

Synchronization of laser systems for communication has been an active area of research for several years on the basis that it could provide a secure communication channel. Multiple quantum well lasers are an ideal choice for such a channel as they can be fabricated with mechanisms that are used for controlling dynamics.

Research in the field of semiconductor materials and devices have always been exciting. Present research and development in the field brings fast changes to the society with the help of better equipments and cheaper technologies. Therefore, today, we see rapid replacements for optoelectronic devices by faster, smaller and cheaper counterparts. Since we cannot neglect nonlinear dynamical effects from the working of semiconductor lasers, our work is rewarded if the research could bring in a better understanding of the quantum mechanics, material synthesis and fabrication technologies needed for creating better semiconductor lasers.

# Index

- adiabatic approximation, 26
- applications of delayed laser systems, 91
- asymptotically stable, 6
- attractor, 6
- Auger process, 32
  
- basin of attraction, 7
- Bernard-Duraffourg condition, 33
- bifurcation diagrams, 11
- biperiodic torus, 6
- bistability, 72
  
- carrier diffusion, 29
- carrier overflow, 32
- carrier transport, 28
- chaos, delay induced, 89
- chaotic communication, 12
- chaotic dynamics, 4
- conservative system, 6
- control of chaos, 11, 89
- crisis, 75
  
- direct modulation, 46
- dissipative system, 6
- distributed Bragg reflector laser, 34
- distributed feedback laser, 34
- dynamical system, 4
  
- Fabry-Perot cavity, 34
- feedback, optoelectronic, 86
- fixed point, 6
  
- gain calculation, 37
- group velocity, 76
  
- heterostructures; separate-confinement, 23
- Hopf bifurcation, 5
- hysteresis, 74
  
- impurities, 21
- interband processes, 32
- intermittency, 5
- intragand processes, 32
  
- Jacobian matrix, 10
  
- Lang-Kobayashi model, 26
- laser
  - distributed feedback, 20
  - quantum cascade, 20
  - quantum well, 20
- laser, quantum cascade, 25
- limit cycle, 6
- Lyapunov exponent, 9
  
- map, 4
- Maximal Lyapunov Exponent, 9, 54, 57

- Maxwell-Bloch equations, 26
- modulation, 45
  - multitonic, 58
  - single tone, 49
  - two tone, 55
- modulation depth, 58
- multiple quantum well lasers, 25
- multistability, 72
  
- nonradiative recombination, 27, 32
  
- OGY method, 11
- optical cavity, 33
  
- period-doubling bifurcation, 5, 49
- phase flow, 4
- phase-space, 6
- phonons, 21
- photon lifetime, 30
- pitchfork bifurcation, 74
- Poincaré map, 7
- power spectrum, 10
- pulse position bistability, 74
- Pyragas method, 11
  
- quantum confinement, 21
- quantum well, 21
- quantum well lasers, 23
  
- routes to chaos, 5
  - MQW Laser, 60
  - Pomeau-Manneville route, 5
  - Ruelle-Takens-Newhouse route, 5
  
- similarity function, 13, 63, 65
  
- strange attractor, 7
- superlattice, 25
- synchronization, 12
  - coupled laser systems, 12
  - coupled MQW lasers, 61
  
- well-barrier hole burning model, 30

